859750

ELECTROMAGNETIC BLACKOUT GUIDE

Effects of High Altitude Nuclear Bursts on Electromagnetic Waves

Volume I

DASA-1229

1 May 1961

Prepared for Defense Atomic Support Agency, Washington 25, D.C.
by General Electric TEMPO, Santa Barbara, Calif.
on Contract DA 49-146-XZ-038
GE Report Identification RM 61TMP-14

LETTER OF PROMULGATION

The "Electromagnetic Blackout Guide" describes the quantitative relationships between nuclear explosions at various altitudes, geographic locations and yields and the absorptive and refractive effects produced as a function of time, space and frequency. This guide provides quantitative data for war games and for evaluating communication systems and weapon systems. Liberal use is made of typical examples to emphasize the utility of this document. This report was prepared for the Defense Atomic Support Agency by General Electric TEMPO and is published for the information and guidance of all concerned.

Robert H. Booth

ROBERT H. BOOTH
Major General, USA
Chief, DASA

TABLE OF CONTENTS

LIST OF ILLUSTRATIONS

CHAPTER 1
INTRODUCTION

CHAPTER 1
INTRODUCTION

1.1 PURPOSE

This Guide is intended to supplement such works as "The Effects of Nuclear Weapons"[1] and "Capabilities of Atomic Weapons."[2] These previously published documents cover, in considerable detail, the expected physical phenomena and damage that can result from nuclear explosions occurring at heights ranging from beneath the surface to altitudes on the order of 10 to 15 kilometers. Correspondingly, low altitude phenomena and effects receive only incidental treatment here. Primary emphasis is placed on nuclear explosions that occur at altitudes above approximately 30 kilometers and the consequences of such explosions on radio and radar systems.

Modern nuclear weapons release tremendous amounts of energy, sub-atomic particles and radioactive debris; and can cause extensive blast, thermal, and radiation damage. Explosions also can affect the electrical properties of large volumes of the atmosphere. High energy radiation (gamma and X rays) and particles (beta particles) may cause partial or complete ionization in the air they penetrate. The ionization, in turn, may cause absorption, refraction, and reflection of electromagnetic waves. As a consequence, nuclear devices may have profound effects on the performance of radar and radio communication systems.

In general, the geographic extent, severity, and duration of the resulting system disturbances will depend on both the yield and altitude of the explosion and on the character of the radar or radio service. Above the very low frequency band (3 to 30 kilocycles), the importance of electromagnetic effects induced by nuclear explosions generally will increase with increasing weapon yield and burst altitude and will decrease with the wave length of the radio or radar service. For most practical purposes, electromagnetic disturbances created by nuclear explosions at altitudes below a few kilometers, will be quite localized and short-lived. Estimates given

in "The Effects of Nuclear Weapons" indicate that thousands of tons of dirt or water will be carried upward by an atomic cloud resulting from a surface burst of a megaton weapon. The resulting particles can act as reflectors to electromagnetic waves and produce echoes on X and K$_u$ band radars pointing at the cloud. Particle sizes are too small, however, to affect lower frequency radar or radio communications systems.

At low altitudes, penetration distances of the high energy radiations are restricted by the relatively dense atmosphere. For example, gamma rays lose half their energy in traveling somewhat less than 250 meters at sea level. In addition, the average lifetime of a free electron is less than a microsecond at altitudes less than about 20 kilometers so that any ionization created will disappear within a small fraction of a second.

In contrast to detonations below 20 kilometers, bursts at ionospheric heights are unmuffled and the primary outputs of weapons can escape to great distances. At the same time, ionization can persist from minutes to hours. Thus, as weapons are fired intentionally or unintentionally in the upper atmosphere or in space, the important consequences probably will be damage to weapon systems operating in the upper atmosphere or in space, or effects on electronic systems depending on electromagnetic waves propagating through or near the region of the burst. The ground blast and thermal effects are likely to be incidental, although they must still be considered.

1.2 SCOPE OF THE GUIDE

Emphasis is given in this Guide to two classes of phenomena associated with high altitude nuclear bursts. The first results from ionization caused by immediate and debris radiation — neutrons, gamma rays, beta particles, and X rays. These can produce major effects in the D and E regions of the ionosphere where collisions between electrons and neutral atoms cause electromagnetic wave absorption. This phenomena has been termed the low ion curtain. The second class is the extensive ionization caused by X rays and high speed debris in the F region. Here, the important effects of a detonation may be refraction, reflection, or absorption resulting from electron-ion collisions. This latter effect has been termed the high ion curtain.

As background for analyzing these effects of nuclear weapons on radio communications, navigation, and radar systems, Chapters 2 and 3 briefly review the principles of electromagnetic wave propagation and system performance criteria. An excellent and extensive body of literature exists on these subjects and is readily available to anyone desiring a more detailed or tutorial development of the subject. The primary purpose here is to summarize, for the user of this Guide, the concepts and notation used in subsequent chapters for qualitative and quantitative analyses of nuclear weapon effects on electromagnetic waves.

In this context, Chapter 2 reviews the pertinent concepts of electromagnetic waves and the physical processes influencing their propagation. Since many of the nuclear explosion effects of interest are caused by changes in the inoization states of the various regions of the atmosphere, both the atmosphere and the normal and abnormal ionosphere are described.

Performance criteria for communications and radar systems are discussed in Chapter 3. Here, principal emphasis has been given to the transmission losses that occur in the propagation medium. To assess the degradation in system performance resulting from nuclear explosions, typical transmission losses are given for the various frequency bands of importance to radio and radar operations. Since factors such as receiver sensitivity, noise and bandwidth considerations, and losses in transmission lines are unique to specific equipments, no attempt has been made to treat these subjects here.

The basic properties of nuclear explosions are reviewed in Chapter 4. Emphasis is placed on primary weapon outputs and the early interactions of these with the atmosphere and the earth's magnetic field. These are then related to the secondary outputs or manifestations that differ with altitude.

The principal effects of interest to propagation are further detailed in general form in Chapter 5, but not for specific weapons at specific altitudes. Absorption of radio waves as a function of frequency, weapon yield, time after burst, and space distribution of weapon products are discussed. This is followed by a treatment of refractive effects including reflection and backscatter. A discussion of F region disturbances and synchrotron noise concluces the unclassified volume.

The classified Guide which supplements this volume, treats in more detail the quantitative relationships between nuclear explosions (at various altitudes, geographic locations, and yields) and the absorptive and refractive effects produced as a function of time, space and frequency. It relates currently used procedures for radio and radar operations to suggested procedures for determining the degradation to be expected following a nuclear explosion, and selecting the best available alleviation measures.

1.3 STATE OF KNOWLEDGE

The physical phenomena and important effects associated with weapons exploded above approximately 30 kilometers are quite different from those of low altitude detonations. Only a small number of nuclear devices have been exploded in this altitude region. There is a large range of altitudes, yields, and geographical positions for which no tests have been made. Until comparatively recent times, these high altitude regions have been relatively inaccessible to direct experimental measurements, and a great deal of research remains to be done just to define natural phenomena fully.

The HARDTACK test series (TEAK and ORANGE conducted in the late summer of 1958), the ARGUS test series (conducted in the early fall of 1958), and extensive theoretical analysis form the basis for the description weapon effects presented in this Guide. Theoretical extrapolations are limited by uncertainties as to the magnitudes of various coefficients of interest — ionization cross-sections, deionization reaction rates, etc. It is sometimes difficult to choose among possible alternative physical processes with confidence at this time. Thus, the reliability of the predicted system degradations is limited. Both in the text and in the pertinent working graphs, indications of the estimated error in the degradation parameter (absorption, refraction, etc.) or in the temporal or spatial extent of the degradation are given. The possible variances should be borne in mind where action decisions are involved.

REFERENCES

1. Glasstone, Samuel, (ed). The Effects of Nuclear Weapons, United States Atomic Energy Commission, Washington 25, D.C.: U.S. Government Printing Office, June 1957.

2. Capabilities of Atomic Weapons (U), TM 23-300, OPNAV Instruction 03400.1B, AFM 136-1, NAVMC 1104 REV, (CONFIDENTIAL)

CHAPTER 2
REVIEW OF PROPAGATION

CHAPTER 2
REVIEW OF PROPAGATION

2.1 ELECTROMAGNETIC WAVES

In this chapter, electromagnetic waves are reviewed primarily in terms useful for analyzing radio and radar propagation. The electromagnetic energy spectrum also includes infrared radiation, visible and ultra violet light, X and gamma rays. While wave analysis is applicable to these higher frequency radiations, other methods are frequently more convenient. Thus, discussion of X and gamma rays, in particular, is deferred to later sections.

Radio and radar energy radiated into free space propagates as transverse electromagnetic waves. These are waves, consisting of electric and magnetic fields at right angles to each other as illustrated in Figure 2-1, that move in a direction perpendicular to the stress fields. To an observer at a large distance from their point of origin, these electromagnetic waves appear to have a plane wave front; both the electric and magnetic fields have uniform values at all points in a plane normal to the direction of propagation. By convention, the polarization of an electromagnetic wave is associated with the orientation of its electric field or E-field. Thus, for the case illustrated, the wave is vertically polarized. A horizontally polarized wave should have a horizontal E-field.

The instantaneous spatial character of an electromagnetic wave is illustrated in Figure 2-2. Here the E and H vectors represent the electric and magnetic field intensities respectively along the path of propagation. An instant later, the entire wave pattern will have shifted to the right. The distance along the direction of travel, between maximum (or minimum) field intensities is the wave length (λ) which is related to the frequency (f) and the phase velocity (v) by the expression:

$$\lambda = \frac{v}{f} \qquad (2\text{-}1)$$

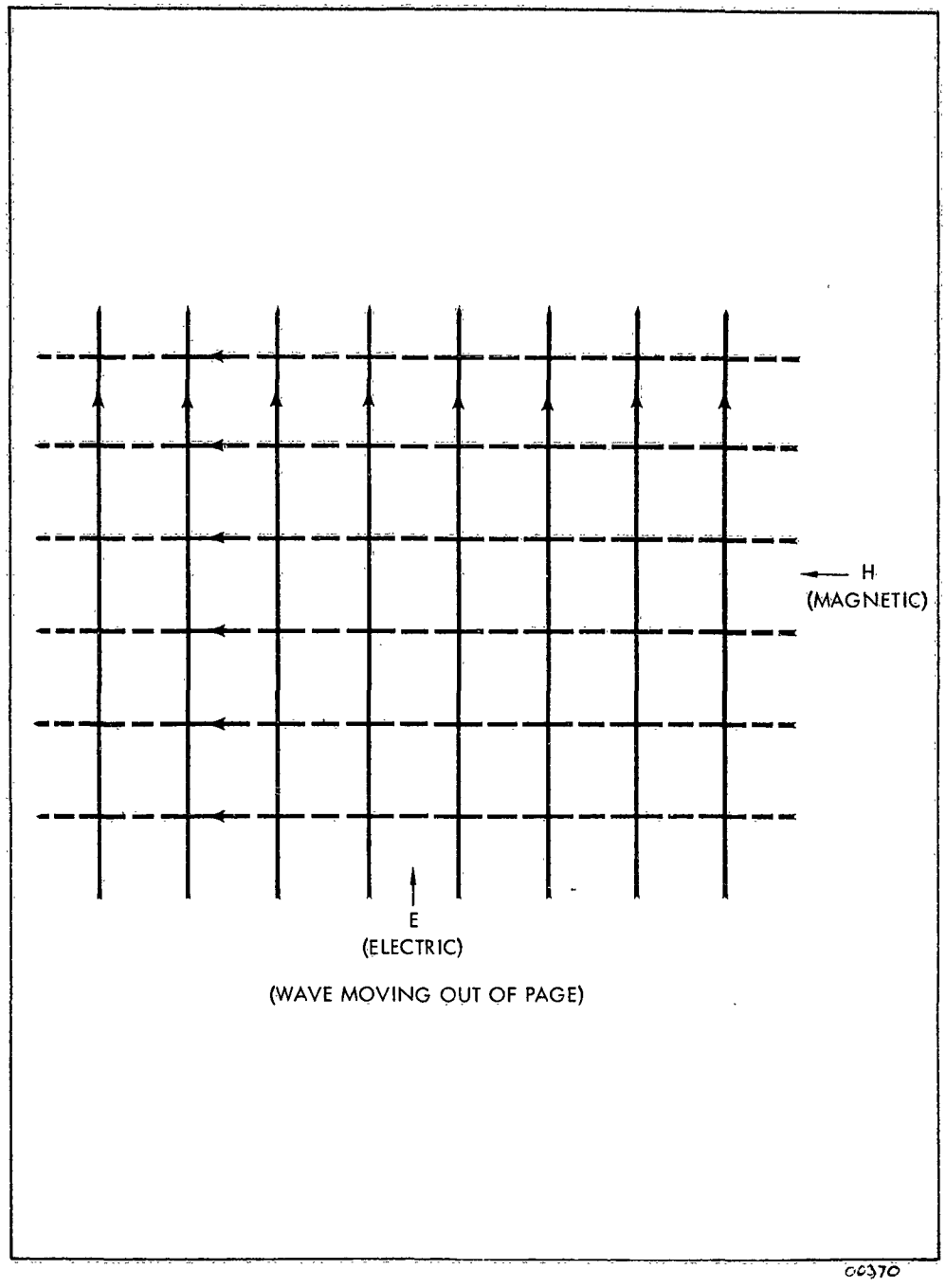

Figure 2-1. Electric and Magnetic Field Lines in Plane Perpendicular to Direction of Propagation

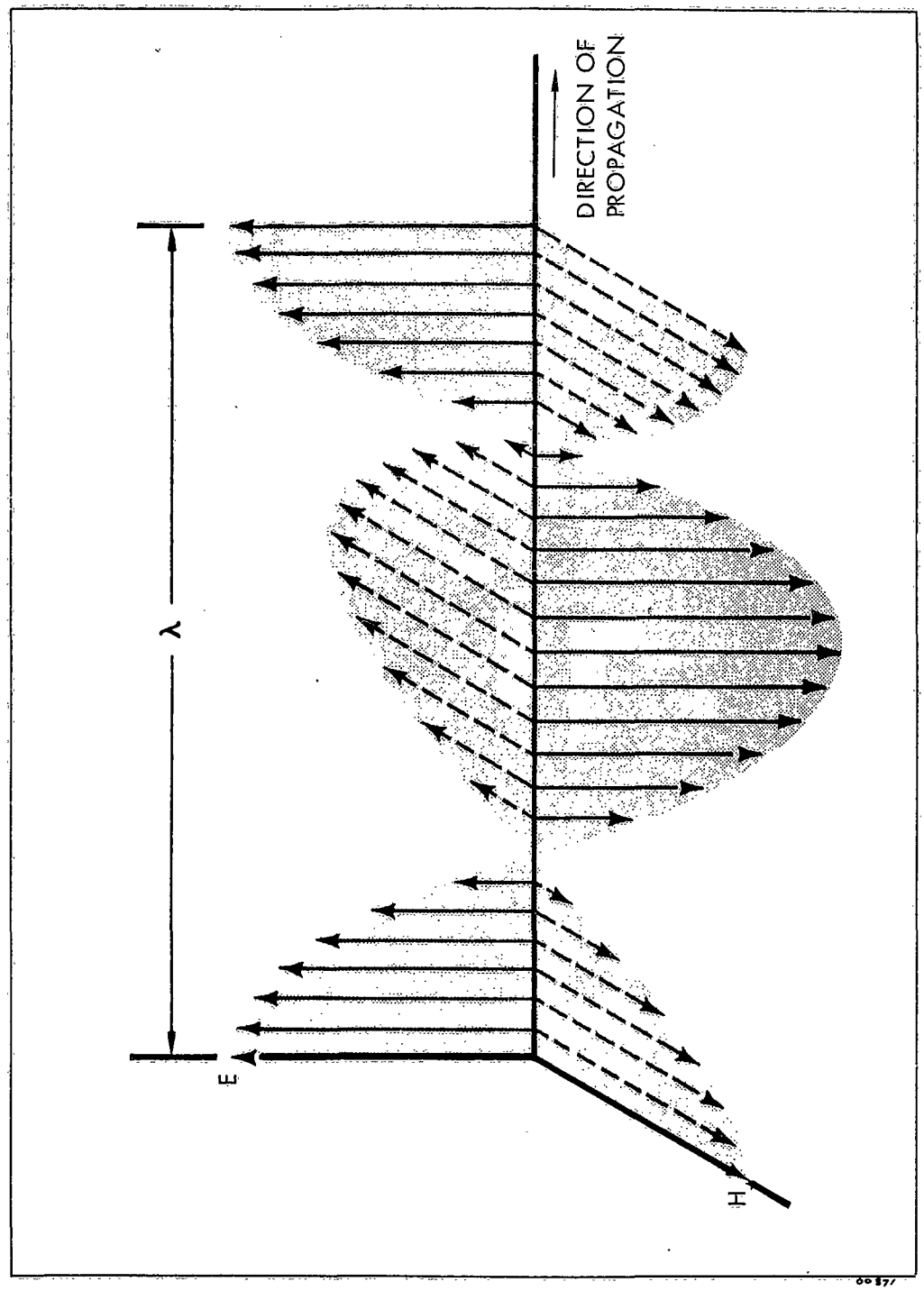

Figure 2-2. Electric and Magnetic Field Vectors Along Propagation Path

The frequency is determined by the source of energy, but the phase velocity is a property of the medium in which the wave is propagating. In a vacuum, for example, the phase velocity is about 3×10^8 meters per second.

2.1.1 Refraction

Because variations in the phase velocity of an electromagnetic wave will cause it to bend or be refracted, it is convenient to have an expression relating the phase velocity to a reference value. The relationship used is the refractive index (μ), which is a characteristic of the medium, and is the ratio of the phase velocity (c) in vacuum (free space) to the phase velocity (v) in the medium.

$$\mu = \frac{c}{v} \tag{2-2}$$

Normally, the phase velocity in the troposphere (lower atmosphere) will deviate only slightly from the free space value, and the refractive index will be very nearly one. In ionized regions such as the ionosphere, however, the refractive index will be less than unity and will be a function of electron density. Waves bend away from regions of low refractive index and into those having the larger index. For this reason, radio waves are refracted or reflected by the ionosphere as illustrated in Figure 2-3. The refraction is expressed quantitatively by Snell's law:

$$\mu_r \sin r = \mu_i \sin i \tag{2-3}$$

As shown, i is the angle between the incident ray (wave) and the normal to the boundary between two regions. Above the boundary, the index of refraction μ_r decreases with increasing height, and r is the angle between the refracted ray in the upper region and the boundary normal. If the discontinuity or refractive index gradient is small between these regions, the wave direction will be altered only slightly as illustrated by the "a" ray. On the other hand, if r becomes 90 degrees at some point of penetration, the wave will be reflected as shown by ray "b". Since $\sin 90° = 1$, condition for reflection of a wave entering the ionized region then is:

$$\sin i \geq \frac{\mu_r}{\mu_i} \tag{2-4}$$

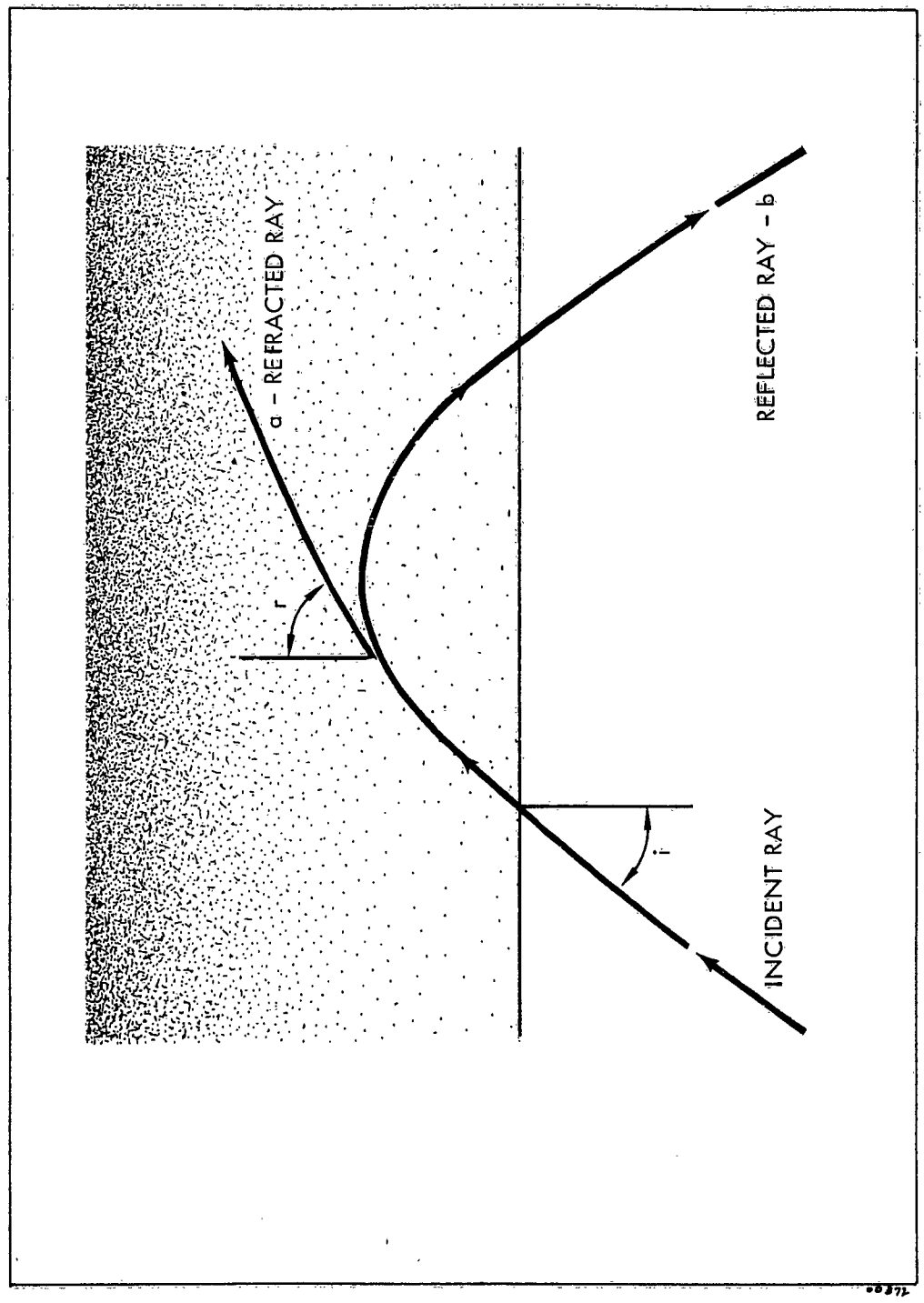

Figure 2-3. Refraction of Electromagnetic Waves

and where

$$\mu_i = 1$$

$$\sin i \geq \mu_r \qquad (2\text{-}5)$$

Such refraction and reflection occurs in the ionosphere because the electric field of an electromagnetic wave will exert a force on the ions and electrons and accelerate them. This transfers energy from the wave to the ions and electrons. Charged particles in motion constitute a current, and the current will increase in magnitude until the electric field reverses direction. Then, as the particles decelerate, energy is returned to the electric field. However, the current lags behind the electric field, so the ionized region acts as a reactance, giving rise to an equivalent index of refraction:

$$\mu = \frac{c}{v} = \sqrt{1 - \frac{Ne^2}{m \pi f^2}} \qquad (2\text{-}6)$$

where

N = ion density,

e = charge on the ions,

m = ion mass, and

f = wave frequency.

Because electrons are many orders of magnitude lighter than positive or negative ions, they are more readily accelerated and constitute the major portion of the current. Consequently, only free electrons normally need to be considered as affecting propagation. Expressing N_e in electrons/centimeter^3, equation 2-6 becomes:

$$\mu = \sqrt{1 - f_n^2/f^2} \qquad (2\text{-}7)$$

where

$$f_n^2 = 80.5 \times 10^6 N_e$$

$$f_n \cong 9 \times 10^3 \sqrt{N_e} \qquad (2\text{-}8)$$

As long as f_n^2/f^2 is less than one, an electromagnetic wave entering the ionized medium perpendicularly ($i = 0^o$) will continue to propagate. When the wave frequency is equal to or less than f_n, the wave will be reflected. The condition $f_n = f$ is thus a transition between transmission and reflection and is called the "critical frequency".

For beyond-the-horizon radio communications, employing waves reflected from the ionosphere, f_n is the critical penetration frequency for vertical incidence. Higher frequency waves propagating vertically upward will penetrate the ionized region, while waves with frequencies of f_n or lower will be reflected. The maximum frequency at which waves will be reflected when making oblique angles of incidence at the ionosphere is related to the critical penetration frequency by the expression:

$$f = f_n \text{ secant } i$$
$$\cong 9 \times 10^3 \sqrt{N_e} \sec i \qquad (2\text{-}9)$$

This frequency is the maximum usable frequency (MUF) for communication links relying on sky waves reflected by the ionosphere, and will depend on ionospheric conditions and the distance between stations.

2.1.2 Magnetic Field Effects

So far, the discussion has neglected the effect of a magnetic field in an ionized region. In the vicinity of the earth, there is a constant magnetic field which influences wave propagation in the ionosphere — a region starting at about 60 kilometers altitude and extending upward. An electron moving freely in a constant magnetic field will move in a circular path or á spiral path along the lines of magnetic flux as shown in Figure 2-4. The frequency of rotation depends only on the strength of the constant magnetic field and is called the gyrofrequency (f_H). For electrons

$$f_H = 2.8 \times 10^6 B \qquad (2\text{-}10)$$

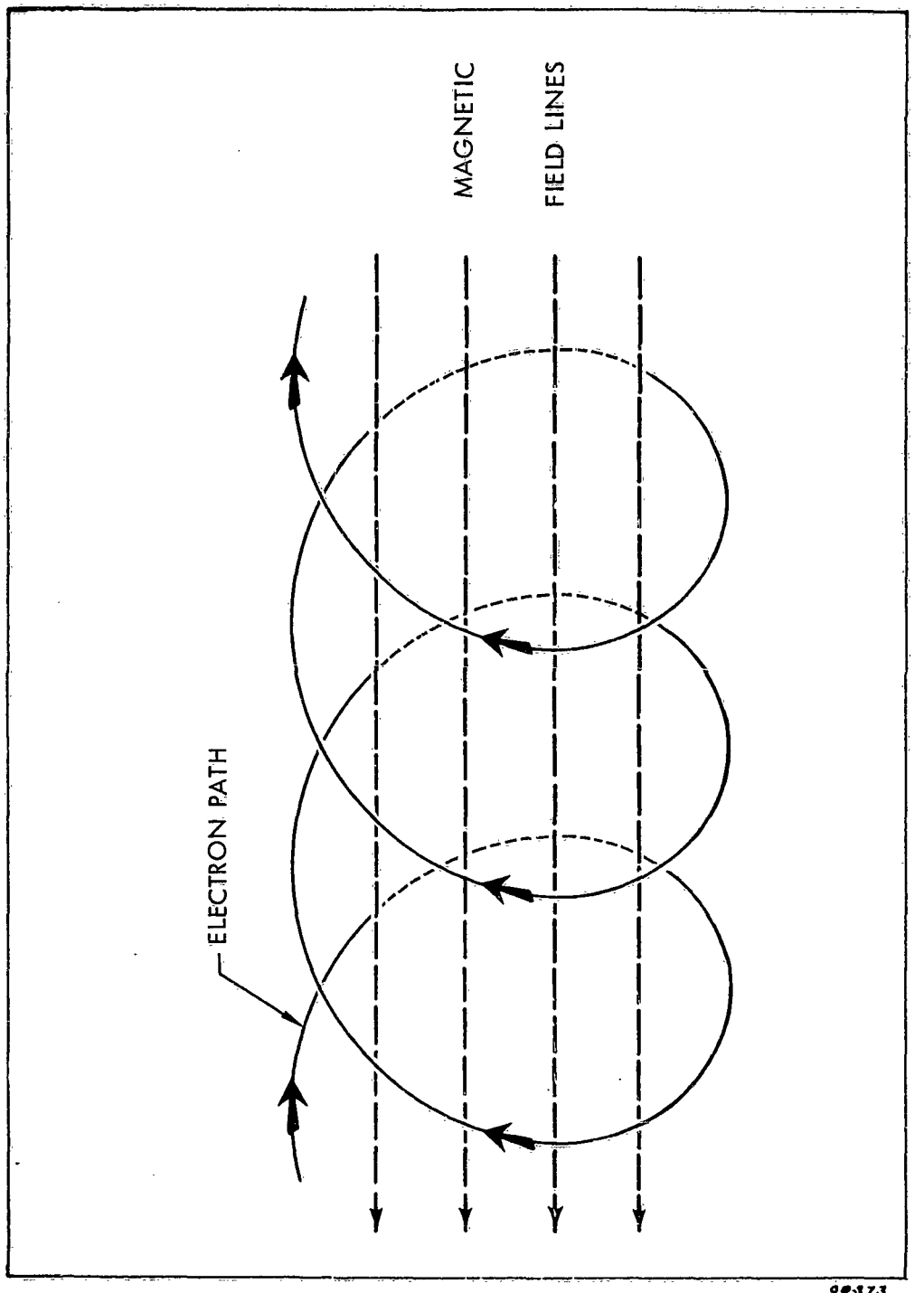

Figure 2-4. Electron Path in a Constant Magnetic Field

where B is the magnetic flux density in gauss. Since the earth's magnetic field is not uniform, the gyrofrequency will vary with location. In general, however, it will be on the order of 1.5 megacycles.

An electron in a magnetic field and forced in its motion by the alternating electric field of an electromagnetic wave will follow an elliptical path in general. When the wave frequency is close to the gyrofrequency, energy abstracted from the wave is not all reradiated by the electrons. Instead, the spiral path continues to increase in diameter as the electron motion becomes synchronous with the electric field causing the attenuation at 1.5 megacycles to be greater than at higher or lower frequencies.

With these interactions between waves and electrons in a magnetic field, an electromagnetic wave passing through an ionized region in the upper atmosphere will be split into two components of different polarizations — the "ordinary" and "extraordinary" rays — which have different phase velocities and attenuations and follow different paths. As a result, the phases of the two components will not generally be the same, causing a wave that was linearly polarized initially to emerge from an ionized medium elliptically polarized. That is, the plane of polarization continuously rotates at the wave frequency, and the electric field does not pass through a zero value, as illustrated in Figure 2-2.

2.1.3 Absorption

Except for the gyroresonance phenomena, the wave-electron interactions described above are reversible processes. That is, the energy acquired by the electrons is returned to the wave which continues to propagate with undiminished intensity, although not necessarily in the original direction. If, however, the electrons collide with other particles before returning their increased energy to the wave, the energy will be lost and the wave attenuated. In the atmosphere, electrons do collide with neutral molecules or pass close enough to ions to be "scattered" by the forces between charged particles. They cannot then give back reversibly the energy absorbed from the wave; some energy is converted into random motion, or thermal energy.

The average number of collisions experienced by an electron per second is the collision frequency, ν, and is proportional to the

particle density (i.e., to the atmospheric density). Collision frequency increases with atmospheric temperature and electron velocity.

Considering the neutral particles as smooth billiard balls, one can formulate the concept of a molecular cross-section area. More accurately, the cross-section is related to the probability that an electron passing through a particular unit volume of air will hit a neutral particle. For interactions between electrons and positive or negative ions, the attraction or repulsion between charges decreases as the inverse square of the distance between particles. This makes the cross-section as much as four or five orders of magnitude greater for a charged particle than for a neutral particle. The interaction at the greater distance may be only a slight bending of the electron path, caused by the forces acting for the time that the electron is relatively near the ion.

The billiard ball concept is not strictly applicable, and scattering is a better descriptive word than collision. An important consequence of the interactions between charged particles is the temperature dependence. The faster an electron moves, the less time it spends near an ion, and the less its path is bent. The "cross-section" is then a strong function of temperature so that scattering is less effective at high temperatures than at low.

In the normal ionosphere, radio wave absorption occurs in a region where the fractional ionization is relatively low. Thus, despite the greater cross-section of ions, electron scattering by neutral particles dominate in the absorption process.

An absorption coefficient can be defined which represents the effects of collisions on the electromagnetic wave:

$$k = \frac{2\pi e^2}{mc} \cdot \frac{1}{\mu} \cdot \frac{N_e \nu}{\omega^2 + \nu^2} \quad \text{nepers/meter} \qquad (2\text{-}11)$$

where $\omega = 2\pi f$.

This approximation neglects the effects of the magnetic field. A wave passing through a region having an absorption coefficient (k) decreases in intensity by a factor e^{-k} per unit path distance. Both μ and k are functions of the wave and collision frequencies,

electron density, and angle between the direction of propagation and magnetic field. When μ is approximately one, the wave is not refracted, and the absorption is called "non-deviative." On the other hand, when μ becomes small, the wave bends greatly and "deviative" absorption may result. Under circumstances in which μ approaches zero and k is large, the wave is highly attenuated.

2.2 THE EARTH'S ATMOSPHERE

The earth's atmosphere influences electromagnetic wave propagation. For that reason, and as background for introducing the modifications in the atmosphere caused by nuclear explosions, the next few sections discuss the normal and abnormal atmosphere. Important regions are the troposphere, stratosphere, mesosphere, and thermosphere as illustrated in Figure 2-5. The troposphere extends from the surface of the earth to the tropopause which has an altitude of 13 ± 5 kilometers. In this region the temperature decreases from a surface value of 273° ± 20°K to 210° ± 20°K. In the stratosphere, extending on upward to 50 ± 5 kilometers, the temperature rises again to 273° ± 20°K at the stratopause. The temperature drops again in the mesosphere to 190° ± 25°K at the mesopause — 85 ± 5 kilometers. At higher altitudes, in the thermosphere, the temperature again increases as the earth's atmosphere blends with that of the sun. The ionosphere mentioned earlier begins in the mesosphere and extends upward.

The density of the atmosphere decreases approximately exponentially with increasing height. Represented mathematically:

$$\rho = \rho_o e^{-\frac{h}{H}} \qquad (2\text{-}12)$$

Where ρ is the density at altitude h, ρ_o is the density at sea level, and H is called the "scale height." For each incremental altitude increase H in height, the density will decrease by a factor e (which is equal to 2.718) or by 63 percent. Because both the temperature and composition of the atmosphere change with altitude, the scale height is not actually a constant, but varies as shown in Figure 2-6. Below approximately 130 kilometers, however, a constant scale height of 7 kilometers will be sufficiently accurate for most computational purposes of this guide.

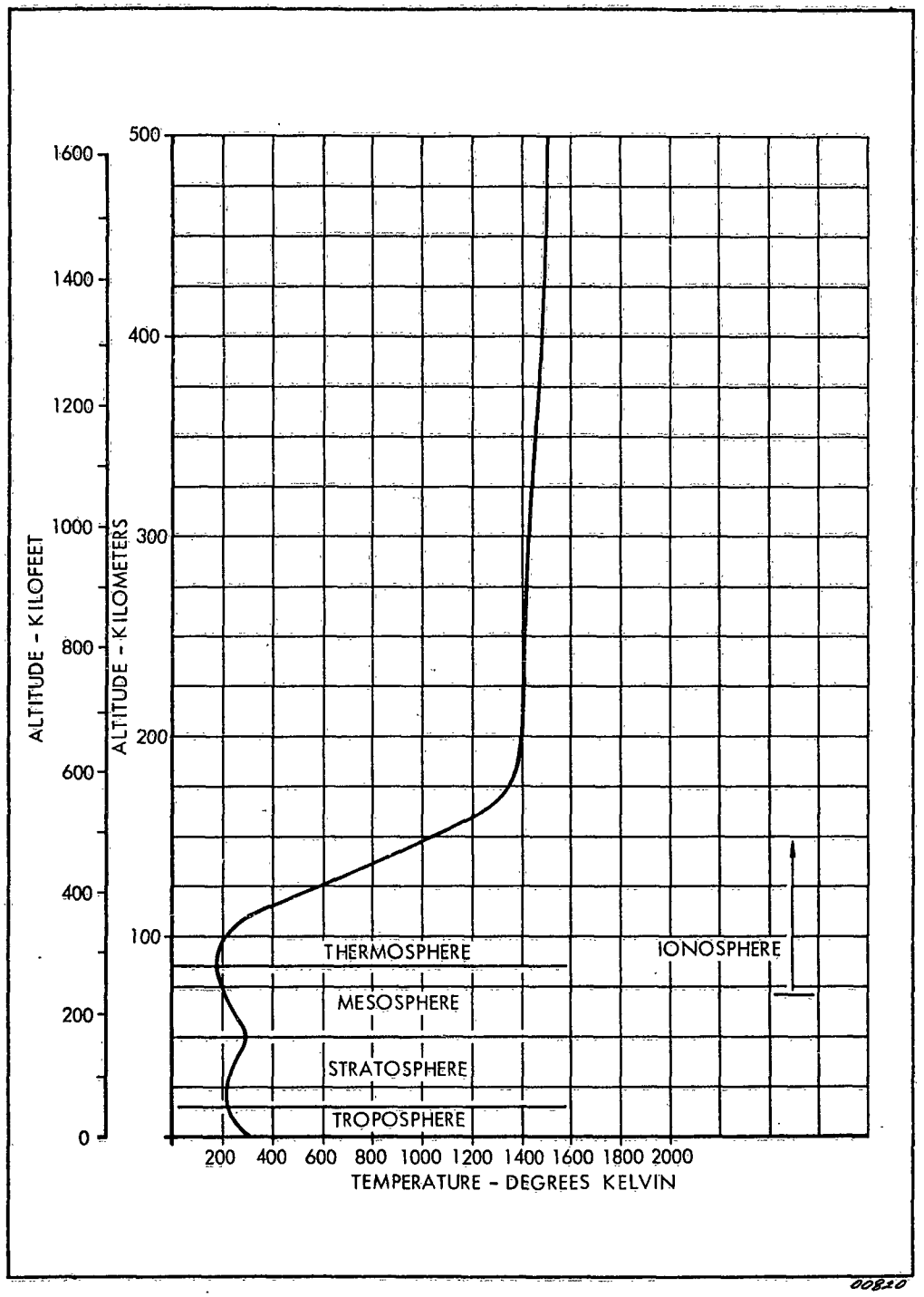

Figure 2-5. Atmosphere Temperature

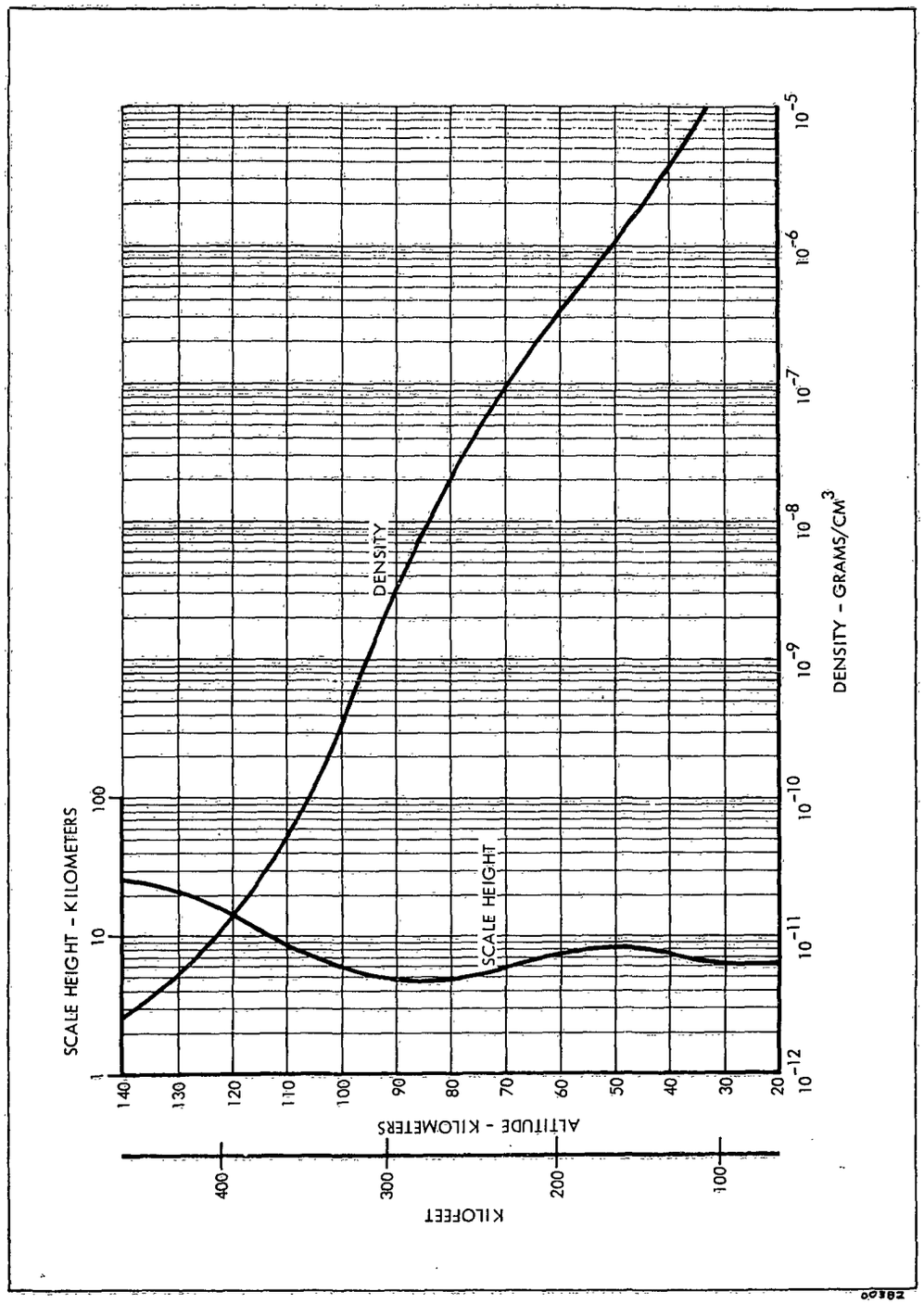

Figure 2-6. Density and Scale Height of the "Normal" Atmosphere

In addition to varying in temperature and density, the atmosphere undergoes changes in composition with altitude. Near the earth's surface, principal constituents of the air are molecular nitrogen (78 percent) and oxygen (21 percent). These diatomic molecular gases continue to be dominant to an altitude of approximately 95 kilometers. Above 90 kilometers, molecular oxygen (O_2) begins to dissociate into atomic oxygen (O). This dissociation of oxygen is caused by ultraviolet radiation from the sun and is nearly complete above 130 kilometers. Minor species, such as ozone (O_3) and nitric oxide (NO), also play important parts in determining the characteristics of the atmosphere, as each species absorbs radiation and enters chemical reactions in a characteristic manner.

The absorption of a particular portion of the radiation spectrum can be expressed in terms of the mass of air, or a particular constituent of air, that must be penetrated to reduce the incident energy by a factor e. To be most useful at various densities, this measure is a mass penetration coefficient, having the dimensions of grams per square centimeter. The mass penetration coefficient of a particular gas constituent(s) divided by density of the same constituent(s) in grams per cubic centimeter will give the penetration distance required to attenuate the radiation by 63 percent. Radiation, of a particular wavelength, entering the atmosphere vertically from above will not be absorbed rapidly at first because of the low density. As the density increases, so will the absorption, and most of the energy will be deposited in the region in which the e-folding distance (energy reduced by the factor e) corresponds to the scale height of the atmosphere. Although the atmosphere will become denser at still lower altitudes with a corresponding increase in attenuation, most of the energy will have been absorbed, and the radiation will have less and less effect.

In the upper regions of the atmosphere, ions and free electrons are produced by ultraviolet radiation, X rays, gamma rays, and cosmic rays. Ionization also may be produced by the impact of high speed particles on the molecules or atoms of the gases. All these causes of ionization appear to be present in the upper atmosphere, but the preponderant ionizing agent is the ultraviolet radiation from the sun. Since this radiation has its maximum effect at the altitude where the e-folding absorption distance is approximately a scale height, and different parts of the ultraviolet spectrum have different mass penetration coefficients, the ionization is a complex function of altitude giving rise to several maxima and minima in the electron

production rates. These regions of ionization are known collectively as the ionosphere and can reflect, scatter, and absorb electromagnetic waves. The ionosphere can have an important role in determining the propagation characteristics of radio and radar signals. Because free electrons have the most pronounced effect on the propagation of electromagnetic waves through an ionized medium, the ionosphere is usually represented by its free electron density as shown in Figure 2-7.

Free electrons and negative ions tend to unite with positive ions and form neutral molecules or atoms. Electrons also may be removed from their free state by attaching themselves to neutral particles forming negative ions. During the daytime, photodetachment frees the excess electrons from negative ions as rapidly as they are formed, however, effectively preventing attachment from being an important removal mechanism. Thus, recombination is the dominant reaction in the lower ionospheric layers during the day and may continue to be a significant factor at some altitudes at night. No completely satisfactory process has yet been established to describe the interacting electron loss mechanisms in the ionosphere (regions above about 60 kilometers). The reaction most likely to occur, however, is a dissociative recombination. This is a process in which an electron recombines with a positive molecular ion and causes it to split into neutral atoms. For example, a molecular nitrogen ion (N_2^+) or oxygen (O_2^+) may recombine with an electron. In the process, the molecule gains enough energy to split it into excited atoms. Thus,

$$N_2^+ + e \rightarrow N + N \qquad (2\text{-}13)$$

$$O_2^+ + e \rightarrow O + O \qquad (2\text{-}14)$$

Under conditions in which the recombination of electrons and positive ions dominate and negative ions can be neglected, such as the D region of the ionosphere, the electron loss rate is expressed as

$$\text{loss rate} = \alpha_e N_e^2 \qquad (2\text{-}15)$$

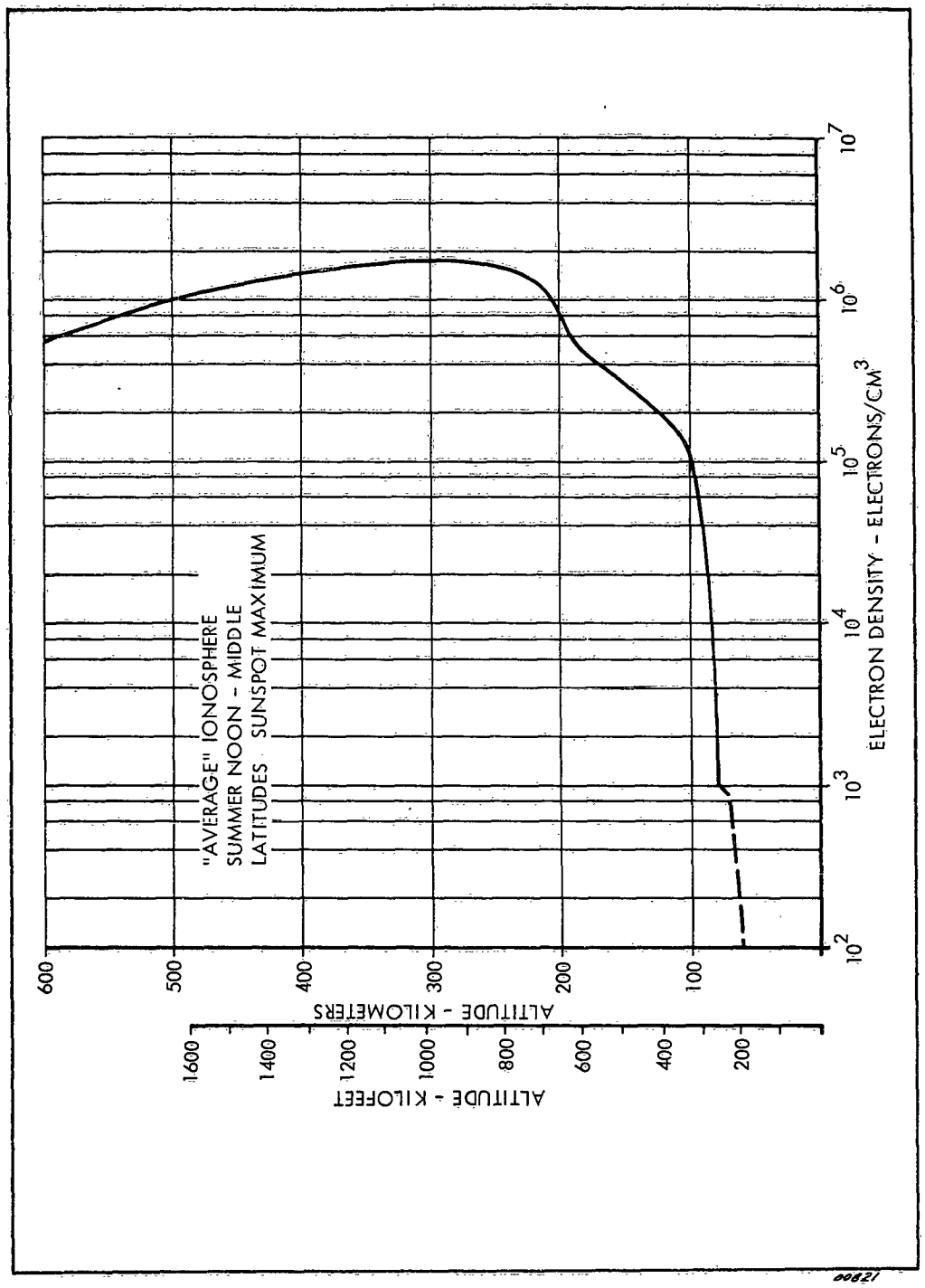

Figure 2-7. The "Average" Ionosphere

where α_e is a recombination coefficient and N_e is the number of electrons/centimeter^3. This equation leads to a relaxation time, or time for the electron density to decrease by 63 percent after removal of the ionizing source, of $1.7\ (\alpha_e\ N_e)^{-1}$.

At F region altitudes where oxygen and nitrogen are largely dissociated, the positive ions are principally atomic oxygen and nitrogen. Direct recombination of electrons with atomic ions is some four to five orders of magnitude slower than dissociative recombination with molecules. More rapid is a charge exchange reaction in which an atomic ion gives its charge to one of the few neutral oxygen molecules present, and the molecular ion later enters a dissociative recombination reaction. For this two-stage process, the electron loss rate is:

$$\text{loss rate} = \text{constant} \times n(O_2) \times N_e \qquad (2\text{-}16)$$

where $n(O_2)$ is the particle density of molecular oxygen per cubic centimeter, and N_e is the electron concentration as previously defined. In this case, the relaxation time is independent of N_e but inversely proportional to $n(O_2)$.

At night and at low altitudes, electron attachment to neutral atoms or molecules becomes an important process. For example, in the troposphere where the atmospheric density is high, the life of a free electron is only a few millionths of a second. This process continues to be important up to the lower portion of the ionosphere.

2.3 NORMAL IONOSPHERE

The free electron density in the ionosphere is determined by the equilibrium conditions between the electron production and loss rates. Both vary with altitude giving rise to stratification or layer formation. Between approximately 60 and 90 kilometers the ionosphere is known as the D region. While the free electron density in this region (approximately 10^3 electrons/centimeter^3 at 80 kilometers) is considerably below that of the upper regions, collisions of electrons with neutral particles can cause considerable absorption at communication frequencies. Because of absorption and the low electron densities, data regarding the D region have been limited, but available evidence indicates that the diurnal variations of the D region and variations with solar activity are similar to those of the E region.

The E region of the ionosphere lies approximately between 100 kilometers and 150 kilometers. During the daytime, the peak electron density is of the order of 10^5 electrons/centimeter^3. At night the layer largely disappears. The E region like the F_1 region can be described in terms of the earth's relative position with respect to the sun so that contours of E-region electron density may be given as a function of local time and latitude. Peak electron densities vary by about 50 percent in the course of the sun spot cycle, being highest in periods of greatest sun spot activity.

The F region is that part of the ionosphere which lies above a height of about 150 kilometers and during the day has two electron density maxima. The F_1 peak density occurs near 160 kilometers shortly after noon and the F_2 peak at about 250 kilometers well after local noon. At night the F_1 layer disappears or merges with the F_2 layer. Peak electron densities of 10^6 electrons/centimeter^3 are recorded for the F_2 region in the daytime while the F_1 layer peaks at about 2.5×10^5 electrons/centimeter^3. The decay of free electrons in the F_1 region has a relaxation time of about 14 minutes. Decay in the F_2 region is slower and is due principally to charge exchange reactions. Substantial electron densities persist through the night.

The behavior of the F_1 region can be related directly to the relation of the earth's movements with respect to the sun. Because of the short relaxation time, the peak electron density at a particular location is reached a few minutes after noon. Plots of F_1 electron density contours can be given as a function of local time and geographic latitude where the local time scale replaces longitude. Variations in maximum electron density with latitude occur from month to month as the sun's subsolar point (latitude where the elevation angle of the sun reaches 90 degrees) moves from northern to southern latitudes or in the opposite direction depending on the season. At the equinox (subsolar point at the geographic equator) there is symmetry in the contours about the equator. For other seasons there is antisymmetry, i.e., the contours for June at a northern latitude corresponding to those for December at the same southern latitude. In addition to the above variations, there are variations with solar activity, the most prominent being an 11-year sun spot cycle.

The simple relationship between the earth's movement relative to the sun and electron density contours does not apply in the F_2 region. Apparently electrodynamic drifts caused by the earth's magnetic field, diffusion, tidal currents, and winds all play a role in modifying the contours. The influence of the magnetic field can be illustrated by noting that if the electron density contours are plotted on a grid of geomagnetic coordinates, the geomagnetic equator can be replaced by a local time scale. However, the usual way of presenting F_2 contours is to divide the earth's surface into three zones and plot the contours against geographic longitude and local time. Within each of the three zones, the magnetic effects are sufficiently alike that no further corrections are made for small variations. The peak electron density at most locations occurs well after noon and declines rather gradually at night. The F_2 region exhibits a larger variation with solar activity than the other ionospheric regions.

2.4 THE ABNORMAL IONOSPHERE

In addition to its regular and generally predictable cyclic variations, the ionosphere is subject to irregular and abnormal fluctuations. During these abnormal periods, ionospheric absorption, critical penetration frequencies, and virtual heights of layers may deviate suddenly and widely from the norm. Ionized clouds with above normal electron densities may intrude into the E layer, giving rise to an inhomogeneous structure which scatters radio waves. These abnormalities may be short-lived, lasting less than a second, or may persist for several days. This sporadic-E layer is one of the more important and persistent anomalies influencing propagation in the ionosphere.

Sporadic-E occurs above the normal E layer and is characterized by regions or clouds having higher electron concentrations than the surrounding medium. At times, the density is sufficient to reflect signals at frequencies of 10 to 15 megacycles and completely mask the higher F layers. Virtual heights vary between 90 and 120 kilometers. The exact nature of the source of sporadic-E is not known (meteor showers, thunderstorms, and ionospheric turbulence have been proposed), and the mechanism may be different for different latitudes. While this phenomenon has some diurnal variation, it does not appear to correlate particularly with the sunspot cycle. In equatorial regions, sporadic-E is weak during daylight hours and varies smoothly with maximum intensity occurring at noon. It appears most frequently in the early morning and evening hours in

temperate and subtropical latitudes, more frequently in summer than in winter, and the effects persist an hour or so after sunset. Its most frequent appearance is in the polar or auroral zones.

A sudden ionospheric disturbance (SID) is characterized by an intense increase in ionization of the lower ionosphere and occurs simultaneously with solar flares. Correspondingly, the frequency of SID's increases and decreases with the 11-year solar cycle. The upper layers of the ionosphere are essentially unaffected. Intense ultraviolet or X ray radiation from the bright eruptions of the sun's chromosphere penetrate deep into the atmosphere, causing increased ionization in the D region over the daylight hemisphere of the earth. This condition may last from a few minutes to several hours and may be sufficiently severe to cause complete loss of radio signals in the short and medium wave length bands. Because of the enhanced ionization in the D region, long wave length radio signals normally reflected by the lower ionosphere, may propagate with increased signal strength.

Ionospheric storms (magnetic storms) are generally characterized by a depression of the F region ionization and an increase in virtual height. These storms are associated with terrestrial magnetic disturbances. The effects are dependent on geomagnetic rather than geographic latitudes and may occur almost simultaneously over the earth. Increased ionization in the D region may accompany the storm and increase absorption. A close statistical relationship between ionospheric storms and sun spots has been established. The effects can last from a few hours to several days. The auroral zones (around the magnetic poles) discussed below may shift to lower latitudes during a magnetic storm.

The regions around the magnetic poles differ markedly from those at low and temperate latitudes. Two explanations are generally offered for the observed phenomena. First, the diurnal and seasonal variation of the radiation from the sun is quite different for these regions than for lower latitudes. Secondly, the incidence of charged solar corpuscles guided into the regions around the poles by the earth's magnetic field produces intense ionization. Abnormal conditions of the ionosphere are almost a normal feature in the auroral zones. The ionization produced by charged particles is located in the lower ionosphere and causes pronounced absorption at nearly all times, day and night.

Meteor trails are a source of abnormal ionization between approximately 80 and 120 kilometers. Meteoric particles intercepted by the earth's atmosphere are heated by collision with air molecules and produce an ionization trail on the order of 25 kilometers in length.

REFERENCES

1. Mitra, S. K. The Upper Atmosphere. (The Asiatic Society Monograph Series, Vol. V), Hafner Publishing Company, New York, 1952.

2. Ionospheric Radio Propagation. (National Bureau of Standards Circular 462.) Washington, D. C., United States Government Printing Office, 1949.

3. Proceedings of the IRE. Vol. 47, No. 2, February 1959, The Institute of Radio Engineers, Inc., New York.

4. Stratton, J. A. Electromagnetic Theory. McGraw-Hill Book Co., Inc., 1941.

CHAPTER 3

PERFORMANCE CRITERIA FOR COMMUNICATION AND RADAR SYSTEMS

CHAPTER 3

PERFORMANCE CRITERIA FOR COMMUNICATION AND RADAR SYSTEMS

3.1 GENERAL

Except for possible direct physical damage to terminal equipments, nuclear explosions will have their important effects on radio communications, navigation aids, radar, etc. by disturbing the medium through which electromagnetic energy must propagate in traveling between transmitters and receivers, and by generating extraneous noise signals. Correspondingly, normal radio and radar performance criteria, that are measures of propagation and noise conditions, are applicable in assessing the effects of nuclear weapons on electromagnetic waves.

For communication circuits, propagation paths may vary in length from a fraction of a kilometer to thousands of kilometers. Over such a variety of distances, radio waves may be affected in different ways by ground and atmospheric conditions. Similarly, radar propagation paths may vary widely even though the transmitting and receiving terminals normally, but not necessarily, employ a common antenna. In general, only a small part of the energy generated by the transmitter will be available in useful form at the receiver.

Energy will be lost in the transmission medium by spreading and absorption, in the couplings between antennas and the medium, and in the terminal equipments. At the receiver, signals must compete with radio noise and interfering signals occupying the same part of the electromagnetic spectrum. This noise may originate in the terminal equipments, in other electrical machinery, or in the propagation medium, and may enter the links at various points and degrade signal qualities. Since power available at the receiver is critical, radio and radar performance criteria are basically measures of transmission losses and noise conditions.

3.2 RECEIVED POWER

Received energy is a function of the transmitted power, transmitter and receiver antenna characteristics, the transmission medium, and distances traversed. With both radio and radar, electrical energy supplied by a transmitter is coupled to the propagation medium by an antenna. If the energy is radiated isotropically (uniformly in all directions) into a lossless medium (free space), the power per unit area at a distance D (large compared to a wave length) from the radiator is:

$$p_a = \frac{p_t}{4 \pi D^2} , \tag{3-1}$$

where p_t is the power actually radiated.

At the receiving terminal, an antenna is used to collect the energy. In general, the effective collecting area (A_e) of an antenna is a function of its dimensions and design, but it may be affected by proximity to the earth and other nearby objects. The power available to a radio receiver (p_r) from a loss-free antenna will be $p_a A_e$. In the free space isotropic radiator case then, the received power will be

$$p_r = \frac{p_t A_e}{4 \pi D^2} . \tag{3-2}$$

With an isotropic receiving antenna, the effective area is $\lambda^2/4\pi$, and the received power will be:

$$p_r = \frac{p_t \lambda^2}{(4 \pi D)^2} , \tag{3-3}$$

where λ is the wavelength in the same units as D. Additional terms enter the radar equation and will be treated in a later section of this chapter.

In actual practice, both transmitting and receiving antennas have directional characteristics. Energy is radiated preferentially in particular directions to increase the power available at the receiver,

and the effective area of receiving antennas will be greater in some directions than in others. The ratio of power available in these preferred directions to that which would have been available from an isotropic antenna is the antenna gain (G). With a directional transmitting antenna equation (3-1) becomes:

$$P_a = \frac{P_t G_t}{4 \pi D^2} \quad . \tag{3-4}$$

3.3 RADIO TRANSMISSION LOSS

The ratio of power actually radiated (p_t) to power received in an equivalent loss-free antenna (p_r), expressed in db, has been defined as the transmission loss (L).[1] That is:

$$L = 10 \log_{10} \frac{p_t}{p_r} = P_t - P_r \quad , \tag{3-5}$$

where $\log_{10}$ is the logarithm to the base 10, and the upper case letters L, P_r, and P_t indicate values expressed in decibels (db). Since the power radiated will always exceed the power received, the transmission loss L will always be a positive number.

3.3.1 Basic Transmission Loss

To separate losses in the propagation medium from the effects of antenna directivities, the transmission loss may be expressed in the form:

$$L = L_b - G_p \tag{3-6}$$

Here L_b, in db, is termed the basic transmission loss and represents the attenuation that would be expected if isotropic antennas replaced those actually being used. G_p is the path antenna gain, in db, and in free space will be equal to the sum of the transmitting and receiving antenna gains ($G_t + G_r$): where both G_t and G_r are expressed in db. In general, G_p will not be appreciably less than the free space value as long as the antenna gains are less than about 40 db.

The basic transmission loss, L_{bf}, for isotropic antennas in free space is:

$$L_{bf} = 32.44 + 20 \log_{10} D_{km} + 20 \log_{10} f_{mc}, \qquad (3\text{-}7)$$

where

D_{km} = path length in kilometers, and

f_{mc} = wave frequency in megacycles.

Curves of basic free space transmission loss, for various frequencies in the useful radio spectrum, are shown in Figure 3-1. As previously noted, the equations expressing power received, apply only so long as the path length is large compared to the signal wavelength.

3.3.2 Ground Wave Loss

When antennas are near the earth's surface and waves have been neither reflected nor scattered by the troposphere or ionosphere, energy propagates as a "ground wave." This wave may be treated as two components — a surface wave and a space wave. At its lower edge, the surface wave actually passes along the earth's surface, and its transmission loss is sensitive to the electrical characteristics of the ground. The space wave is the sum of a direct wave and a ground reflected wave as shown in Figure 3-2. Because the two components of the space wave follow different paths, the two waves may arrive at the receiver with a phase difference and may add constructively or destructively. That is, the sum may be greater or less than either of the components. The phase difference will depend on antenna heights and the distance between them. Thus, for an elevated transmitting antenna, the space wave field intensity (or transmission loss) will vary with elevation angle; contours of equal intensity will have the familiar antenna lobe structure.

The basic transmission losses for vertically polarized waves propagating over a smooth, spherical earth are shown in Figure 3-3. The computations on which these curves were based make use of idealized "average" ground constants (conductivity - σ = 0.005 mhos/meter and dielectric constant - ϵ = 15) and antenna heights of 30 feet (about 9 meters) — see Reference 1. For frequencies below a few megacycles, these are short antennas and energy is transmitted primarily by surface waves. Horizontally polarized surface waves are effectively short-circuited by the earth and are attenuated too rapidly for use in radio communications. Between approximately 10 and 100 megacycles, a transition occurs between surface and space wave modes of propagation. Above 100 megacycles the energy propagates as a space wave, and the transmission loss is relatively unaffected by polarization.

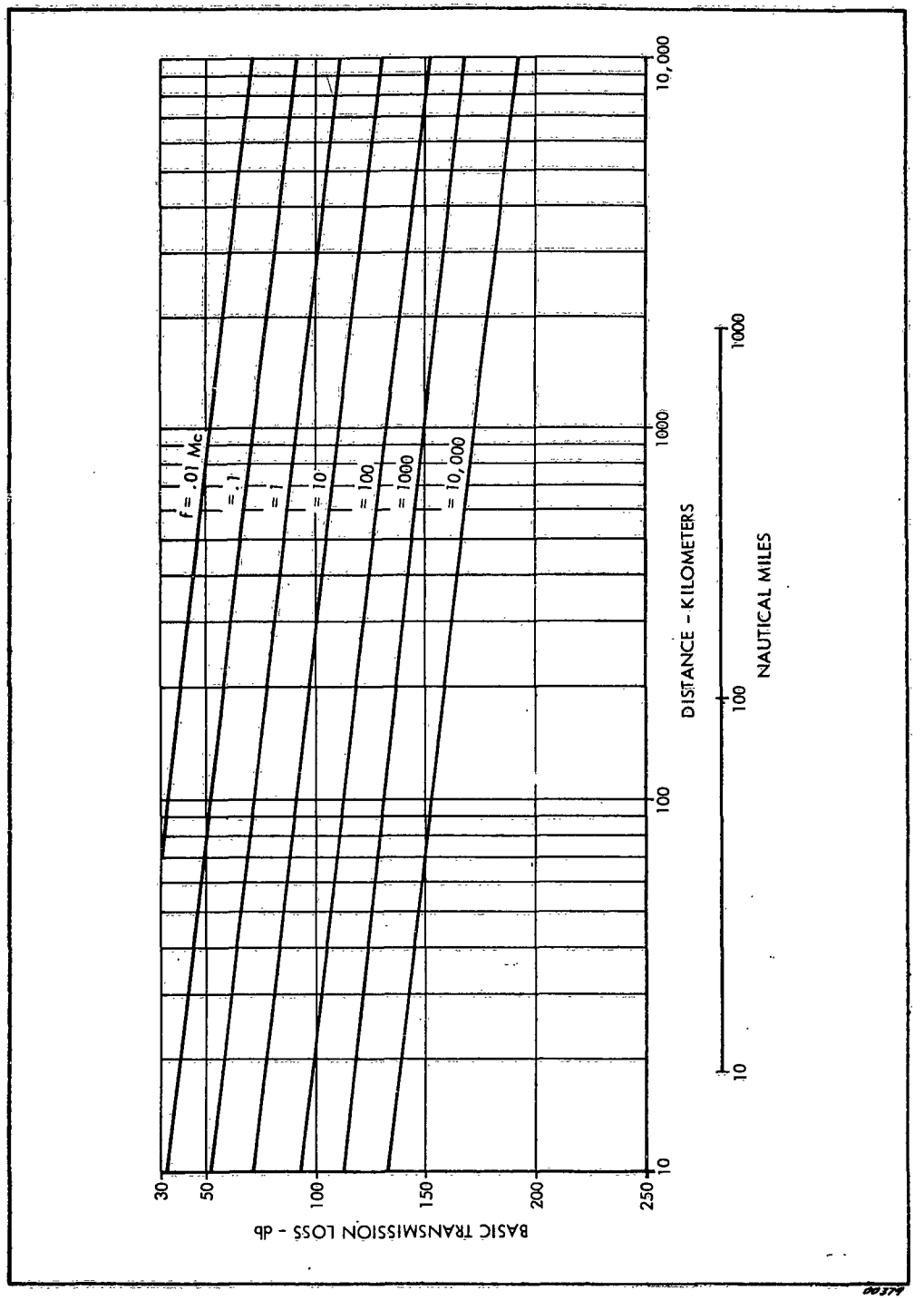

Figure 3-1. Basic Transmission Loss for Isotropic Antennas in Free Space

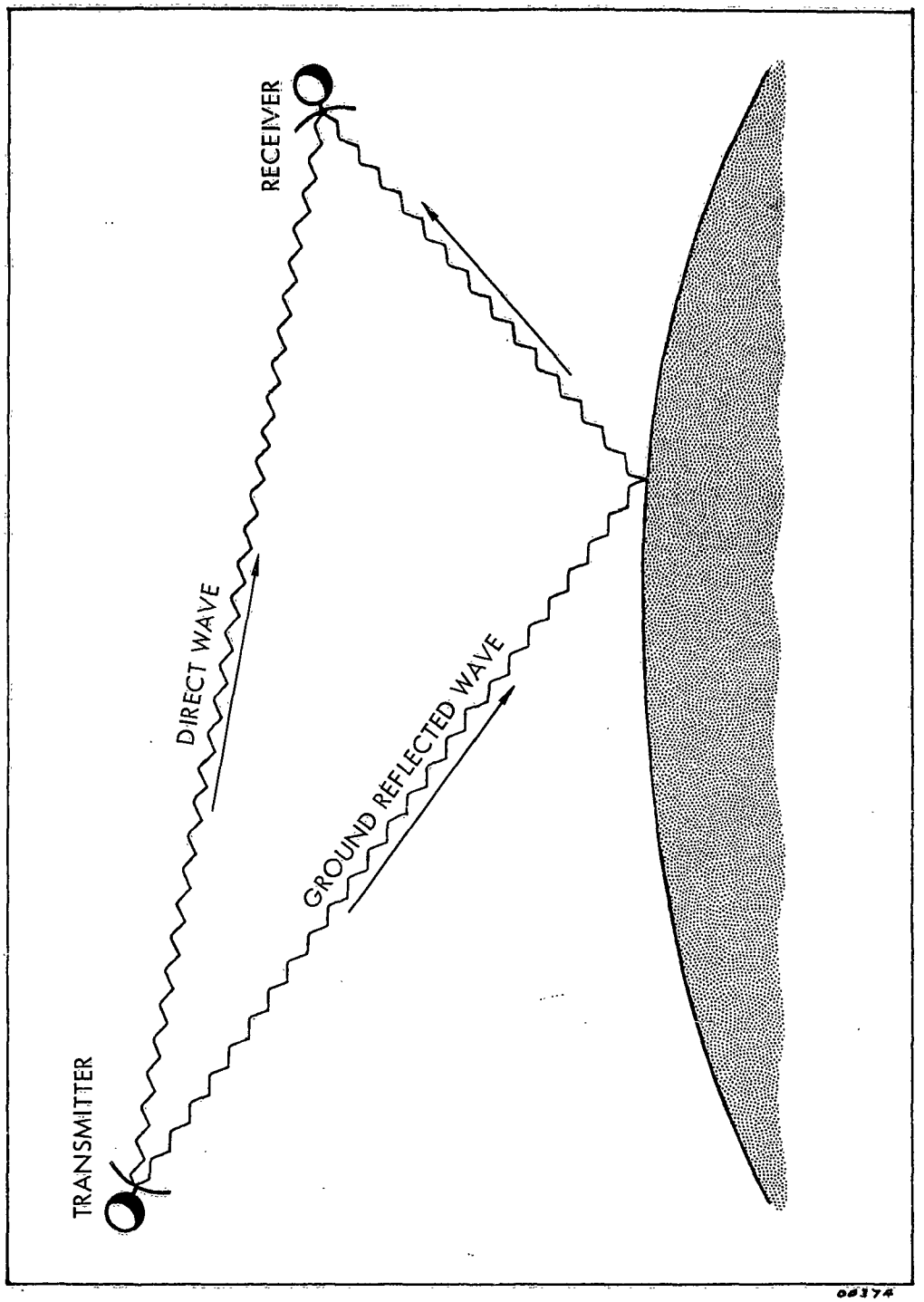

Figure 3-2. Space Wave

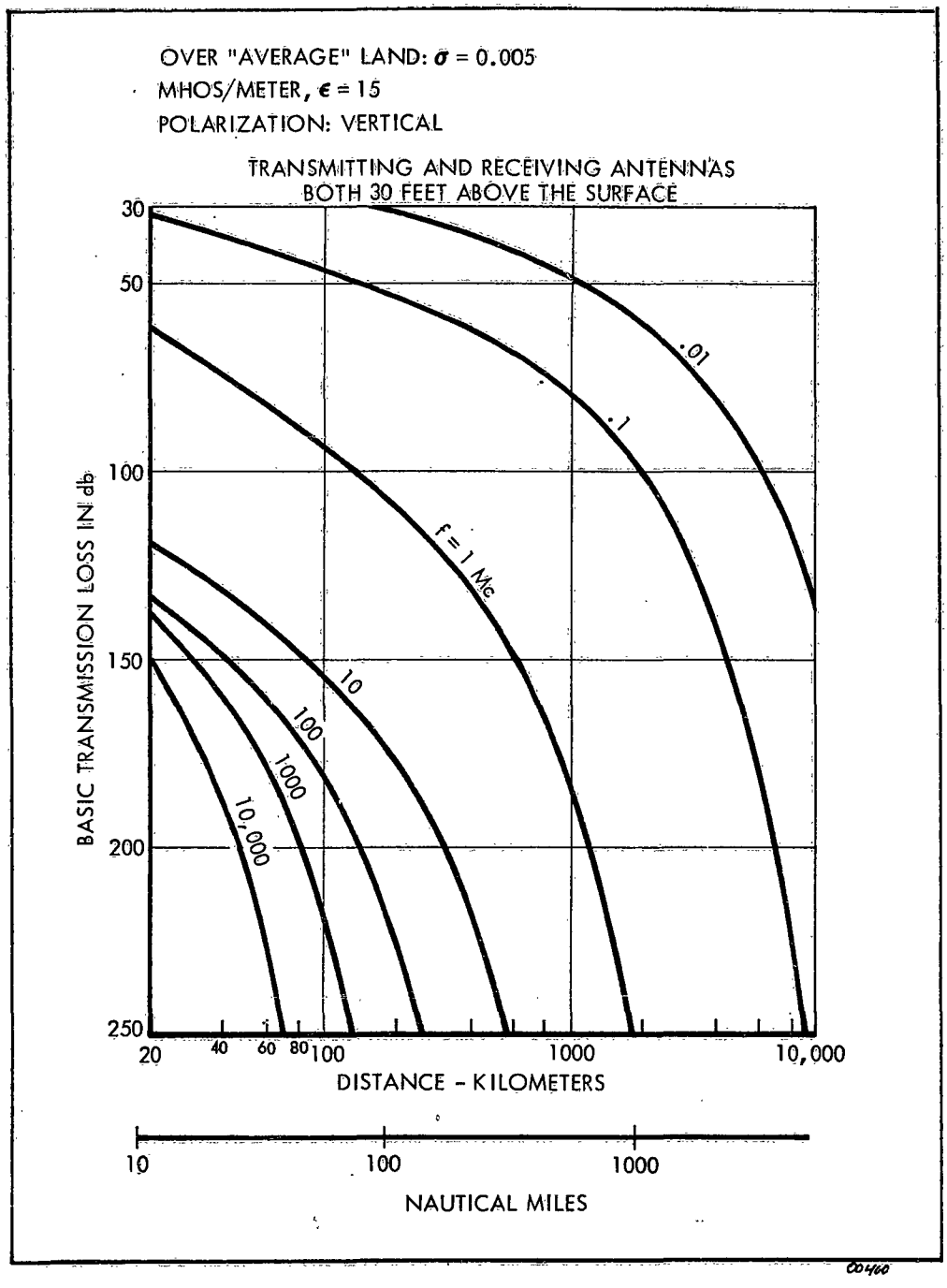

Figure 3-3. Basic Transmission Loss Expected for Ground Waves Propagated over a Smooth Spherical Earth

As frequency increases above about 10,000 megacycles, water vapor and oxygen in the atmosphere cause a marked increase in absorption, making these frequencies useful only for special short-range applications.

Except for frequencies below a few megacycles, ground wave transmissions are limited primarily to line-of-sight paths. The space wave, which carries most of the energy at higher frequencies, propagates in nearly straight lines with its transmission loss increasing approximately as the square of the distance travelled. Beyond the line of sight, losses increase at a much faster rate as the receiving antenna recedes further into the "shadow region."

The line of sight is related to the radio horizon which may be expressed approximately in terms of antenna height (h) as:

$$d \text{ (miles)} = \sqrt{2h \text{ (feet)}} \qquad (3\text{-}8)$$

$$d \text{ (kilometers)} = 2.91 \sqrt{2h \text{ (meters)}} \qquad (3\text{-}9)$$

The maximum line-of-sight transmission path will be the sum of the distances to the transmitting and receiving antenna horizons.

3.3.3 Beyond the Horizon Propagation

Point-to-point communication circuits extending well beyond the radio horizon may employ ground waves at very low frequencies, sky waves that have been reflected by the ionosphere, or energy that has been scattered by inhomogeneities in the troposphere or ionosphere. As discussed in Chapter 2, electromagnetic energy is reflected by the ionosphere when the wave frequency is less than the MUF or critical frequency for oblique incidence. Thus, waves will follow paths as illustrated in Figure 3-4. At frequencies on the order of 10 kilocycles, the lower edge of the ionosphere acts as a sharply defined reflecting surface with an altitude of about 70 kilometers during the day and approximately 90 kilometers at night. For analysis purposes, propagation in this frequency range may be viewed as taking place in a wave guide comprised of two spherical shells — the ionosphere and the earth's surface. The transmission loss varies some with the time of day and earth conductivity, as illustrated in Figure 3-5 which consolidates computed charts contained in Reference 1. These curves apply to transmission between short vertical dipole antennas having gains $G_t = G_r = 1.76$ db. The path antenna gain thus is $G_p = 3.52$ db.

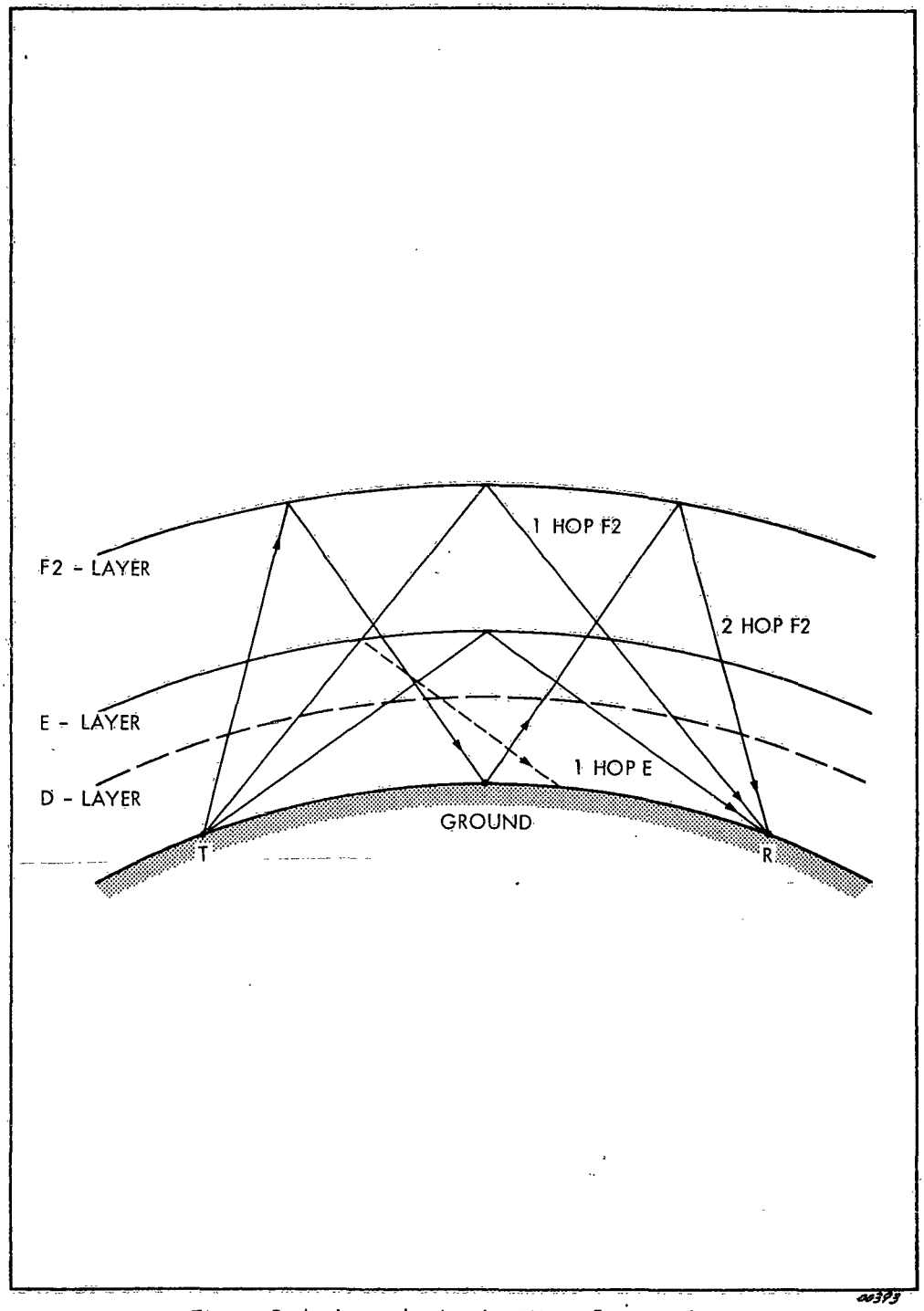

Figure 3-4. Ionospheric Sky-Wave Propagation

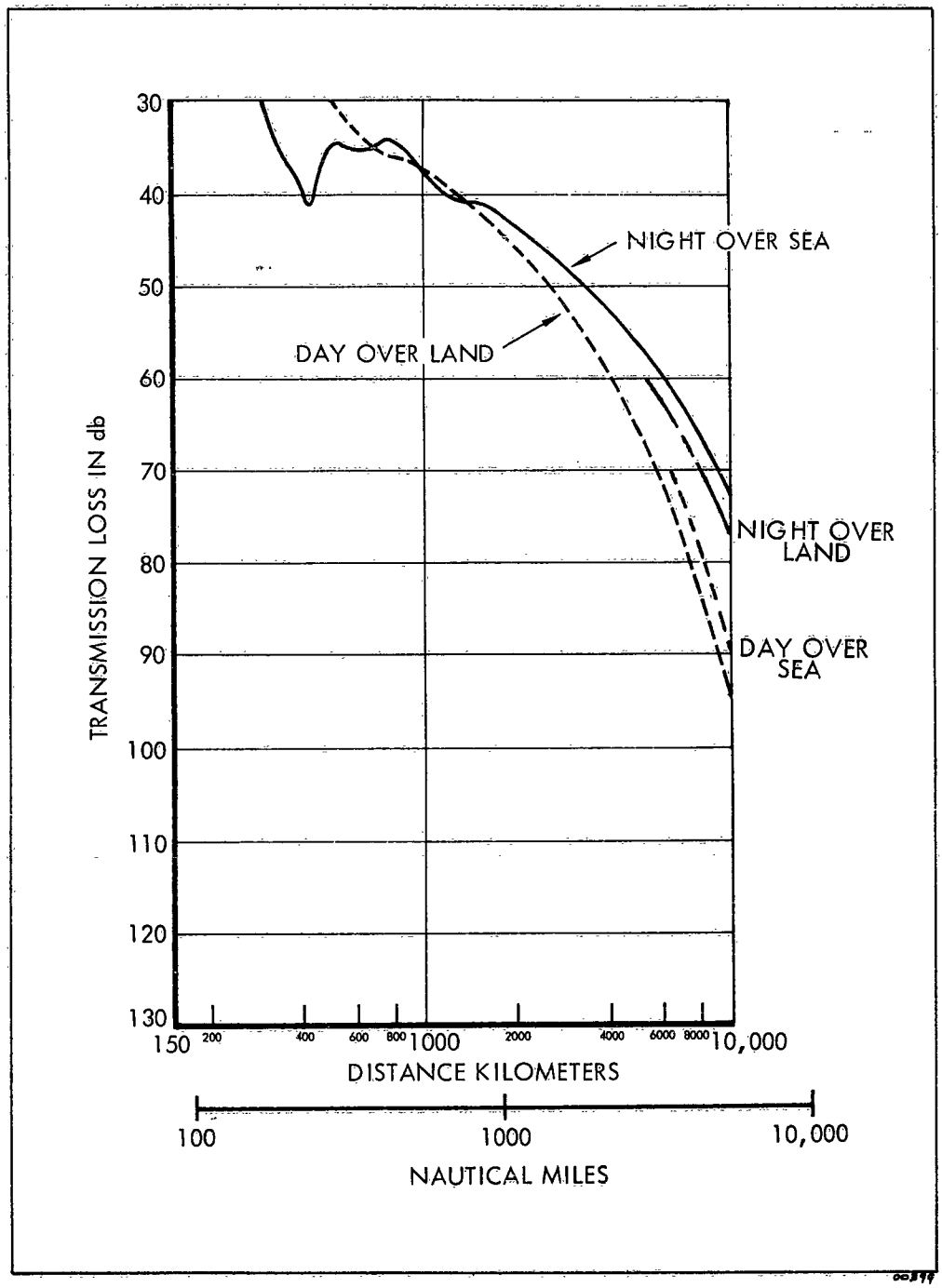

Figure 3.5. Transmission Loss Expected Between Short Vertical Electric Dipole Antennas - f = 10 Kilocycles

As the frequency increases sufficiently to penetrate to the E and F layers, the waves will behave more like the rays illustrated in Figure 3-4 and energy will be transmitted to the receiver via one or more ionospheric reflections. In these modes, the transmission loss will be a combination of the spreading losses, in a manner analogous to the free space propagation, and absorption or fading losses. At night, in the absence of the D layer, the transmission loss will be primarily that due to spreading and that caused by ground reflections in multi-hop modes. During the daytime, however, absorption in the D layer and losses incurred at the ground reflection point for multi-hop modes may range from a few db to a few tens of db. Calculated transmission losses, taken from Reference 1, are shown in Figures 3-6 and 3-7.

The median absorption loss that must be added to the basic transmission losses for daytime propagation by ionospheric reflections of signals above a few megacycles is given in the Reference 2 Signal Corps Technical Report as:

$$L_a = \frac{615.5\, n \sec \phi\, (\cos 0.881\, \psi)^{1.3}\, (1 + 0.0037\, S)}{(f + f_H)^{1.98}}, \quad (3\text{-}10)$$

where

L_a - will be in db,

ϕ - is the angle between the ray path and the vertical at 100 kilometers,

ψ - is the sun zenith angle,

S - is the smoothed Zurich sun spot number (for this purpose, $S_{min} = 10$ and $S_{max} = 150$),

f_H - is the gyrofrequency at 100 kilometers (approximately 1.5 megacycles for the United States), and

f - is the wave frequency.

As can be seen, propagation by ionospheric reflection is dependent upon the sun's zenith angle, the sun spot cycle, and the gyrofrequency. This is an empirically determined relationship and averages a number of other factors that influence behavior of the ionosphere. As at lower frequencies, nighttime losses are primarily those arising from spreading and absorption at ground reflection points. It might

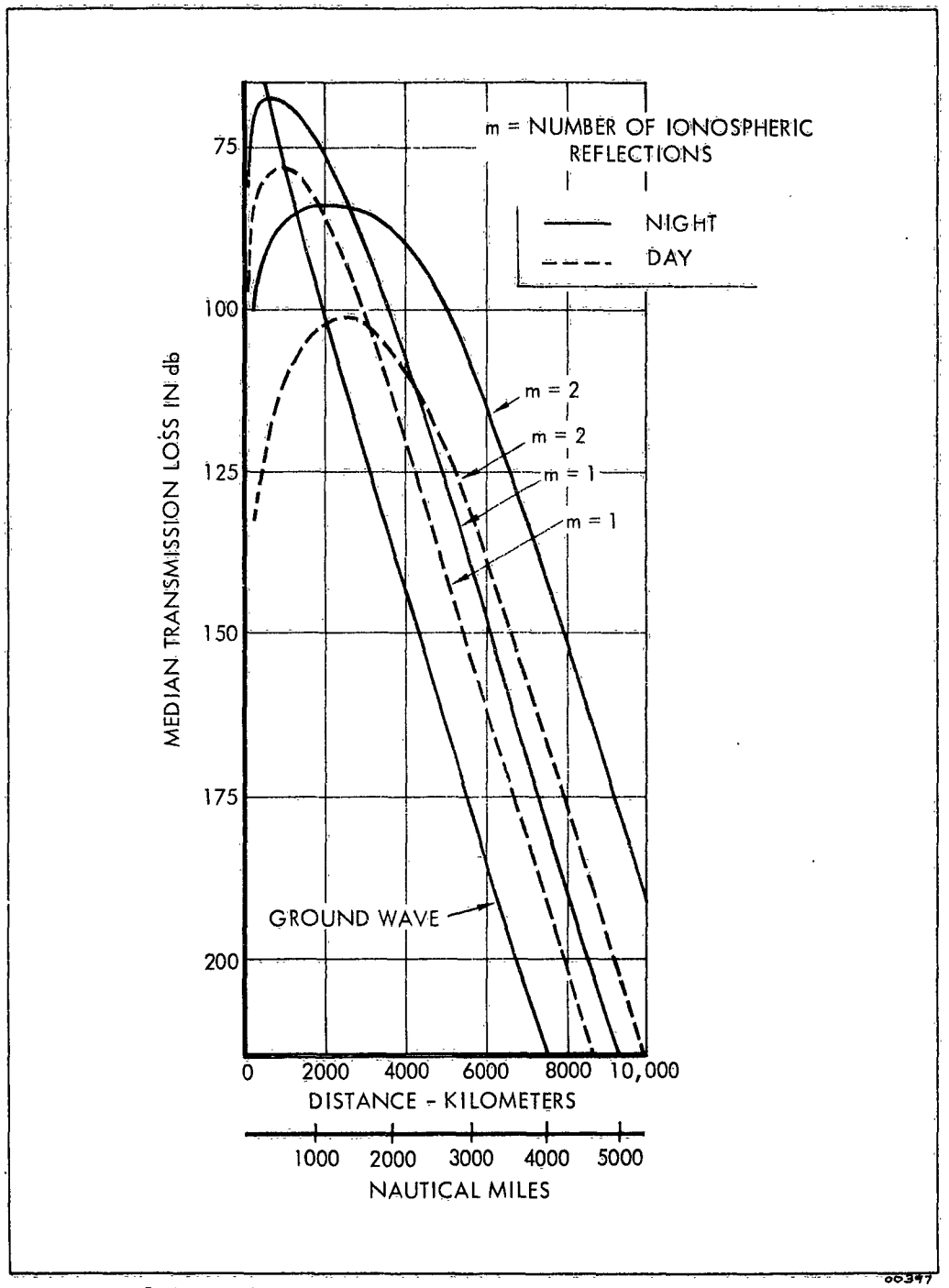

Figure 3-6. Median Transmission Loss over Land at 100 kc Day h = 70 km Night h = 90 km

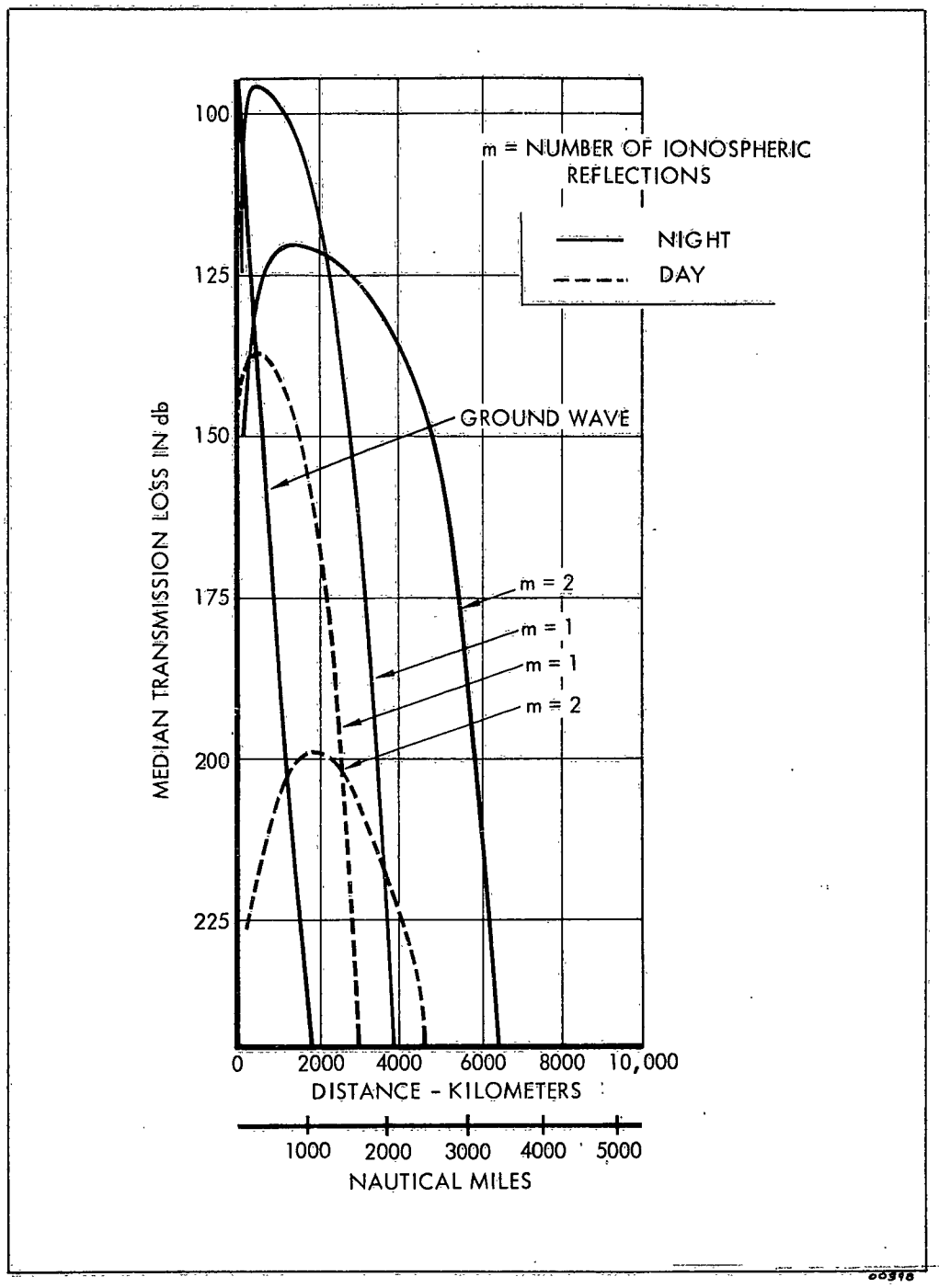

Figure 3-7. Median Transmission Loss Over Land at 1000 kc Day
h = 70 km; Night h = 110 km

also be noted that additional deviative absorption occurs in the E and F layers when the wave frequency is close to the MUF. Because of this deviative absorption, and for other reasons, the optimum traffic frequency (FOT) for a particular communication circuit will normally differ from the MUF. The FOT is the frequency that will permit effective communication 90 percent of the time during undisturbed ionospheric periods, and is usually about 85 percent of the MUF.

Sky wave transmission losses illustrated in the above figures represent median values about which the actual losses will fluctuate. The ionosphere itself varies with time, and received sky waves are not, in general, reflected from a single point. Rather, the downcoming waves are composed of a number of waves that have followed different paths and, hence, may arrive with amplitude and phase differences — absorption and interference fading. Also, waves are split into ordinary and extraordinary waves which may recombine on leaving the ionosphere with a polarization different from that of the receiving antenna — polarization fading. As the electron density varies in the ionosphere (for example, near sunrise or sunset) the MUF may oscillate about the transmission frequency, and the downcoming wave may "skip" beyond the receiver — skip fading.

For reliable communications, the received power must equal or exceed some minimum value. The minimum intensity depends on the information to be transmitted, equipment characteristics, and noise conditions. This required intensity, in turn, establishes along with the communication path length and ionospheric conditions, a lowest required radiated power (lrrp). It also fixes a lowest useful high frequency (luf) for which the received power will be equal to or greater than the minimum required.

At frequencies above the MUF, scatter communication links may still be used for beyond-the-horizon communications. In these cases, energy is scattered from inhomogeneities in the ionosphere — forward propagation ionospheric scatter (FPIS); or in the troposphere — forward propagation tropospheric scatter (FPTS). Median transmission losses for these propagation modes are illustrated in Figure 3-8. As can be seen, the FPIS losses are relatively insensitive to distance, but are dependent on frequency. By contrast, the FPTS mode losses are relatively independent of frequency and do vary significantly with distance.

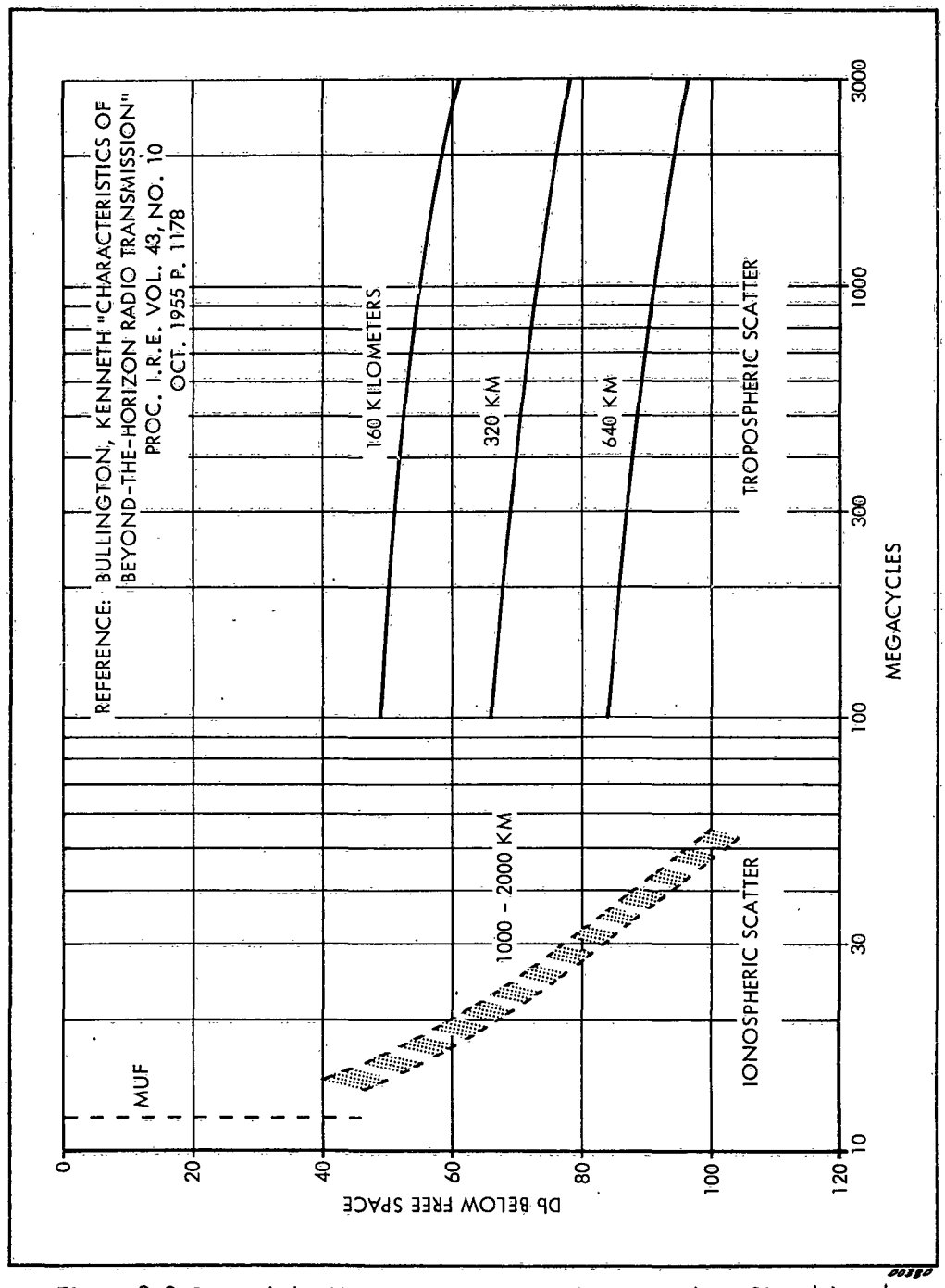

Figure 3-8. Beyond the Horizon Transmission Loss - Medium Signal Level Versus Frequency

3.3.4 Radio Frequency Bands

The radio spectrum is divided into decade bands extending in frequency from a few kilocycles to several megacycles as summarized in Table 3.1.

3.3.4.1 THE VERY LOW FREQUENCY (VLF) band is used for long distance communications and for maritime and aerial navigation systems. The Navy, for example, uses VLF radio to communicate with forces spread throughout the world. Both ground wave and sky wave propagation modes are important in this frequency band. Ground wave attenuation is relatively low, and the sky wave is reflected at the lower edge of the ionosphere with little absorption. Thus, transmission losses are relatively unaffected by ionospheric heights or disturbances. Variations in the height of the ionosphere will cause phase changes which may be important in navigation applications and in synchronous communications circuits.

3.3.4.2 THE LOW FREQUENCY (LF) band and the next higher band are used by the Navy as part of its fleet broadcast system, and is used by the Army for medium and long range tactical communications. During the daytime, the sky wave is heavily abosrbed in the D layer making the sky wave unusable. Normal applications rely on the ground wave which, with reasonable transmitter powers, permits communications over distances of several hundred kilometers.

3.3.4.3 THE MEDIUM FREQUENCY (MF) band, in addition to the applications and propagation characteristics noted in the previous paragraph, is used for commercial broadcast radio. Daytime coverage is provided by the ground wave. At night, the sky wave will extend the useful service area, but may also cause interference between stations transmitting on the same frequency.

3.3.4.4 THE HIGH FREQUENCY (HF) band is used extensively commercially and by the military services for long range communications. These applications rely on the sky wave and service is correspondingly sensitive to ionospheric conditions. One to three ionospheric reflections may be involved in typical circuits with 800 kilometers to 8000 kilometers separations between transmitting and receiving stations. Energy losses at the ground and ionosphere reflection points generally prevent service requiring more than three hops.

TABLE 3.1

Radio Frequency Bands

Band	Frequency Range	Wavelength Range	Illustrative Uses
Very Low Frequency (VLF)	3-30 kc	100-10 km	Long distance communications with ground wave and sky wave.
Low Frequency (LF)	30-300 kc	10-1 km	Medium and long range tactical communications primarily using ground wave.
Medium Frequency (MF)	300-3000 kc	1000-100 m	Commercial broadcast using the ground wave: at night sky wave extends coverage and causes interference between stations.
High Frequency (HF)	3-30 Mc	100-10 m	Long range military and commercial communications employing sky wave ionospheric reflections.
Very High Frequency (VHF)	30-300 Mc	10-1 m	Line-of-sight communications and radar. Forward propagation ionospheric scatter (FPIS) links and forward propagation tropospheric scatter (FPTS) links.
Ultra High Frequency (UHF)	300-3000 Mc	100-10 cm	Line-of-sight communications and radar. FPTS links.
Super High Frequency (SHF)	3-30 kmc	10-1 cm	Precision line-of-sight radars.

3.3.4.5 THE VERY HIGH FREQUENCY (VHF) band and the ULTRA HIGH FREQUENCY (UHF) band ground waves are rapidly attenuated, and sky waves are seldom returned from the ionosphere (in the usual reflection sense). Thus, primary applications have been line-of-sight communication and radar services. However, the lower portion of these bands (30-50 megacycles) is finding increasing usage in beyond-the-horizon radio employing forward propagation ionospheric scatter (FPIS) links. These links operate at ranges from about 1000 to 2000 kilometers. Scattering occurs in the lower E layer (75 to 90 kilometers) and normal transmission losses exceed the free space values for corresponding distances by 40 to 100 db. The VHF band also is being used for meteor scatter links. In this case, scattering occurs at altitudes of about 100 kilometers, and losses may be over 10 db less than in the FPIS mode. The upper portion of the VHF band and the UHF band are finding increasing application in forward propagation tropospheric scatter circuits operating over distances on the order of 200 to 600 kilometers. Here too, transmission losses are from about 50 to 100 db more than the free space values for comparable distances.

3.3.4.6 THE SUPER HIGH FREQUENCY band is principally used by the military for high precision line-of-sight tracking radars.

3.4 THE RADAR EQUATION

Radar systems employ electromagnetic waves to detect, track, and identify objects. Part of the transmitted energy is reflected or scattered by the radar target and a small portion of this energy returns to the receiver. From the direction of arrival of the signal and its round trip travel time, target location and movement can be determined. As in the case of radio communications, radar performance depends on the amount of energy received, which is given by the radar equation:

$$p_r = p_t \frac{G A_e \sigma S}{(4\pi)^2 R^4} \qquad (3\text{-}11)$$

where

p_t = transmitted power,

p_r = received power,

G = gain of transmitting antenna,

A_e = effective area of receiving antenna,

σ = radar cross-section of target,

R = range to target, and

S = an absorption loss factor.

As can be seen, the radar equation differs from the radio form by the inclusion of terms representing two-way transmission and a target reflecting area. A term included here is the absorption factor which is usually omitted in the standard literature — its importance will be treated in subsequent chapters. Both sides of the equation could be divided by the transmitted power putting the expression in a form equivalent to the radio transmission loss. More frequently, however, maximum range is a more meaningful parameter for radar purposes, giving rise to the radar range equation:

$$R_{max} = \left(\frac{p_t G A_e \sigma S}{p_{min} (4\pi)^2} \right)^{1/4} \qquad (3\text{-}12)$$

In this equation, p_{min} represents the minimum received power that permits a specified level of radar performance. It will depend on the specific design of equipments and the type of service (that is, detection, tracking, etc.). More extensive treatments of these factors are available in the reference literature and cannot be reproduced here. In brief, however, the minimum power term must include consideration of such items as signal-to-noise ratio, detection probability, false-alarm rate, and tracking errors.

Radar performance considerations not included in the radar equations are the effects of variations or anomalies in the refractive index along the transmission path. As might be expected, where primary outputs are direction and distance, such variations may cause more serious degradation to radar than to radio. Under some circumstances, transitory variations in the refractive index or those confined to small regions may be especially serious. Such cases arise in missile guidance and in other applications involving predictions of future positions.

REFERENCES

1. Norton, Kenneth A. Transmission Loss in Radio Propagation: II, (NBS Report 5092, U.S. Department of Commerce) Boulder, Colorado: National Bureau of Standards, Boulder Laboratories, 25 July 1957.

2. Laitinen, P.O. and Haydon, G.W. Analysis and Prediction of Sky-Wave Field Intensities in the High Frequency Band, (Technical Report No. 9, Third Printing) Fort Monmouth, New Jersey: Signal Corps Radio Propagation Agency, March 1956.

3. Norton, Kenneth A. Transmission loss in radio propagation. Proc. of the IRE, Vol. 41, January 1953, pp. 146-152.

4. Kelley, L.C. and Silva, A.A. Revised Radio Noise Data, (Project 700) Fort Monmouth, New Jersey: Signal Corps Radio Propagation Agency, March 1960.

5. Basic Radio Propagation Predictions, Central Radio Propagation Laboratory Series D, National Bureau of Standards.

6. Ridenour, L.N. Radar System Engineering, MIT Radiation Lab. Series, Vol. 1, New York, N.Y.: McGraw-Hill Book Co., Inc., 1947.

7. Marcum, J.I. and Swerling, P. Studies of target detection by pulsed radar, IRE Transactions on Information Theory, Vol. IT6, No. 2, April 1960.

CHAPTER 4

QUALITATIVE DESCRIPTION OF NUCLEAR EXPLOSIONS

CHAPTER 4

QUALITATIVE DESCRIPTION OF NUCLEAR EXPLOSIONS

4.1 WEAPON OUTPUTS - PRIMARY

The energy output of a nuclear explosion is expressed in terms of the equivalent energy output of such conventional explosives as TNT. When exploded, a ton of TNT releases approximately 4×10^{16} ergs so a megaton yield corresponds to the release of 4×10^{22} ergs. Most of the energy is generated during the final few generations of nuclear fission and fusion, occupying a time of about 10^{-8} seconds. This energy first appears as high energy motion of the fission fragments (atoms and neutrons) and nuclear emissions such as gamma ray photons. By collisions and other interactions the energy quickly is distributed among all the particles present, plus radiant energy photons. Tremendous temperatures and pressures are created.

In the absence of any surrounding air (such as a burst in free space), the energy will leave the original weapon volume by various mechanisms: X rays, gamma rays, neutrons, and as the kinetic energy of the particles that constituted the weapon and its associated structures. These are all "immediate" forms of energy release, generated during the final few shakes (10^{-8} seconds), although the transport of this energy from the weapon volume may take a longer time. Some additional energy is generated at later times that is properly included in the effective total yield of the weapon. This includes the energy released by radioactive decay of the various fission-product atoms and the decay of neutrons. Most such radioactive decay events are accompanied by the radiation of beta rays (high velocity electrons) and gamma rays (photons).

The partition of the energy among these various forms depends on the weapon configuration used, such factors as the ratio of fission yield to fusion yield, the efficiency, the yield, and the total mass of structure surrounding the weapon. At high altitudes, far the greatest part of the energy released by a typical weapon, about three-quarters, leaves the weapon volume as thermal or X ray radiation. About

one-quarter of the energy escapes as kinetic energy of particles. Something less than ten percent is nuclear radiation emitted by the fission products as "debris radiation."

The location of the fission debris determines where the debris radiation effects will be observed. However, this location or distribution of the debris in space is determined by the interaction with the environment of the large immediate release of energy and will differ markedly for low-altitude and high-altitude nuclear explosions. Following sections of this chapter discuss major factors determining debris location for different burst altitudes.

The processes of fission product decay consist of the spontaneous radioactive decay of the many different nuclides (the nucleus of a particular isotope of a particular element) which result from nuclear fission. These atomic nuclides range in the periodic table from krypton to the rare earth elements. Each decay reaction is characterized by a half-life, a time within which half of the atoms of that species will have undergone the reaction. After twice this half-life, there will be only one-fourth of the original atoms of this species left; after three times, there will be one-eighth, i. e., the decay is exponential. Each original atomic species decays to another nuclide which may also be radioactive, and so on, in a chain of decay reactions that averages three steps before a stable nuclide is reached. As the half-lives of these reactions vary from fractions of a microsecond to millions of years, it is not possible to represent the net radioactivity by a single half-life. Over a very wide range of times from seconds to days or years, the time variation of the radioactivity is closely approximated by $t^{-1.2}$, or it varies slightly faster than inversely with time. This cannot be true down to zero time or the radioactivity would be infinite. A selected approximation for small times is given in Cahpter 5 (Figure 5-1).

Similar to the half-life concept is the half-distance concept. Absorption of various kinds of photon radiation was discussed in Chapter 2 as a function of the mass penetration coefficient. This is easily usable for radiant energy of one wavelength, but is not an accurate concept for broad spectrum radiation or for charged particle radiation such as beta rays and high speed debris particles.

However, for each particle type or wavelength of radiation at a given air density there is a distance at which the radiation intensity is cut in half. For a single wavelength of radiant energy, the radiation

intensity will be reduced to one-quarter in twice this distance and to one-eighth in three times this distance. This extrapolation is frequently not true for broad spectrum radiation and particle radiation.

Some perspective is given in Table 4-1 which shows in the first column the half distance for the major radiation components at sea level. In the second column, the half distances at 100 kilometers altitude are shown. The third column indicates the altitude at which the half distance for each type of radiation is 100 kilometers. This aids appreciation of the detonation altitude at which each radiation type may cause significant and extensive effects.

There are three cautions in the use of these numbers. Since constant air density is inherent in the concept of a half distance at a specified altitude, these half distances are principally applicable along constant altitude, horizontal paths. Where the half distance is only a small fraction of a scale height, it may be used for upward or downward paths with only minor error. Charged particles, such as beta rays, are constrained to move along magnetic field lines so the half distance applies only when the magnetic field and beta ray path are horizontal. As indicated, extrapolation from half distance to a quarter or an eighth the radiation intensity is limited to narrow band photon radiation.

TABLE 4.1

Typical Half Distance of Particles and Radiations

Weapon Output	Half Distance: Sea Level	Half Distance: 100 km Altitude	Altitude at Which 100 km is Half Distance
Gammas	120 m	400,000 km	50 km
Neutrons	120 m	400,000 km	50 km
Betas	3 m	10,000 km	75 km
X rays	3 cm	100 km	100 km
Ultraviolet	.16 cm	5 km	125 km
Debris Particles	.03 cm	1 km	140 km

4.2 LOW ALTITUDE

A detailed description of the physical phenomena and damage criteria of low-altitude bursts (below about 15 kilometers) is given in documents such as "The Effects of Nuclear Weapons"[1] and classified reports. In this section a brief summary of the major effects are given.

The intense heat and pressure following a nuclear burst causes the products of the explosion, in the form of hot gases, to move rapidly outward producing a blast or shock wave. Of the 85 percent of the bomb energy which is in the form of heat energy roughly two-thirds contributes to the blast wave.[1] The remaining one-third radiates as thermal energy primarily in the visible and infrared range.

For a one megaton detonation the fireball region of intensely hot and luminous gases will have reached its maximum diameter of several kilometers within a few seconds. By about 10 seconds the gases are no longer luminous, but because of their intense heat rise at a rapid rate like a hot air balloon. As the gases rise and expand they cool. The bottom of the cloud following a megaton detonation will rise to about 20 kilometers within approximately 10 minutes. The top of the cloud may reach 30 or 40 kilometers depending on the burst energy.

The initial nuclear radiations, i. e., gamma rays and neutrons, emitted within the first minute or so following an explosion represent about 5 percent of the bomb energy, and may cause personnel injury several kilometers from ground zero. Gamma rays and beta rays will continue to be radiated from the rising cloud.

The ionization of the atomsphere produced by the gamma rays, neutrons, and thermal radiation is essentially all contained within a few hundred meters of the fireball. Outside of the fireball the free electrons attach themselves almost immediately to neutral oxygen molecules. Within the fireball the elevated temperature may change the electron loss rates sufficiently to maintain the ionization for a few seconds. Very little data is available concerning the electron loss rates in the fireball region. Measurements of electromagnetic propagation through the fireball region while near ground level indicate that there are essentially no effects due to high electron densities.

As the fireball rises, the debris radiation bombards the surrounding atmosphere causing ionization in the immediate vicinity of the rising

cloud. Because the electrons are rapidly attached to neutral particles, the density of free electrons remains quite low and no appreciable effect on electromagnetic signals will occur. For large yield bursts, where the fission debris cloud will rise to heights of about 30 kilometers, the upgoing gamma radiation may reach D-region altitudes with sufficient intensity to cause abnormally high electron concentrations above the cloud, and attenuation of electromagnetic waves.

Land or water or subsurface bursts may introduce into the atmosphere large quantities of impurities. These particles of dust, debris, water droplets, or ice crystals in the atomic cloud act as reflectors for electromagnetic signals. Although most of the particles are quite small (one millimeter or less in diameter) there are sufficient numbers present in the early stages after the explosion to produce echoes on X- or K-band radars. This condition may last for minutes or hours, depending on the bomb yield, types of particles picked up in the burst, and the rate at which the atomic cloud spreads in the atmosphere. Because of the small size of the particles, electromagnetic radiation of the longer wave lengths associated with lower frequency radar or with radio communication systems, will not be affected.

4.3 HIGH-ALTITUDE BURSTS

As the altitude at which a burst occurs is raised, all of the radiation types in Table 4-1 can penetrate further and further before being stopped by interaction with the air. As a result, ionization capable of affecting radio propagation can be produced at greater distances. Also, the debris becomes more widespread, so radiation from it will produce continuing ionization at greater distances.

4.3.1 The Fireball

The tremendous release of energy of a burst, principally in the form of X rays and kinetic energy, very rapidly heats a volume of air surrounding the bomb debris. The initial X-ray penetration heats air to such high temperatures that softer X rays and ultraviolet radiation are given off, which are in turn absorbed by the next surrounding shell of air. This "degrading" of the thermal energy toward less energetic forms continues until the radiation is in the visible part of the spectrum. Since air is relatively transparent to the visible and to the near IR and near UV parts of the spectrum, a fair portion of the energy can then escape to great distances as the thermal radiation.

When the "fireball" or entire mass of incandescent air and debris has cooled by radiation to the point where it is no longer a very bright object, it still differs markedly from normal air. At such later times, this mass will be called the "disturbed region" in studying its subsequent history. At the time when its brightness decreases rapidly it may have a temperature of up to 10,000 degrees centigrade. It has a pressure corresponding to this temperature by the laws of gas dynamics. It is almost completely dissociated into atomic oxygen and nitrogen instead of the molecular forms of these gases. Except on the outer fringes, almost every atom is ionized into an electron and a positive ion.

The great pressure within the fireball causes it to expand. In doing so, it does work against the atmosphere. This interaction produces a high velocity shock wave. Continued expansion of the fireball (or disturbed region) makes it less dense than the surrounding air. This buoyancy makes the disturbed region rise, just as a hot air balloon would: until it has risen to an altitude where its density matches the ambient atmosphere. While fireballs from ground bursts may rise to 20 to 40 kilometers, the disturbed region of a high-altitude burst may, by buoyancy, be raised above its initial altitude by considerably more than this.

When the altitude of burst gets so high that the initial penetration of thermal energy, before expansion, is over a kilometer, the sudden heating gives the whole fireball a sudden upward impetus. Both the pressures and the associated pressure gradients of the atmosphere are increased by orders of magnitude above their normal value. These pressure gradients accelerate upward all parts of the fireball except the very bottom. The upward acceleration continues until inward travelling waves from the surface of the fireball have released the vertical pressure gradients. The larger the initial fireball, the longer does the upward acceleration last, and the higher is the upward velocity of the disturbed region after release of the pressure gradients. This boost to the disturbed region can cause it to rise far above the level to which buoyancy alone would take it.

Like a projectile, the expanding disturbed region boosted above the buoyancy level will be acted upon by gravity. It will rise ballistically, coast to a stop, then begin to fall again. All during this rise and fall it is expanding against the surrounding atmosphere which is more rarefied than at lower altitudes. The expansion

laterally may thus be more rapid and more extensive than would be possible for a disturbed region raised by buoyancy alone. The region settles back to a new equilibrium altitude determined by the density to which it has expanded.

The initial thermal radiation distributes its energy over a mass of air many times that of the debris. In general, the debris represents a small central volume within the fireball that rises and expands similarly but remains a distinguishable region far smaller than the fireball. Nuclear test explosions TEAK and ORANGE in August 1958 showed that both the ionospheric disturbances associated with the disturbed region and the absorption of radio waves associated with the expansion of the debris, extended outward for thousands of kilometers. However, the disturbed region expanded five to ten times faster than the debris.

As the altitude of burst is raised above 100 kilometers, the X-ray produced disturbed region may exceed 100 kilometers in radius within microseconds after the burst. The debris particles may be contained within a hundredth of this radius. In addition to the expansion and rise produced by pressure gradients, the earth's magnetic field begins to have an appreciable effect on the expansion of the disturbed region. Ionized air is a good conductor of electricity, and moving ionized air carries the magnetic field with it. That is, the motion of electrons and ions produces a current that distorts the magnetic field. The outward radial expansion of charged particles in the disturbed region bends the field lines outward to exclude them from the center of the region.

This restraint can produce magnetic braking action which, for burst altitudes above 200 kilometers, may be the principal force acting to limit the expansion of the fireball. At very great altitudes, on the order of 1000 kilometers, when the air surrounding the burst is truly negligible, the debris expansion expels the magnetic field from an even larger pocket. Bending the magnetic field lines increases the energy stored in the magnetic field, eventually absorbing most of the expansion energy of the debris and halting the expansion. Like stretched rubber bands pressing in on the expanded disturbed region, the magnetic field will then tend to make the region reverse itself and contract. The details of this magnetic containment beyond this point are not known, as instabilities may cause the volume to break up into turbulent eddies, allowing the magnetic field to return to nearly its original position.

For regions between 100 kilometers where magnetic braking action begins to enter and 1000 kilometers where magnetic containment is the principal control on the fireball, the study of fireball and debris motion is extremely complex. The X-ray energy produces ionization and thermal motion of the air surrounding the burst. The debris starts in a much smaller volume and its kinetic energy soon becomes principally the radial motion of expansion. Although the air is tenuous, all the charged particles resulting from X-ray ionization are coupled to the debris expansion by the outward motion of the magnetic field, so are swept up by the expanding shock wave surrounding the debris. It is likely that a part of the debris, expanding downwards from the burst height, is eventually slowed and stopped by the denser atmosphere and comes to rest in a fairly thin widespread layer. Exact mechanisms involved, altitude and extent of the debris, are very poorly known at this time.

4.3.2 Ionization by Immediate Radiation

High energy radiation, such as X rays and neutrons, may cause significant ionization of the various regions of the ionosphere if the half distance for these radiations is appreciable at the burst altitude, for example, for neutrons when the burst is above 50 kilometers and for X rays when the burst is above 100 kilometers. In each case the lateral half distance is 100 kilometers. For bursts at 30 kilometers or even lower, enough neutrons can penetrate upward through the atmosphere to reach altitudes of 40 to 60 kilometers and cause D-region ionization which produces absorption.

When the burst is in or above the D region, the neutrons radiate as from a point source and are virtually unhampered by interaction with the atmosphere until they reach altitudes below 60 kilometers. The radiation intensity will decrease inversely as the square of the distance from the burst, but may remain large until limited by the curvature of the earth as shown in Figure 4-1. That is, the earth's curvature prevents straight line radiation from reaching the D region at point A without first traversing a layer of denser air at lower altitudes. Before reaching the ionosphere again, however, the neutrons are absorbed.

The large portion of the bomb yield that is contained in the X-ray radiation means that some effects will be observed far beyond the fireball as defined in the preceding section. Instead of complete ionization, fractional ionization which still involves large electron

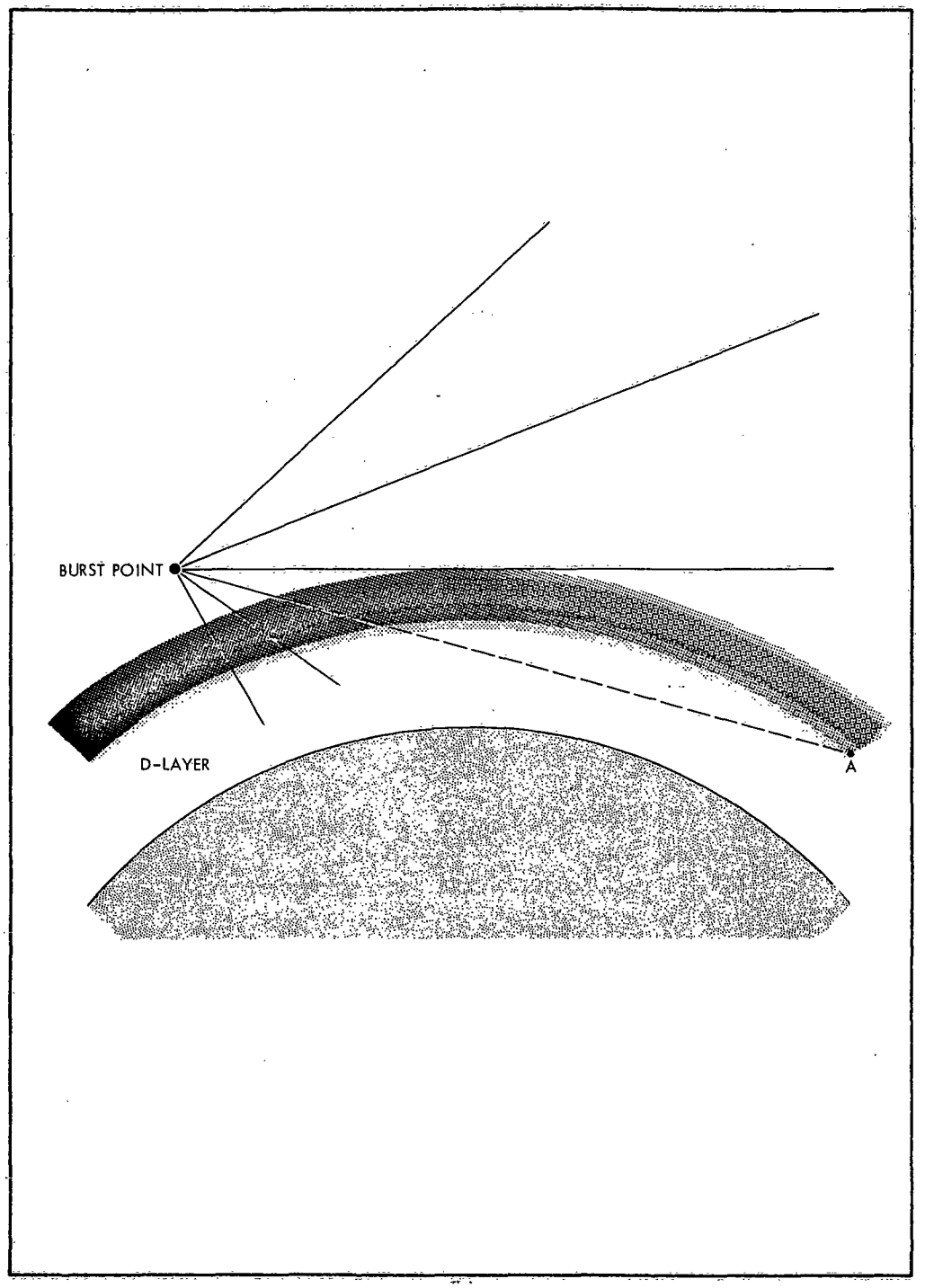

Figure 4-1. Effect of Earth Curvature on Neutron Range

densities can be produced over large areas in the D region by a burst in or above the D region. The transient ionization produced may create significant absorption for short periods. X radiation, being principally emitted within a few microseconds, can also be treated as radiating from a point source.

4.3.3 Ionization by Debris Radiation

Although the beta and gamma radiation from fission debris constitutes only a small portion of the total bomb yield, it may be the most significant cause of degradation to communication or radar systems. The continuing nature of the radiation makes it possible to maintain significant D-region electron densities for considerably longer than the transient ionization from the immediate radiation. The penetration characteristics of these two, particularly beta radiation, cause the major part of the ionization produced to be at altitudes that can produce significant absorption of radio waves. The expansion of the fireball distributes the debris relatively uniformaly over a large area so extensive effects to whole networks or systems can be caused.

When the debris cloud is still small, the debris gamma rays for a burst in or above the D region can be treated as radiation from a point source producing extensive effects varying inversely with the square of the distance from the burst until limited by the earth's curvature. When the debris cloud is very widespread, is uniform, and above the D layer by a height small compared to the debris cloud size, the gamma radiation may be treated as coming from an infinite-plane source. In such case, the radiation intensity that falls on the top of the D region, say 80 kilometers, is uniform and is the sum of contributions from all parts of the debris cloud, out to infinity. The greatest contribution arises, however, from that part of the cloud that is nearly overhead. The magnitude of the radiation intensity will depend on the fission yield of the weapon, rather than the total yield. It will also depend on the area over which the debris is spread, so can be said to be a function of the yield per unit area. As fission product radioactivity decreases with time, the intensity is also a function of the time after the burst.

Beta particles differ from gamma rays in one important respect. Being charged (electrons) they are affected by the earth's magnetic field and tend to move along the field lines in helical or spiral paths as indicated in Figure 2-4. Thus, the beta radiation moves along a tube defined by the magnetic field and will impinge an area in the

D region having the same magnetic field lines as their emission point in the debris cloud. As a consequence, the D region ionization, resulting from beta particles, will be offset from the debris cloud by an amount depending on the magnetic field dip angle. The radiation intensity is also defined by the yield per unit area and the time after burst, but no assumptions are necessary that the debris cloud is an infinite plane.

Roughly half the beta rays start with an upward component of velocity and half start with a downward component. The latter move down into the D region (when the debris is above the D region) in almost straight lines if the initial velocity is along the magnetic field lines and in tight spirals like a screw thread if the velocity along the field lines is small compared to the total velocity. The tightly spiralling beta particle travels a longer path to reach each altitude. On the average, it loses its energy by collisions at a higher altitude. Beta rays start with all possible angles, or tightnesses of spiral, and distribute their energy over a range of altitudes from 90 down to 50 kilometers The average lifetime of secondary electrons produced in this range is long enough to make this radiation effective in causing radio blackout.

Considering the earth as a giant magnet, all lines originating in the southern hemisphere terminate in the northern hemisphere as shown in Figure 4-2. Since the North geographic pole (Latitude 90 N) and the North magnetic pole (Latitude 78 N, Longitude 70 W) are displaced, the magnetic field lines are symmetrical about a tilted plane called the magnetic equator which does not coincide with the geographic equator. The concepts of magnetic latitude and longitude are defined from this plane and the two magnetic poles. From a map on which magnetic longitude and latitude lines are superimposed, points which have the same latitude, except that one is north and one south of the magnetic equator, and have the same longitude are called conjugate to each other. One of these points is spoken of as the magnetic conjugate of the other. The half of the beta radiation, which starts upward, continues to spiral along the magnetic field lines until it reaches the magnetic conjugate point. There most of it penetrates to D-region altitudes and causes ionization and radio blackout conditions similar to those at the burst location.

As may be seen in Figure 4-2, the field lines are more widely spaced at their maximum altitude over the magnetic equator, and converge near both terminals on the earth's surface. An electron follows a true helix of constant pitch angle, as in a screw thread,

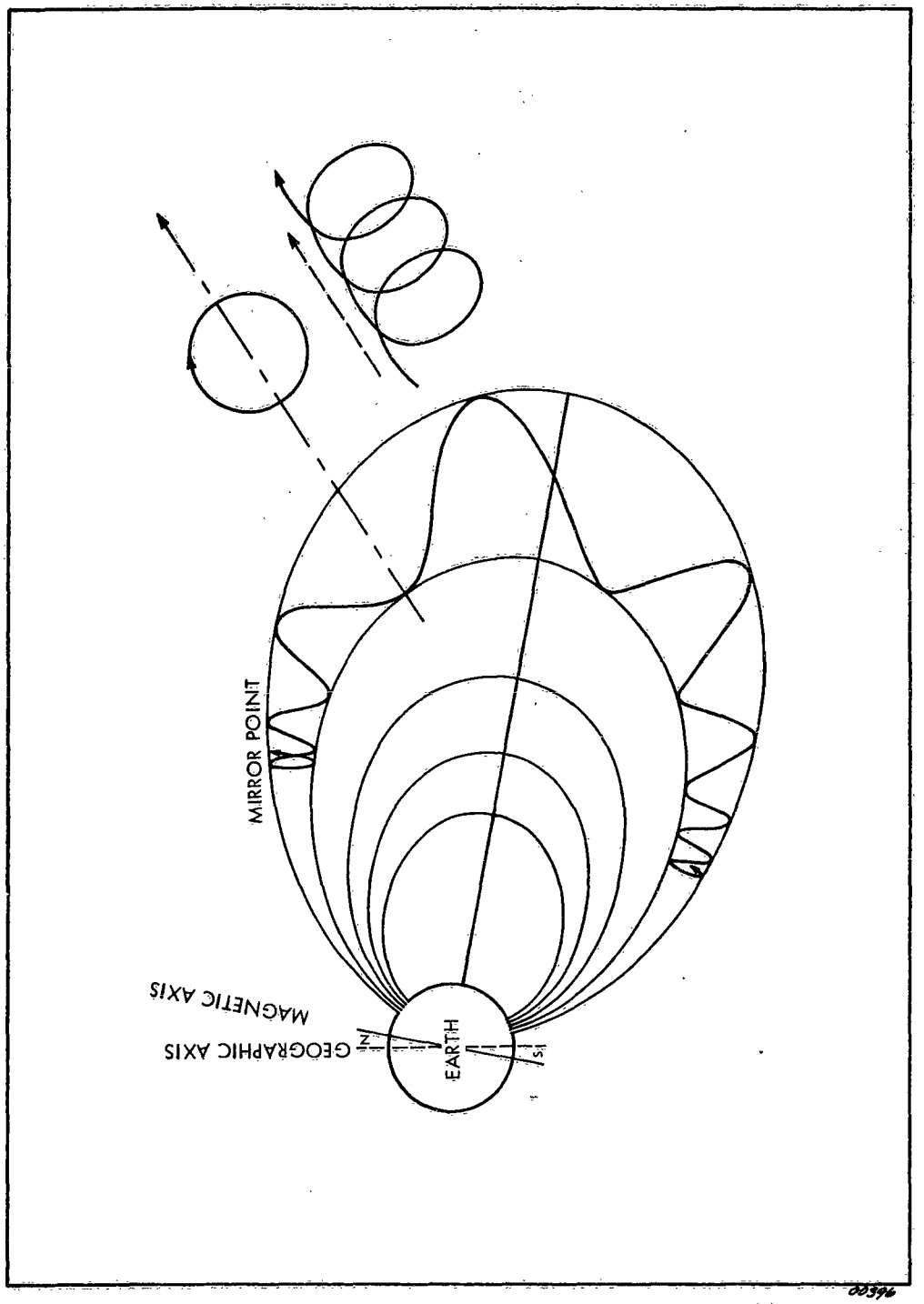

Figure 4-2. Trapped Beta Rays in Geomagnetic Field

only if the field is uniform. Where the field lines converge the pitch angle gets less, or the spiral gets flatter and flatter. For a spiralling electron, a point may be reached where the magnetic field is strong enough so that the spiral becomes completely flat, and the electron can go no further along the field line but rather starts to spiral back up the magnetic field line. This point is called the mirror point. Its altitude for any electron depends on the altitude at which the electron originated and the pitch of the spiral path when it originated. The flatter the spiral when the electron originates the higher will be the mirror point.

When the mirror point is in the D region or below, collisions absorb the electron's energy, and reflection to the conjugate point does not occur. When the debris from which the beta particles originate gets higher and higher above a hundred kilometers, a larger and larger fraction of the electrons are reflected from mirror points above the D region. These can bounce repeatedly between two mirror points, one near the burst, the other at the conjugate point, i.e., can be trapped in the magnetic field, with small chance of collision with air.

Trapped electrons obviously do not produce D-layer ionization until such time as the occasional collisions with air particles lower its mirror points to the denser atmosphere. While trapped, such beta rays, like the trapped electrons of the natural Van Allen belts, can constitute a radiation hazard to missile and space flights. They can also radiate electromagnetic noise (called synchrotron radiation) over a wide frequency spectrum because they are moving at nearly the speed of light over a tightly curved path with radius of 1 to 100 meters. The ARGUS test detonations of August and September 1958 demonstrated that a long-lived belt of trapped electrons could be artificially created.

In connection with ARGUS, one additional phenomenon must be described. As indicated in Figure 4-2, the magnetic field strength decreases with altitude above the earth. Looking along a magnetic field line, an electron will not describe the perfect circle it would in a uniform field. Instead the path curvature is greater on the lower side and less on the upper side. As shown, the net result of this is a sideways motion or eastward drift in longitude. In the many turns of the spiral for each passage between mirror points, the drift can be appreciable. Each passage between mirror points takes only about 0.1 second, and the resulting drift can soon carry the electron path around the world. Typicall, a trapped electron

path can drift around the world in from a half hour to several hours. Soon then a tube of trapped electrons from the burst to its conjugate points will be spread into a belt around the world, with all mirror points at the same magnetic latitude, north and south, that they had in the original tube.

4.3.4 Other Effects

The fireball (or disturbed region) and debris expansion from a high-altitude nuclear detonation continue for a long time. One of the results of this may be extensive modification of the normal ionosphere. The unclassified literature concerning TEAK and ORANGE, two explosions of the HARDTACK series held in August 1958 at Johnston Island (about 1300 kilometers southwest of Hawaii), reports or suggests the following phenomena.

Extensive F-region disturbances were recorded at stations throughout the Pacific, including Johnston Island, Palmyra, Midway, Oahu, Fanning, Jarvis, Apia, Rarotonga, and New Zealand. Reference 9 indicates that one characteristic was a supersonic wave travelling in the F region which in the vertical ionosonde records at each station showed a sudden increase in the electron density as the wave passed over the station, followed by a drop in electron density to values far below the normal nighttime F-region values. This drop in F-region electron density was prolonged; it must lower the MUF and affect adversely high frequency communication links using the F region in the depleted area.

Some disturbances to VLF systems were noted at very great distances from the bursts (continental United States). These consisted of sudden changes in the time of transmission from transmitter to receiver, evidenced by the sudden phase shifts in the received signal. The path of the VLF waves was well shielded by the curvature of the earth from line-of-sight effects from X rays, gamma or beta rays. One theory to explain the results is that some of the immediate neutrons travelled in straight lines to point far above the earth's surface. Neutrons decay radioactively into protons and electrons, with a half-life for the decay of 13 minutes. The charged particles resulting from the decay must spiral along magnetic field lines to the denser part of the atmosphere, where they may produce enough effects in the lower D region of the ionosphere to explain the noted VLF phenomena.

Visible aurora was noted following TEAK and ORANGE both near the burst and near the conjugate point. Beta radiation is believed to be the cause of this.

REFERENCES

1. Glasstone, Samuel, (ed). The Effects of Nuclear Weapons, Washington, D. C.: U. S. Gov't Printing Office, 1957.

2. Cullington, A. L. A man-made or artificial aurora, Nature 182, 1365-6, 1958.

3. Matsushita, S. On artificial geometric and ionospheric storms associated with high-altitude explosions, J. Geophys Research 64, 1149-1161, 1959.

4. Maeda, H. Geomagnetic disturbances due to nuclear explosions, J. Geophys Research 64, 863-4, 1959.

5. McNish, A. G. Geomagnetic effects of nuclear explosions, J. Geophys Research 64, 2253-2265, 1959.

6. Malville, J. M. Artificial auroras resulting from the 1958 Johnston Island nuclear explosions, J. Geophys Research 64, 2267-2270, 1959.

7. Welch, J. A., Jr. and Whitaker, W. A. Theory of geomagnetically trapped electrons from an artificial source, J. Geophys Research 64, 909-922, 1959.

8. Newman, P. and Peterson, A. Optical electromagnetic, and satellite observations of high-altitude nuclear detonations, J. Geophys Research 64, 923-938, 1959.

9. Cummack, C. H. and King, G. A. M. Disturbance in the ionospheric F region following the Johnston Island nuclear explosion, New Zealand Jour. of Geology and Geophys. 2, 634-41, 1959.

CHAPTER 5

PROPAGATION EFFECTS OF HIGH ALTITUDE NUCLEAR EXPLOSIONS

CHAPTER 5

PROPAGATION EFFECTS OF HIGH ALTITUDE NUCLEAR EXPLOSIONS

5.1 ABSORPTION

The preceding chapter describes how the radiation from high-altitude nuclear explosions leads to the production of free-electron concentrations in the ionosphere. As discussed in Chapter 2, electron loss processes, such as recombination of the electrons with positive ions and attachment of the electrons to molecules to form negative ions, act to reduce the number of free electrons. The net density of free electrons present at each time and place results from these opposing processes.

Electromagnetic waves passing through an ionized region may be refracted and absorbed. This section treats absorption which is caused by electron collisions. Determining the path attenuation due to absorption of electromagnetic waves requires consideration of the electron production rate, electron loss rates, the resulting net electron density, the collision frequency, the absorption coefficient resulting from these, and finally the integrated absorption along the path of the electromagnetic wave.

The radiation from nuclear fission debris, beta and gamma rays, produces free electrons by interaction or collisions with air molecules. Typically, a single 1 Mev gamma or beta ray will produce over 30,000 ion pairs (an electron and a positive ion). The amount of ionization produced in each small volume of air depends on the air density, intensity of the incident radiation, and the absorption characteristics of air for that kind of radiation.

A convenient approach is to consider that the fission debris is distributed in a layer somewhat above the ionosphere. Beta radiation, confined to travel along the magnetic field lines will impinge on the top of the ionosphere with a radiation intensity proportional to the amount of fission debris per unit area.

For example, the radiation intensity, I_β, due to debris beta rays is defined as the radiation energy released per unit area per second from the fission debris. For uniformly distributed debris:

$$I_\beta = \frac{W K_f K_\beta F(t) C}{A} \text{ watts/meter}^2, \qquad (5\text{-}1)$$

where

W = weapon yield,

K_f = fraction of weapon yield in fission,

K_β = fraction of fission energy released as beta radiation,

$F(t)$ = fraction of the total debris radiation energy being released per second,

A = debris area, and

C = dimensions constant = 4×10^{15} if W is in megatons and A is in square meters.

The factor W/A depends of course on the weapon yield and on the size of the area over which the fission debris has been dispersed. This area is a function of time, the yield, and the altitude of burst as discussed in Chapter 8. K_f and K_β are given functions of the particular weapon used. $F(t)$ expresses the variation with time of the beta (and gamma) debris radiation.

Empirically, fission decay follows the time variation $t^{-1.2}$ fairly accurately from minutes to days after an explosion (see Chapter 4). For a particular example described in the unclassified literature,[1] the early time behavior is given by Figure 5-1. The constituents of a particular weapon and the surrounding structure might alter this figure moderately but would not change the significant points that the $t^{-1.2}$ law is followed after the first minute, and that for times under a few seconds the radiation rate is more nearly constant. Curve B on Figure 5-1 indicates the integral of Curve A, or the cumulative fraction of the energy released prior to the time indicated.

For gamma radiation, which is not confined by the magnetic field, the radiation intensity, I_γ, can also be given in terms of fission

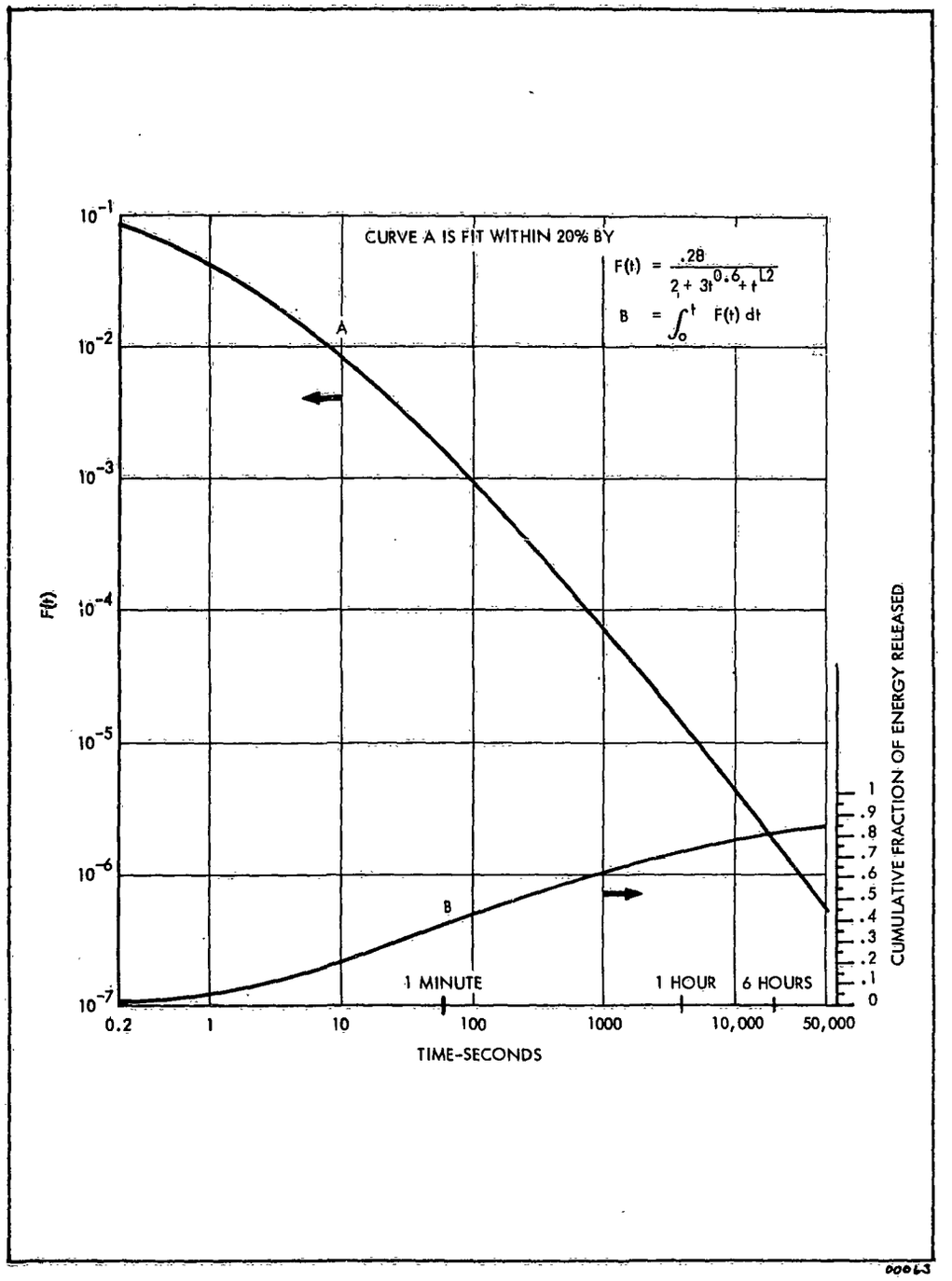

Figure 5-1. Fraction of Debris Energy Released as a Function of Time

yield per unit area if the debris is assumed to be uniformly spread over an infinite area. Where the radius of the debris area is large compared to the altitude separation between the debris and the altitude at which ionization is produced, use of yield per unit area serves as a good approximation.

The maximum production of electrons by gamma and beta rays will occur in the D region of the ionosphere. A typical example for one level of beta and of gamma radiation intensity is shown in Figure 5-2. Since gamma radiation is the more penetrating, it produces a maximum number of ion pairs at about 30 kilometers in altitude. The less penetrating beta radiation produces maximum ionization at approximately 70 kilometers.

The electron-loss processes vary with altitude. In the denser part of the atmosphere, the very large number of neutral molecules present makes attachment of electrons to form negative ions an important process. Its importance decreases with altitude, so the lifetime of an electron before it is lost increases with altitude. As a result, the ionization produced by gamma radiation is less effective than that from beta radiation because it disappears more quickly. Thus, subsequent ionization curves need treat only the debris beta radiation. Figure 5-3 shows the equilibrium electron densities vs. altitude for the beta radiation intensity of Figure 5-2.

During the daytime, solar radiation brings another process into the picture. Negative ions are easily split by photons of sunlight into free electrons and neutral molecules, so the equilibrium will shift toward a higher ratio of electrons to negative ions. The visible and infrared parts of the solar sprectrum responsible for this photodetachment are not strongly absorbed by the atmosphere so that the process has a constant effect as long as the sun is shining on the D region of the ionosphere, and is not dependent on the solar zenith angle. In Figure 5-3, the curve labelled Day applies from about 20 minutes before ground level sunrise to 20 minutes past sunset. The Night curve applies during the dark hours.

The data of Figure 5-3 is based on the interaction of a large number of factors including the relative importance with altitude of the attachment of electrons to neutral molecules and to positive ions, the photodetachment of electrons from negative ions, and the change in electron-ion recombination rate as the atmosphere becomes

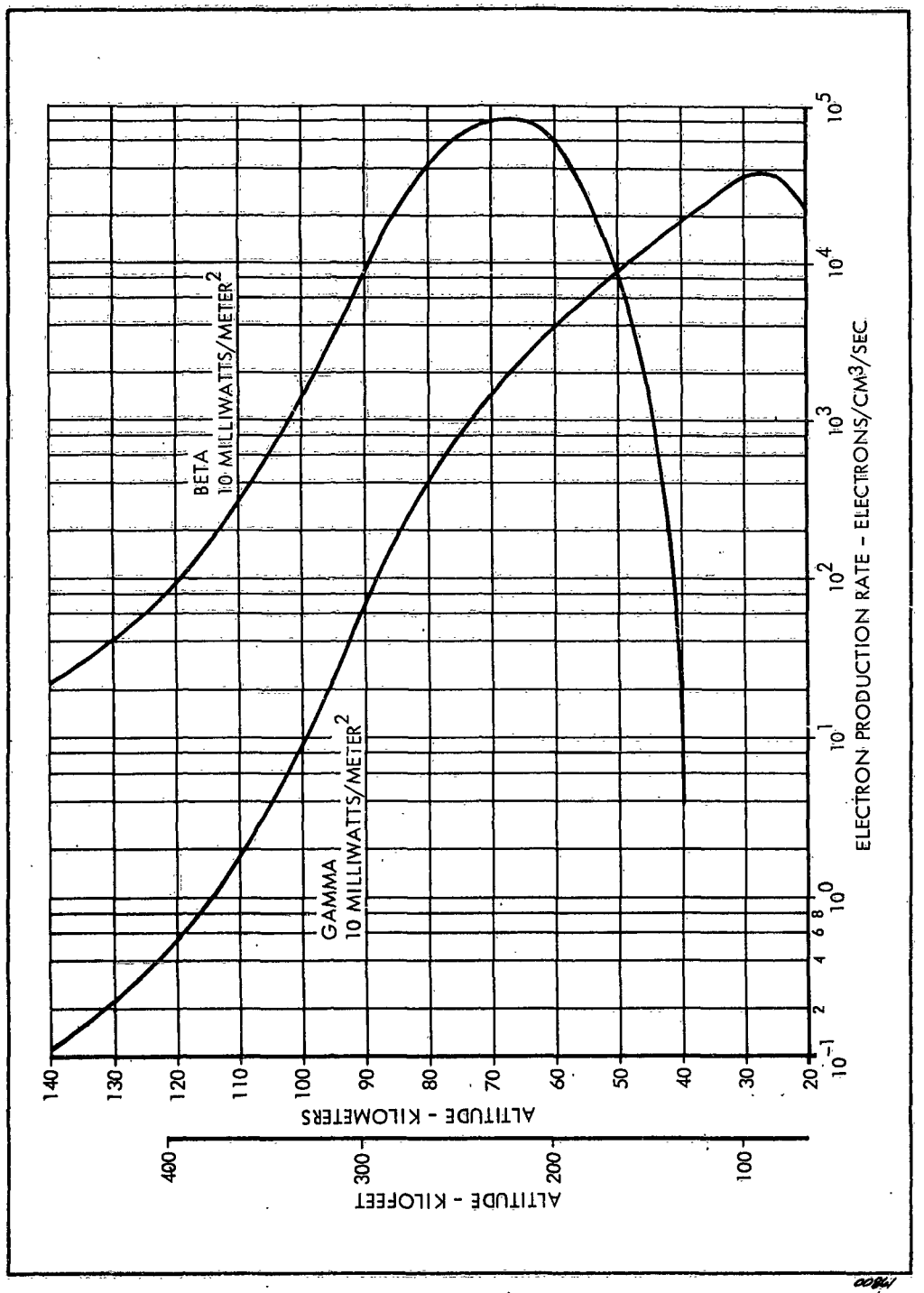

Figure 5-2. Debris Radiation Production Rate Functions

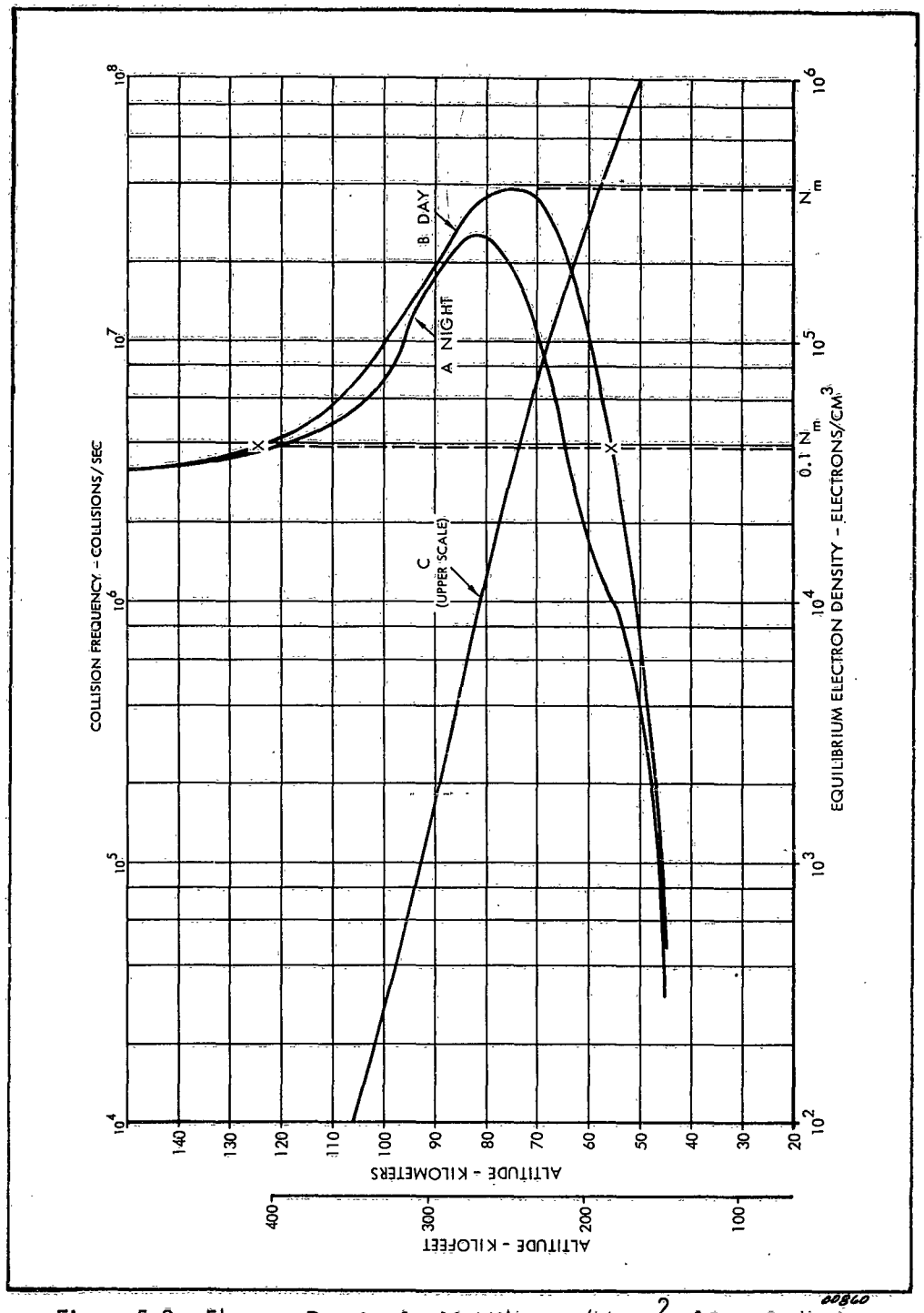

Figure 5-3. Electron Density for 10 Milliwatts/Meter^2 of Beta Radiation

increasingly dissociated above 100 kilometers. The electron densities are a function of the radiation intensity. Depending on radiation intensities and altitudes, the functional relationship varies between one involving $I^{1/2}$ and one involving I.

The electron density present changes the index of refraction and the conductivity of space for electromagnetic radiation. Exact expressions are very complex, involving the components of earth's magnetic field as well as electron density, collision frequency, and wave frequency.[2] However, if the wave frequency is large compared to the gyrofrequency (which is about 1.5 megacycles), or if the collision frequency is large compared to the gyrofrequency (below about 80 kilometers), the magnetic field can be neglected:[3]

$$\mu^2 = 1 - \frac{4\pi e^2}{m} \frac{N_e}{\omega^2 + \nu^2} + \left(\frac{ck}{\omega}\right)^2 \qquad (5\text{-}2)$$

$$k = \frac{2\pi e^2}{mc} \cdot \frac{1}{\mu} \cdot \frac{N_e \nu}{\omega^2 + \nu^2} \text{ nepers/meter} \qquad (5\text{-}3)$$

Since absorption is usually expressed in db, we define a as

$$a = 8.686 \times 10^3 \, k \tilde{=} 4.62 \times 10^4 \frac{N_e \nu}{\omega^2 + \nu^2} \text{ db/km} \qquad (5\text{-}4)$$

where

μ = index of refraction,

k, a = absorption coefficient,

N_e = electron density,

e, m = charge and mass of the electron,

ν = collision frequency, and

ω = wave frequency = $2\pi f$

In Figure 5-3 the upper scale and Curve C show the collision frequency as a function of altitude. From this and the electron density, the absorption coefficient, a, can be found as a function of altitude for a particular frequency. This is illustrated for 50 megacycles in Figure 5-4. The integrated absorption per-kilometer over a vertical path through the D region gives the total path attenuation, L_a, due to absorption expected for one-way vertical transmission. For the case above and for a range of other values of beta radiation intensity from a tenth of a watt to a microwatt per square meter, Figure 5-5 shows the one-way vertical path absorption at 50 megacycles due to beta and gamma rays, for a range of radiation intensities.

For wave frequencies much larger than the collision frequency, the absorption is proportional to f^{-2}. The maximum absorption for a given electron density occurs when the wave frequency equals the collision frequency. For wave frequencies much less than the collision frequency, absorption is independent of frequency. For electron densities of the case discussed above, the f^{-2} approximation is reasonably good from 10 megacycles upward.

For paths other than a vertical one, integration of the absorption must be computed along the path. If the fission debris is uniformly distributed above the region that the ray traverses, the total path absorption for an inclined path can be found by multiplying the vertical path absorption by the secant of the angle of incidence (angle between ray path and vertical).

Inherent in the above sequence of calculations determining absorption are approximations and uncertain coefficients at each step. The cumulative effect is such that, if the radiation intensity is known, the absorption may be in error by as much as a factor of 3. For example, if absorption indicated above is 30 db, the loss might be as much as 90 db or as little as 10 db. On top of this are uncertainties in the radiation intensity at a specified time after a burst which, as discussed in Chapter 8, has a considerable degree of uncertainty also.

5.2 REFRACTION

The change in the index of refraction caused by free electrons also affects the direction and velocity of propagation of electromagnetic waves. If the electron density is arbitrarily distributed, it is

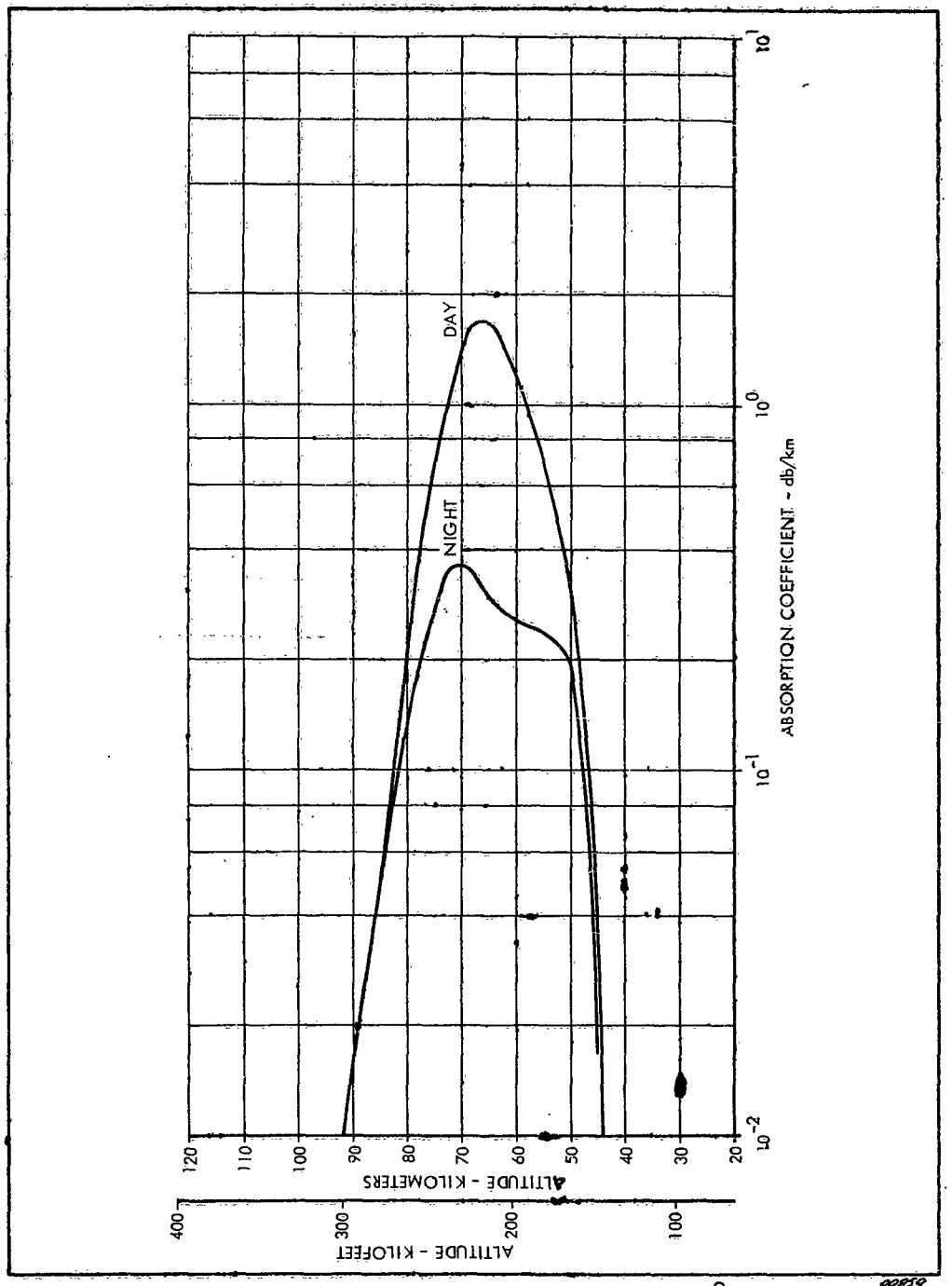

Figure 5-4. Incremental Absorption for 10 Milliwatts/Meter^2 of Beta Radiation, f = 50 Mc

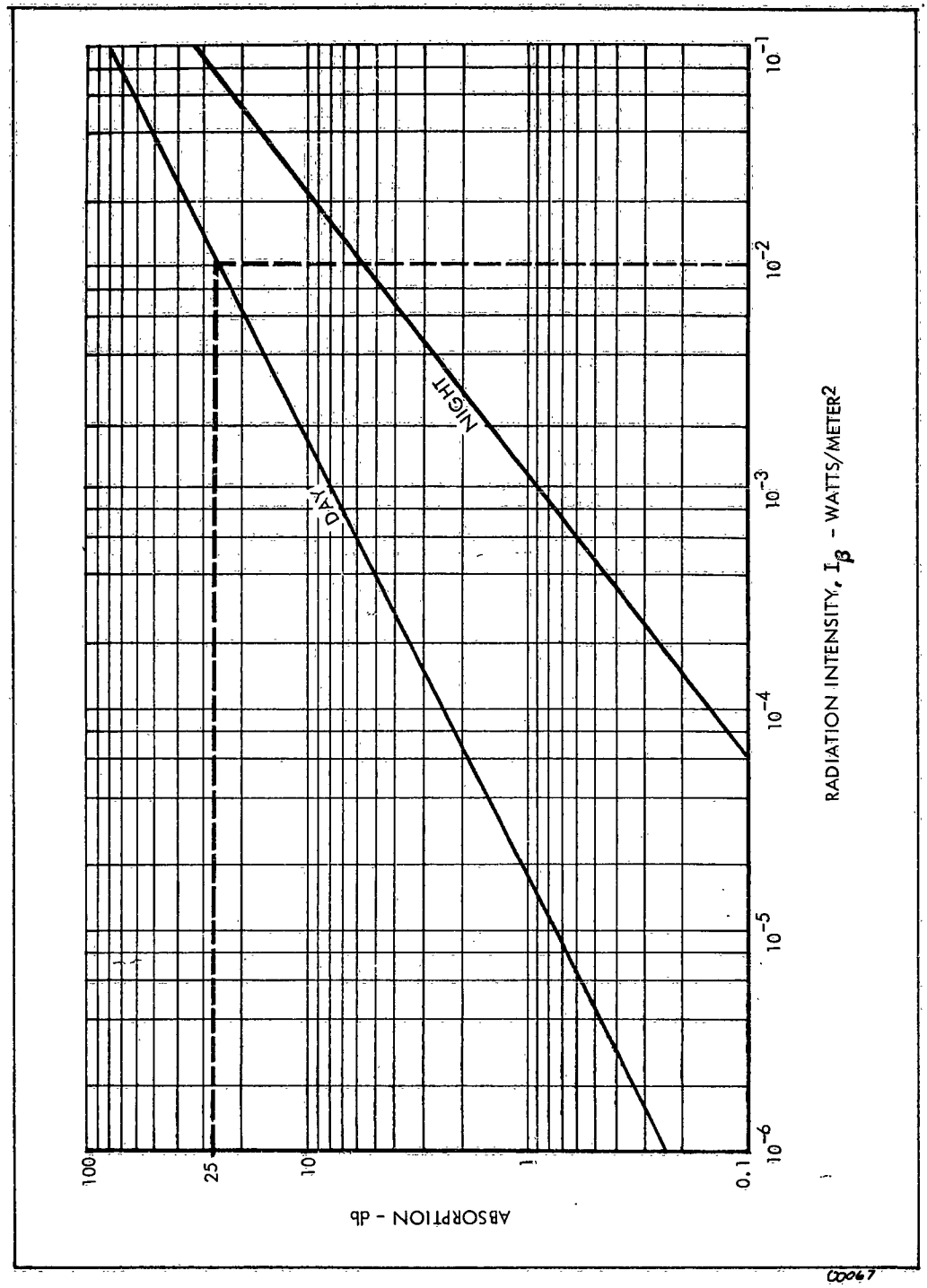

Figure 5-5. One-Way Vertical Path Absorption for Beta Radiation - f = 50 Mc

difficult to give any single rule determining the amount of bending other than actually tracing the ray path point by point. When the electron density distribution can be approximated by fairly simple models such as plane or spherical stratification, approximations can be used to estimate the amount of refraction.

Bending of the ray path results from changes in electron density in the direction perpendicular to the ray path. The ray bends toward the highest index of refraction or away from the highest electron density. Large electron density gradients can produce angular path changes of many degrees, which can seriously hamper or prevent, radar detection, acquisition, or tracking. Accompanying lesser electron density gradients on the fringes of an ionized region will be lesser angular errors or bearing errors of the order of milliradians, which can seriously degrade tracking radars. In addition to angular errors there are range errors resulting principally from the altered propagation velocity of the radar wave along the ray path. For small amounts of refraction, range errors are proportional to the average electron density along the propagation path.

Rate errors are introduced if the angular and range errors change with time. Since the propagation path from a radar to a moving target will traverse different portions of an ionized region as a function of time, significant rate errors can be introduced. The time decay of ionization will cause rate errors even for a fixed path; however, these will usually be negligible in comparison to the rate errors caused by target motion for typical high speed targets. Bearing rate errors much less than a milliradian per second and range rate errors less than a meter per second can be excessive when trajectories are to be extrapolated for great distances.

In the D region where electron collisions with neutral particles are high, applicable refraction is accompanied by large absorption. Thus, refraction is of primary interest when it occurs in the lower E region (~90 kilometers) or higher. But even here absorption may become important when the electron density is large enough to cause large refraction of very high frequencies. This absorption results from collisions of electrons with positive and negative ions as discussed in 2. 1. 3. At low electron densities, electron-ion collision frequencies are small and can be neglected. As the electron density is increased, electron-ion collisions become increasingly important and may cause absorption to be the major source of degradation.

For electron densities insufficient for total reflection, local variations in electron density may cause scattering of part of the incident energy. Scattered energy can produce clutter in radar systems or provide anomalous communication modes. Local variations in electron density can be caused by normal or burst produced turbulence. Above the D region where particle collisions are rare, the earth's magnetic field may cause the variations in electron density to be nonisotropic, appearing as columns of ionization aligned with the magnetic field. At the present time, knowledge of the turbulence sources and amount of field alignment is largely qualitative in nature.

In Sections 5.2.1 and 5.2.2 approximate methods are given for estimating bearing and range errors when the ionized region can be considered plane or spherically stratified. One or a combination of these models can be used in many cases to approximate the actual ionization. For other cases a ray tracing procedure must be used preferably with the aid of a digital computing machine. In Section 5.2.3 the results of an exact ray tracing procedure are presented. A spherical model was used to illustrate the refractive errors which may be caused in radar systems.

5.2.1 Plane Stratification

With plane stratification, variations of electron density occur in only one direction. This variation is a good approximation to the normal ionosphere where electron density essentially varies only with altitude, Z. Figure 5-6 shows a radar propagation path which enters a horizontally stratified region. The true and apparent positions of the target and the bearing error are shown. Approximate[4] expressions for the bearing error $\Delta\theta$ and range error ΔR are:

$$\Delta\theta \approx \frac{\bar{N} \tan \theta_T}{2N_c} \text{ and} \qquad (5\text{-}5)$$

$$\Delta R \approx \frac{\bar{N} R_T}{2N_c} \qquad (5\text{-}6)$$

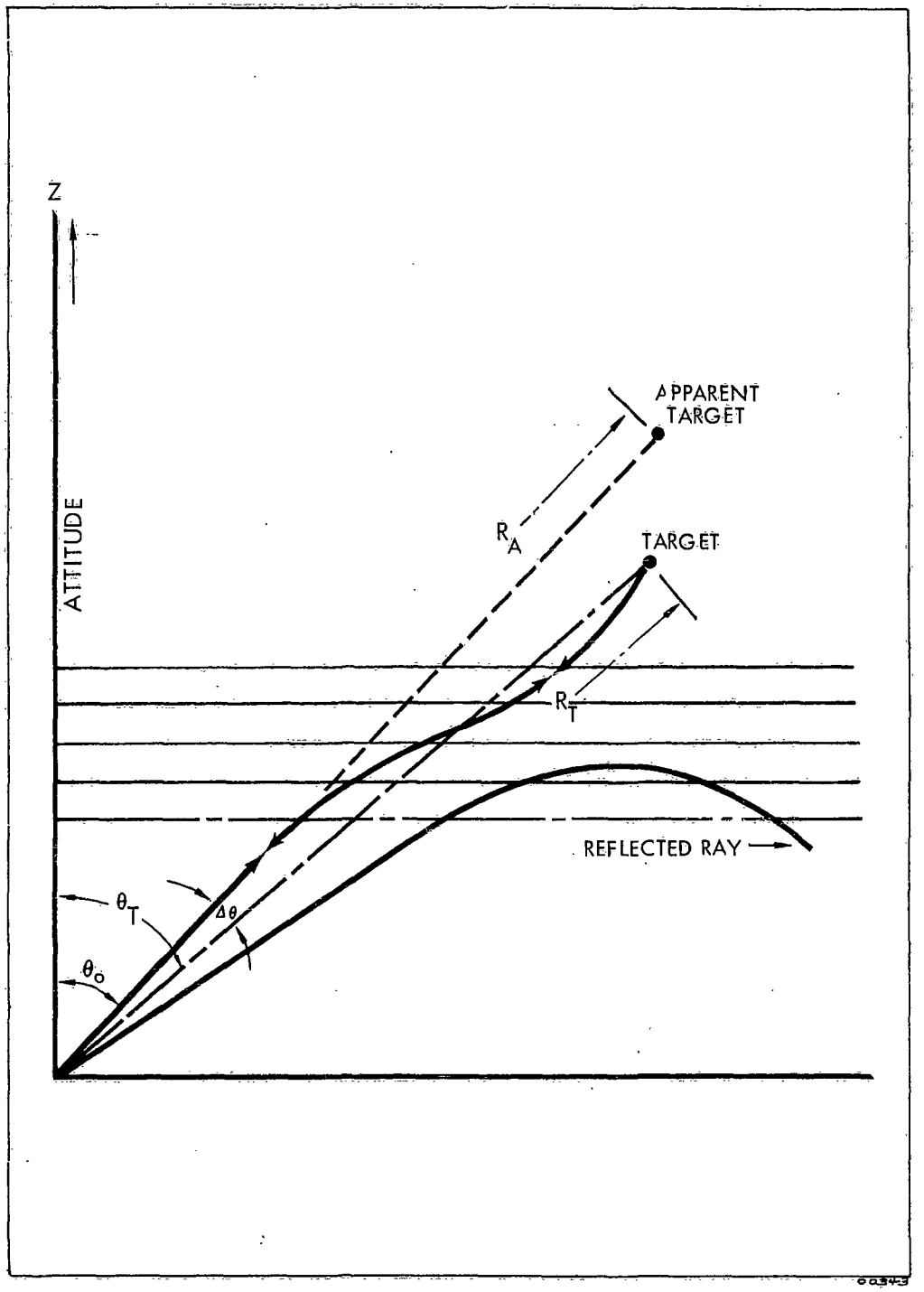

Figure 5-6. Geometry for Refraction in Horizontally Stratified Medium

where

$\bar{N}$ = average electron density over the whole path to the target

N_c = critical electron density, which would cause reflection at normal incidence for the frequency used

θ_T' = angle of line to the target with vertical and,

R_T = range to target (see Figure 5-6).

These approximations for a generalized horizontal stratification are accurate within about 25 percent as long as the peak electron density does not exceed $N_c \cos^2 \theta_o / 4$. If the refraction is sufficiently large, energy entering one medium from another may be returned to the original medium, as discussed in Chapter 2. Reflection occurs when

$$N_e = 1.24 \times 10^{-8} f^2 \cos^2 \theta_o \qquad (5\text{-}7)$$

For normal incidence $\theta_o = 0$, and $N_c = 1.24 \times 10^{-8} f^2$. An example of reflection is also shown in Figure 5-6.

If the target is above the plane stratified layer, the bearing and range error can be given as a function of the maximum electron density within the layer, the thickness of the layer, Z_m, and the height of the target, Z_T. The distribution of electron density within the layer will affect the errors, but results accurate within a factor of about 1.5 can be obtained if the thickness of the layer is defined as the distance between points at which the electron density is down by a factor of 10 from the maximum value, and the layer has only one maximum. Also the peak electron density must not exceed $N_c \cos^2 \theta_o / 4$, thus

$$\frac{N_m}{f^2} \leq 3.1 \times 10^{-9} \cos^2 \theta_o \qquad (5\text{-}8)$$

where N_m = maximum electron density in the layer. The bearing and range errors are proportional to $\frac{N_m}{f^2}$ for these conditions.

For general applicability in a graphical presentation of these errors, it is convenient to use normalized coordinates. Thus, Figure 5-7 presents the bearing error, $\Delta\theta$, multiplied by the ratio $\frac{Z_T}{Z_m}$ as a function of $\frac{N_m}{f^2}$. Also, the range error, ΔR, is divided by the layer thickness, Z_m.

EXAMPLE: What is the bearing and range error and total two-way path absorption caused by the electron density distribution shown in Figure 5-3 for debris beta radiation in the daytime? Assume horizontal stratification and the following conditions.

radar elevation angle = 30 degrees = $90 - \theta_o$,

radar frequency = 50 megacycles, and

target altitude = Z_T = 150 kilometers.

The peak electron density, N_m, is 3.9×10^5 electrons/centimeter^3 as marked on the abscissa of Figure 5-3. The ratio N_m/f^2 then is $3.9 \times 10^5/(50 \times 10^6)^2$ or 1.6×10^{-10}. Also, as marked in Figure 5-3, the density decreases by a factor of 10 at 53 and 123 kilometers giving a layer thickness, Z_m, of 70 kilometers.

Go to Figure 5-7 and enter the abscissa at $N_m/f^2 = 1.6 \times 10^{-10}$. Follow the dashed line vertically until it intersects the solid curve θ_o 60 degrees which is the angle of incidence corresponding to the radar elevation angle, 30 degrees. Following the dashed horizontal line left from the intersection to the ordinate, read the ratio $\Delta\theta\, Z_T/Z_m$ as 0.45 degrees. The bearing error, $\Delta\theta$, then is $0.45 \times 70/150 = 0.21$ degrees or 3.68 milliradians.

To find the range error, return to Figure 5-7. Again follow the dashed vertical curve from the point on the abscissa 1.6×10^{-2} until it intersects the dashed curve $\theta_o = 60$ degrees. Trace the dashed horizontal curve to the right to the ordinate and read $\Delta R/Z_m = 9 \times 10^{-3}$. The range error ΔR then is $9 \times 10^{-3} \times 70 = 0.63$ kilometers or 630 meters.

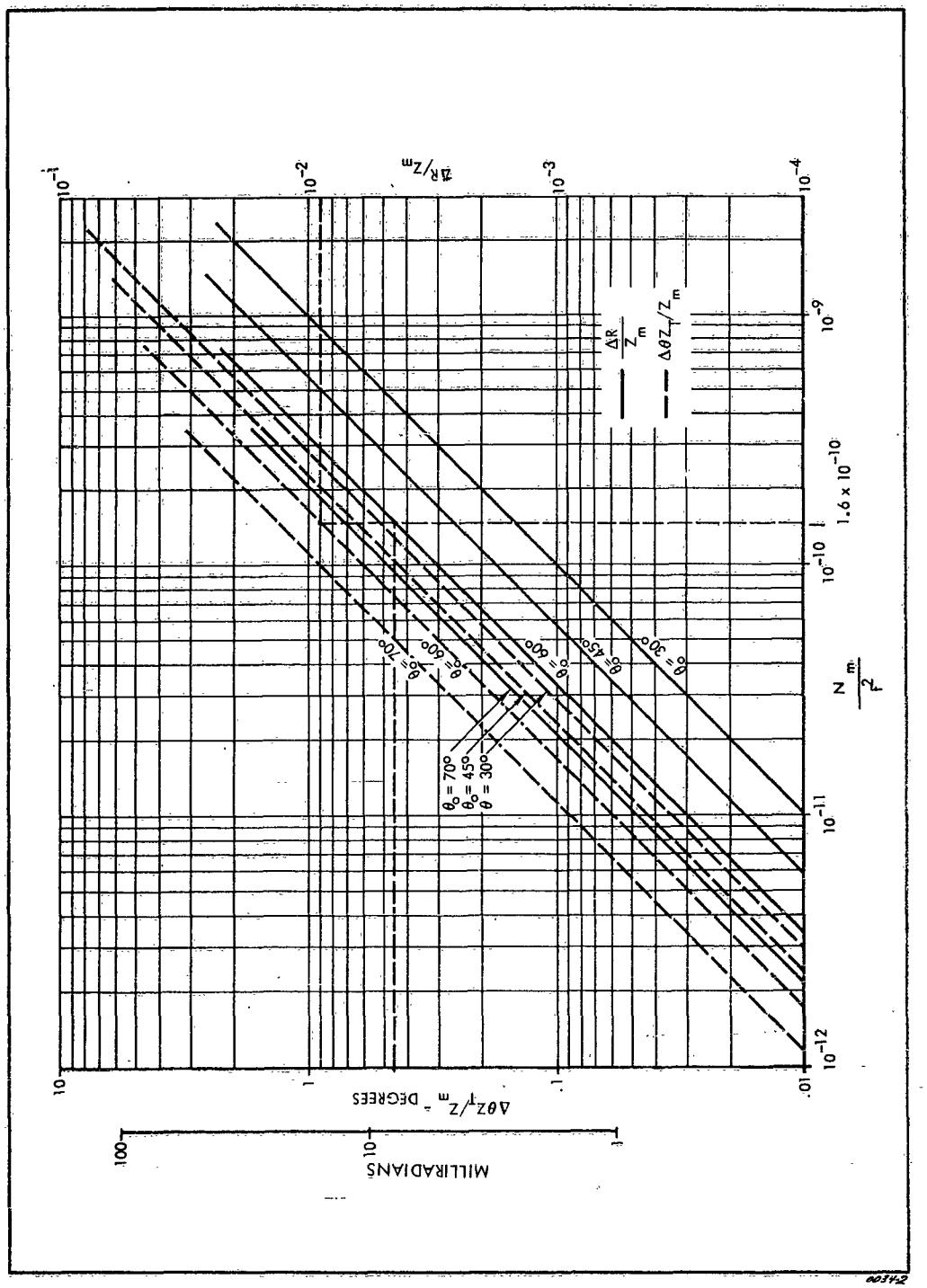

Figure 5-7. Bearing and Range Errors in Horizontal Stratified Medium

As previously mentioned, D-region refraction is accompanied by appreciable absorption. The one-way vertical path absorption may be obtained from Figure 5-5 by entering on the abscissa where $I_\beta = 10^{-2}$, or 10 milliwatts/meter^2, and going vertically to the intersection with the day curve. Then, moving left horizontally to the ordinate, obtain one-way vertical path absorption L_a = 25 db. Multiply by the secant of the angle of incidence (secant 60 = 2) and taking twice the one-way absorption, since the radar energy traverses the absorption region twice in reaching the target and returning, gives 100 db total path absorption.

EXAMPLE: What are the bearing error, range error and path absorption for the same conditions given in the above except for a frequency of 500 megacycles?

From Section 5.1, the absorption scales inversely as frequency squared. Bearing and range errors also scale inversely with frequency squared as shown in Figure 5-7. Note in this figure that the abscissa contains the factor $1/f^2$ and that the curves are straight lines. Thus, for instance, increasing f^2 by ten reduces N_m/f^2 to one-tenth its previous value and at the same time reduces the range and bearing error parameters, $\Delta R/Z_m$ and $\Delta\theta\, Z_T/Z_m$, by a factor of ten. Correspondingly, the bearing and range errors and path absorption for a 500 megacycle radar would be:

bearing error = .0021 degrees = .0368 milliradian

range error = 6.3 meters

path absorption = 1 db

EXAMPLE: For an elevation angle of 30 degrees what is the highest frequency reflected from the daytime beta ionization shown in Figure 5-3?

The peak electron density shown in Figure 5-3 is 3.9×10^5 electrons/centimeter^3. For an elevation angle of 30 degrees, θ_o is 60 degrees. Substituting these values in the equation given for reflection in Chapter 2 (Equation 2-9) and solving for frequency gives:

$$f \cong 9 \times 10^3 \sqrt{N_e} \times \sec i;\ i = \theta_o \text{ for horizontal stratification}$$
$$\cong 9 \times 10^3 \sqrt{3.9 \times 10^5} \times 2 \cong 11 \text{ megacycles.} \qquad (5\text{-}9)$$

5.2.2 Spherical Stratification

In a homogeneous atmosphere, the ionization immediately after the burst decreases with distance symmetrically in all directions. The rate of decrease is a combination of the inverse square law and an exponential decay caused by absorption of the ionizing radiation. For a limited range of radius, $N = Ar^{-n}$ is a reasonable approximation where A and n are constants chosen to match electron density, N, and radial distance from the burst, r, at two points. The value of the constant A will depend on the type and intensity of the ionizing radiation; while the exponent n will be primarily determined by the distance from the radiation source, the electron production rate, and the electron loss rates or mechanisms. While it would be difficult or perhaps impossible to determine these constants in an operational stiuation, such a spherical model is useful in illustrating some important aspects of refraction errors on radar systems. In a spherical model, refraction errors can be obtained exactly when n = 2 and approximately for any n greater than 2.

For an exponential atmosphere, the electron density contours tend to be flattened on the bottom, and are not concentric. Here r should not necessarily be considered the distance from the burst point, but the radius of curvature of the electron density contours in the region of concern.

Figure 5-8 shows refraction of a propagation path through a spherically stratified region when the target lies in a plane containing the transmitter and center of the ionized region. The radius r_o is the closest point of approach of the ray path to the center of the model. The angle Ψ is the amount of refraction and $\Delta\theta$ is the bearing error. Even with approximate solutions, finding the bearing and range errors as a function of radar elevation angle is tedious requiring several intermediate steps. Finding the errors given a target location is a trial and error process.

A solution for the refraction error, Ψ, and the range error, ΔR, can be given as a function of the electron density at the closest point of approach.[4] Figure 5-9 shows the refraction for an illustrative

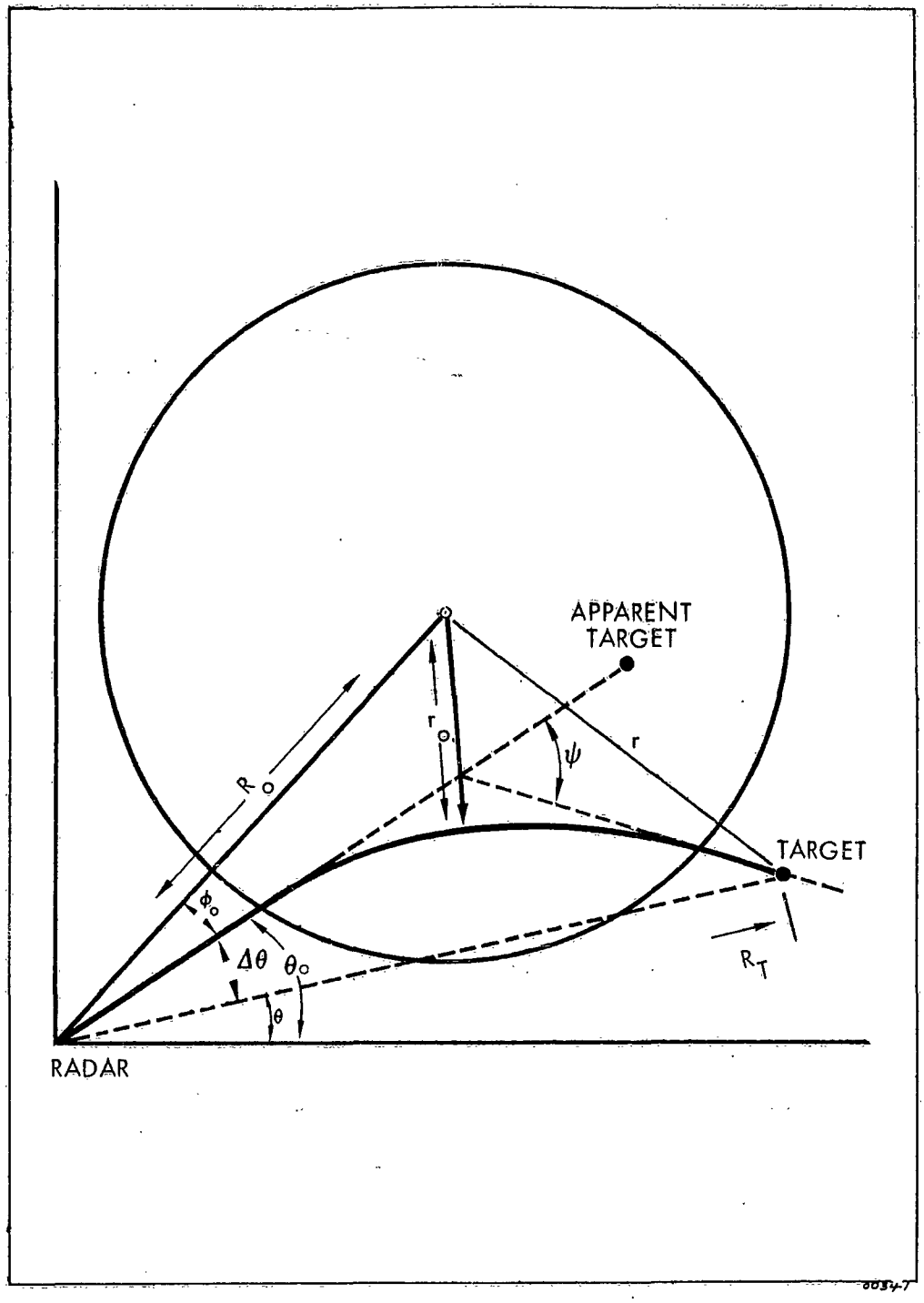

Figure 5-8. Geometry for Refraction by Spherically Stratified Region

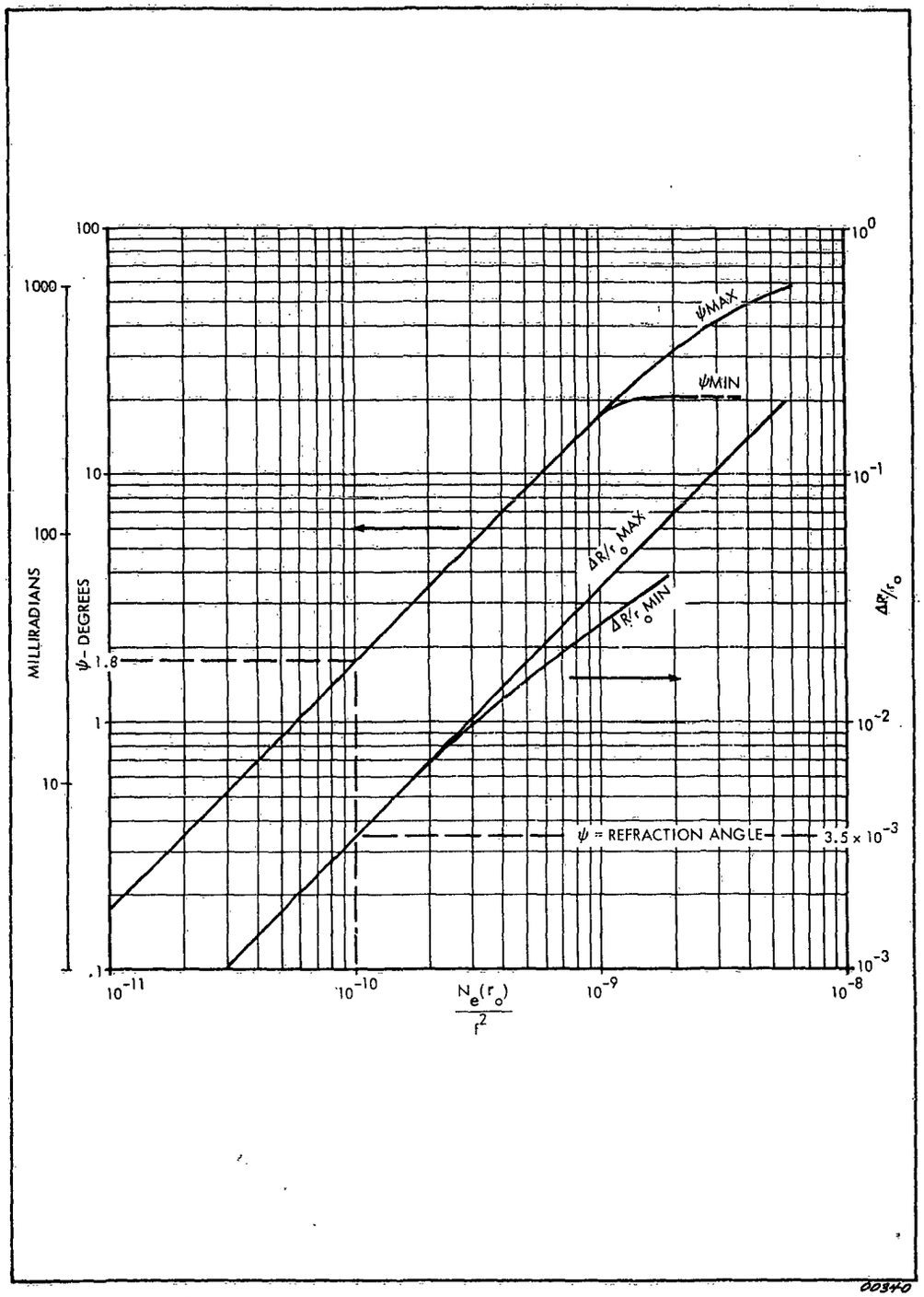

Figure 5-9. Refraction and Range Errors in Spherically Stratified Medium

case. Two approximations which give an upper limit, ψ max, and a lower limit, ψ min, are compared and agree well up to refraction of 20 degrees.

The bearing error $\Delta\theta$ is nearly equal to the refraction angle, ψ, only when the actual range to the target, R_T, is large compared to the distance to the center of the model, R_o. The relation between ψ and $\Delta\theta$ is given by

$$\Delta\theta = \psi - \sin^{-1}\left[\frac{R_o}{R_T}\left[\sin(\psi + \varphi_o) - \sin\varphi_o\right]\right] \qquad (5\text{-}10)$$

where φ_o is defined in Figure 5-8. This relationship strictly applies for target distances sufficiently greater than R_o that negligible refraction is taking place near the target, i.e., the target is outside the electron cloud.

When ψ and $\Delta\theta$ are small (less than about 10 degrees)

$$\Delta\theta = \psi(1 - R_o/R_T) \qquad (5\text{-}11)$$

For the illustrative model, Figure 5-9 can be used to find the bearing and range error for a ray that passes within a distance r_o of the center. A straight line between radar and target can be used to find r_o and thus the electron density at the closest point of approach if the resulting refraction error, ψ, is less than a few degrees. If, when the straight line estimate of r_o is used, ψ is larger than a few degrees, the results are only a lower limit to the actual refraction errors.

EXAMPLE: Find the bearing and range errors for propagation through a spherically stratified region with the following conditions:

r_o = 100 kilometers, $N_e(r_o) = 10^8$ electrons/centimeters^3, and

R_o = 300 kilometers,

R_T = 1200 kilometers, $f = 10^9$ cps.

The ratio $N_e(r_o)/f^2$ is 10^{-10}. Entering Figure 5-9 at the abscissa point 10^{-10} and continuing upward to the intersections with the ψ and $\Delta R/r_o$ curves, we see that $\psi = 1.8$ degrees and $\Delta R/r_o = 3.5 \times 10^{-3}$. Thus, $\Delta R = 3.5 \times 10^{-3} \times 100 = 3.5 \times 10^{-1}$ or 0.35 kilometers.

5.2.3 Ray Tracing Through a Spherically Stratified Region

The refractive errors through a particular spherically stratified region have been computed in detail to illustrate the concepts discussed in the previous sections and to indicate the kinds of errors that may be caused by intense ionization. In an example at the end of this section, the results are compared with the approximate method given in Section 5.2.2.

The electron density contours of this ionization model are defined by

$$N_e = \frac{10^{33}}{r^{12}}$$

for: r = distance from center of model in kilometers

N_e = electron density in electrons/centimeters^3

The center of the model is located at elevation, E, of 30 degrees, zero degrees azimuth, and 564 kilometer slant range measured from the radar site. Figure 5-10 shows the relation between the radar and ionization model in the plane of zero azimuth. Also shown are the ray paths for rays leaving the radar at several elevation angles. A frequency of 1 kilomegacycle was used in determining the refraction. Because the electron density increases rapidly near the center of the model, there is significant bending of the ray path.

The refraction becomes so severe as the elevation angle of radar rays approaches the elevation angle of the burst that there is a region, shown by half tones, into which no radar ray of this frequency penetrates, no matter how powerful the radar is. By analogy to sonar this is called the "thermocline effect," and leads to a radar "blackout" region (shown by half tone). In three dimensions, this blackout region is a cone in which the target is shielded from the radar. Because rays near this region intersect each other, two elevation

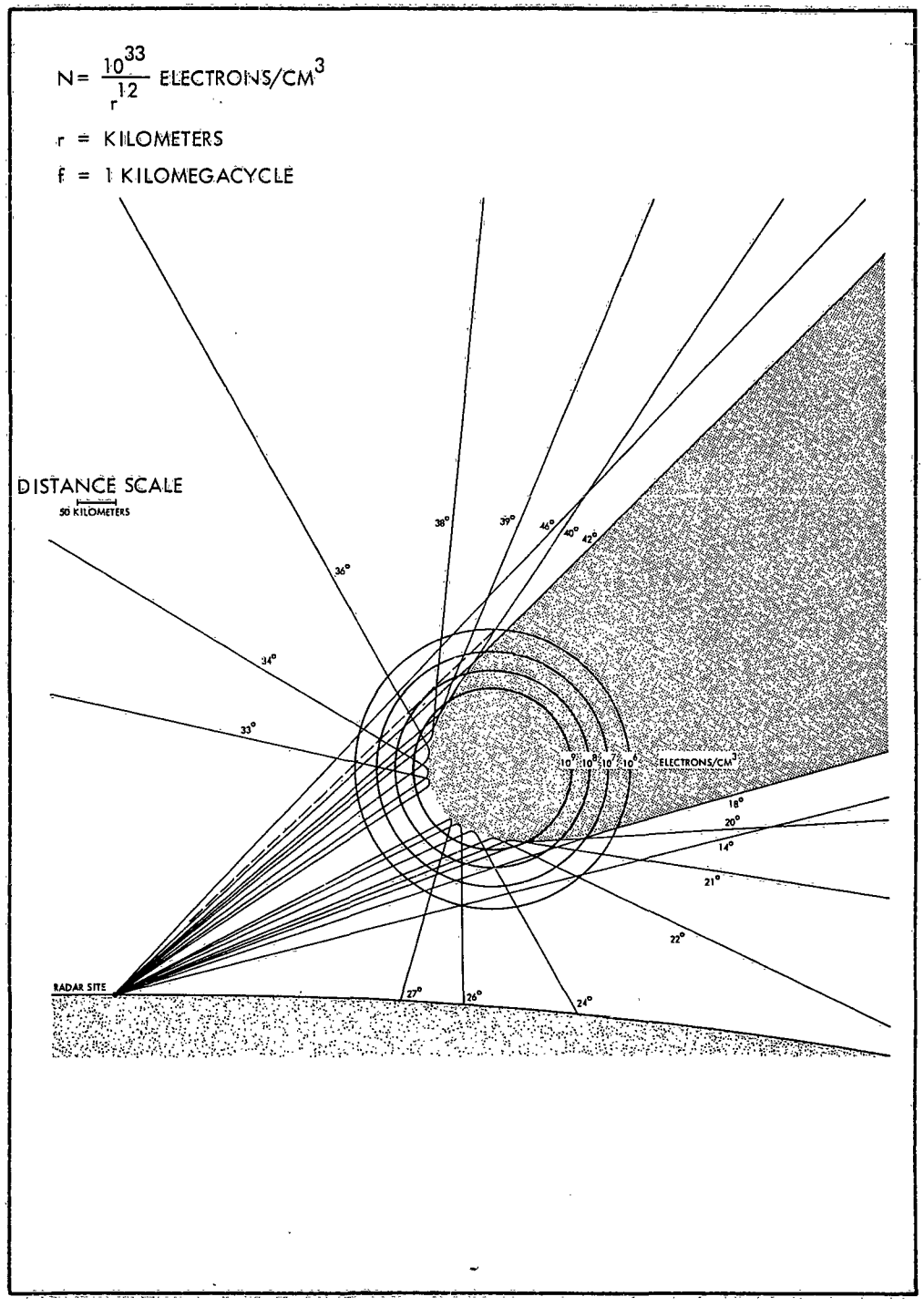

Figure 5-10. Radar Propagation Paths through Spherically Ionized Region

angle paths to the same target exist, and multiple targets may be visible. Some rays are reflected down to the ground and can cause clutter in the radar. However, the absorption along these highly refracted paths is generally found to be high.

The amount of elevation error, or azimuth error if the ray path is not in the zero azimuth plane, is a function of the location of the target. The elevation and azimuth errors for a target located at a slant range of 1200 kilometers have been computed as a function of radar elevation and azimuth angles.

Figure 5-11 shows contours of constant elevation error, ΔE, in one quadrant and constant azimuth error, ΔA, in another quadrant as a function of the ray direction at the radar site. The contours have been terminated when the total bearing error is about 10 degrees. Due to symmetry the errors in the other quadrants are just the mirror image of the quadrant shown. For total bearing errors less than about 10 degrees the errors shown scale as N_e/f^2 where N_e is the electron density along the path. For targets at slant ranges greater than 900 kilometers, the error scales approximately as $R_T/1200$ where R_T is the actual slant range. Thus, doubling the frequency to 2 kilomegacycles or locating the target at 4800 kilometers would reduce the error by a factor of four. Range errors can be found from the approximate methods of Section 5.2.2, or if the refraction is not too large, range errors may be estimated from the average electron density along the path.

$$\Delta R \approx \frac{\bar{N} R_T}{2N_c} \qquad (5\text{-}6)$$

where $\bar{N}$ and N_c are defined in Section 5.2.1.

Rate errors are produced when the bearing error changes with time. If the target is moving, the bearing errors will change with time introducing elevation and azimuth rate errors. An estimate of the magnitude of these errors can be obtained from Figure 5-11 by locating the target elevation and azimuth at two points in time. The difference in elevation or azimuth errors corresponding to the two target positions divided by the time difference is the rate error.

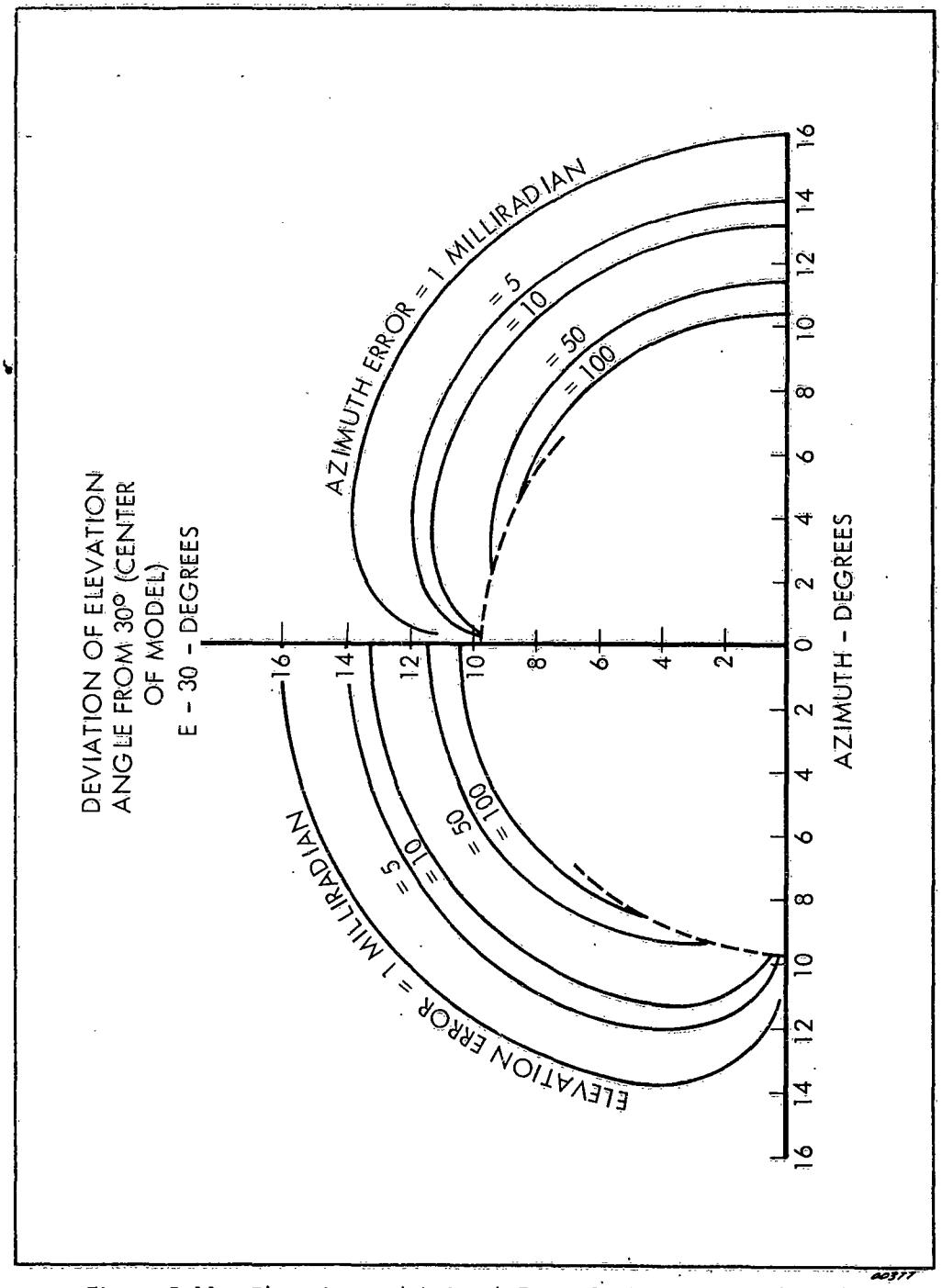

Figure 5-11. Elevation and Azimuth Errors for Propagation through a Spherical Model - f = 1 kMc

As a simple example, assume that the target is travelling at a velocity of 7 kilometers per second at a constant slant range of 1200 kilometers and remains in the zero azimuth plane so that the bearing error is only in elevation. For these conditions the radar elevation angle changes by 0.333 degrees per second $\left(\frac{E_1 - E_2}{\Delta t} = \frac{v}{R_T} \right)$. From Figure 5-11, the elevation rate error can be found for a particular elevation angle of interest. For instance, when the elevation changes from 40.4 to 41.4 degrees the elevation error changes from 100 to 50 milliradians. To change the elevation angle by one degree required 1/.333 = 3 seconds. The elevation error changes by 50 milliradians, which is 50/3 = 16.7 milliradians per second. This procedure is helpful in estimating the maximum rate error that may be introduced but becomes fairly involved if the target range and direction are both changing.

The approximate methods given in Section 5.2.2 can be used to find the bearing and range errors. Again consider the zero azimuth plane and an elevation angle of 43 degrees. In Figure 5-10, a dashed straight line is drawn from the radar at a 43 degree elevation angle. The radius from the center of the model to this line determines the electron density at the closest point of approach. For the particular elevation angle chosen, the electron density at the closest point of approach can be read directly from Figure 5-10 as 10^8 electrons/centimeters^3. For a frequency of one kilomegacycle the ratio $N_e(r_o)/f^2$ becomes 10^{-10}. From Figure 5-9 the refraction error, ψ, is 1.8 degrees or 31.4 milliradians and $\Delta R/r_o$ is 3.5×10^{-3}. The range error becomes $\Delta R \approx 3.5 \times 10^{-3} \times 120 \approx 0.4$ kilometers. The elevation error is found from

$$\Delta E = \psi\left(1 - \frac{R_o}{R_T}\right) = 31.4\left(1 - \frac{564}{1200}\right) = 16 \text{ milliradians.}$$

Checking in Figure 5-11, we see that this is in good agreement with the results found by exact ray tracing.

The range error can also be estimated from the average electron density along the path.

$$\Delta R \approx \frac{\bar{N} R_T}{2N_c} \qquad (5\text{-}6)$$

For the path tangent to the 10^8 contour, a rough estimate of the average electron density might be

8×10^7 electrons/centimeters^3 over 50 kilometers of path length

5×10^7 electrons/centimeters^3 over 100 kilometers of path length

5×10^6 electrons/centimeters^3 over 100 kilometers of path length

Then

$$\bar{N} = \frac{(8 \times 10^7 \times 50) + (5 \times 10^7 \times 100) + (5 \times 10^6 \times 100)}{R_T}$$

$$= \frac{9.5 \times 10^9}{R_T}$$

$$N_c = 1.24 \times 10^{-8} f^2 = 1.24 \times 10^{-8} \times 10^{18}$$

$$= 1.24 \times 10^{10}$$

$$\Delta R = \left(\frac{9.5 \times 10^9}{R_T}\right) \frac{R_T}{2(1.24 \times 10^{10})} \approx 0.4 \text{ kilometers}$$

5.3 DISTURBANCES OF THE UPPER IONOSPHERE

The fireball expansion and shock waves discussed in Chapter 4 can disturb the normal E and F layer over an area thousands of kilometers in diameter. The nature of one ionospheric wave, noted on ionosondes after TEAK, indicated a sudden increase in electron density which could be the compression or shock wave, followed by a prolonged decrease in electron density which could be the radially moving fireball material greatly expanded and hence with an electron density below the ambient value.[5] This effect was observed following TEAK over a large area and the time at which the effect started at any point was approximately proportional to the distance between that point and the burst.

Reduction of the normal F-layer electron densities can cause loss of support for reflection of H-F radio propagation by greatly reducing the MUF. In addition to the reduction in electron density a phenomenon known as spread F was recorded following TEAK. Spread F is the term applied to the F layer when the virtual height of ionosonde records is not sharply defined, indicating reflection from a diffuse region. One proposed theory of spread F is that electrons are aligned along the magnetic field causing reflection or scattering of the incident wave when the wave becomes perpendicular to the field lines. Scattering and defocussing of the incident energy may cause sufficient losses to degrade circuits even though the energy is returned from the inosphere. Another phenomena recorded following the Pacific tests which may be associated with the disturbed region expansion was enhancement of sporadic E. Sporadic E is associated with small clouds or patches of ionization which are above the ambient density of the E region. H-F reflection can occur from these clouds and in the normal inosphere partially explains operation of multi-hop links when there is lack of support at some of the F-layer reflection points.

In addition to the change in the level of ionization, the normal stratification of electron density may be affected by travelling disturbances. The change in stratification or tilting of the F layer changes the path of reflected rays and may defocus the available energy or alter the MUF. Also, tilting can change the direction of arrival of the wave so that it no longer has maximum antenna gain for systems employing directional antennas. Further, the tilt causes anomalous multipath conditions and, if changing, may cause doppler shift and fading.

5.4 NOISE

High altitude nuclear bursts create noise in the radio spectrum primarily by two mechanisms. The disruption of the electrostatic balance around the explosion causes an electromagnetic pulse which can propagate to large distances from the burst. The pulse is of short duration, lasting less than a second in most cases, with most of the energy in or below the VLF band. Interference caused by the pulse will be similar to that produced by lightning flashes in the atmosphere.

Spiralling of the beta rays discussed in Chapter 4 causes these high speed electrons to be in continual acceleration. This results in the

emission of electromagnetic energy which is termed synchrotron radiation.[6] Unless the energy of the electron is large, as for the fission fragment beta rays, little energy is radiated.

Beta rays emitted from the fission debris cause synchrotron radiation as they travel upward from the debris to the magnetic conjugate point or downward from the debris into the earth's atmosphere. If the upward travelling beta rays are trapped (see Chapter 4) a persistent source of synchrotron radiation can be produced which spreads around the world. Downward travelling beta rays which penetrate into the D region are lost by collisions producing a transient noise source whose magnitude is related to the beta radiation intensity.

The radiated power is nearly isotropic for H-F, but becomes highly directional for UHF. The radiation pattern for each electron is a conical shell having the cone angle of its helix pitch. The composite of many electrons is a doughnut-shaped pattern that is only several degrees wide at UHF. The UHF directional properties make effects of the trapped electrons negligible at magnetic latitudes above 50 - 55 degrees if the earth's field lines are not disturbed. No stable trapped electrons at altitudes below 5000 kilometers will radiate toward antennas at these latitudes. At this altitude, the magnetic field is so weak that the radiation is down many orders of magnitude. Washington, D. C. (48 N geomagnetic) is borderline in that 10 electrons/centimeter^3 could produce a localized sky temperature of 100 degrees Kelvin (important only if masers or parametric amplifiers are used). However, at the magnetic latitude of New Orleans the radiation received could be four orders of magnitude greater. Further, if the geomagnetic field lines are sufficiently-disturbed by the detonation or a combination of detonations, synchrotron noise may be more isotropic and be important at higher magnetic latitudes for brief periods.

Synchrotron radiation will be attenutated if it passes through absorption regions as discussed in Section 5. 1. Most of the H-F and VHF noise produced by beta rays directed downward from the debris will be absorbed. Upward directed beta rays may cause noise levels 20 to 40 db above the background in the H-F and VHF bands, which could degrade satellite or ground communication for a short time.

In addition high-altitude nuclear explosions may affect atmospheric and galactic noise reaching radio and radar receivers.

Atmospheric and galactic noise are major sources of interference in the H-F band. Atmospheric noise originates in thunderstorms, rain, snow or dust storms. The noise displays the same propagation characteristics as ordinary radio transmissions so that interference is received from distant storms. Galactic noise is of extra terrestrial origin and under many circumstances may be the principal source of noise between 10 and 100 megacycles. Atmospheric and galactic noise will be attenuated if the noise propagates through absorption regions caused by the nuclear burst. When both the desired signal and interference are attenuated, system performance may or may not be degraded. Of course, reduction of the signal below local noise or receiver set noise will cause blackout.

REFERENCES

1. Maienschein, F. C., et. al. Gamma Rays Associated with Fission. Paper 670, Second Geneva Conference.

2. Mitra, S. K. The Upper Atmosphere. The Asiatic Society Monograph Series.

3. Archer, D. H. Absorption and Refraction of Electromagnetic Waves in an Ionized Atmosphere (RM 59TMP-11). Santa Barbara; Technical Military Planning Operation, General Electric Co., 1959.

4. Archer, D. H. Position and Rate Errors Due to Refraction through Ionized Regions (RM 59TMP-26). Santa Barbara: Technical Military Planning Operation, General Electric Co., 1959.

5. Cummack, C. H. and King, G. A. M. Disturbance in the ionospheric F region following the Johnston Island nuclear explosion, New Zealand Jour. of Geology and Geophys., Vol. 2, (No. 3), August 1959.

6. National Academy of Science Symposium at Washington, D. C., 29 April 1959, Papers published in J. Geophys Research 64, August 1959.

7. Mitra, S. K. The Upper Atmosphere. The Asiatic Society Monograph Series, Vol. V, New York: Hafner Publishing Co., 1952.

8. Stratton, J. A. Electromagnetic Theory. McGraw-Hill Book Co., Inc., 1941.

9. Epstein, P. S. Proc. of National Academy of Science 16, 627, 1930.

10. Haselgrove, J. "Ray theory and a new method for ray tracing," The Physics of the Ionosphere, Report of 1954 Cambridge Conference, p. 355.

11. Minzner, R. A., Champion, K. S. W., Pond, H. L. The ARDC Model Atmosphere. 1959, AFCRC-TR-59-267, August 1959.

12. Schwinger, J. On the classical radiation of accelerated electrons, Phys. Rev. 75, 1912 (1949).

13. Landau and Lifschitz. The Classical Theory of Fields. Addison Wesley, 1951.

14. Rosner, H. Motions and radiation of a point charge in a uniform and constant external magnetic field (MSD 206-950-3), Republic Aviation Corporation, 15 November 1958.

15. Dressler, A. J. Effect of magnetic anomaly on particle radiation in geomagnetic field, J. Geophys Research, Vol. 54, (No. 7), July 1959, p. 713.

16. Ludwig, G. H., McIllwain, C. E., Val Allen, J. A. Satellite Observations of Electrons Artificially Injected into the Geomagnetic Field. State University of Iowa, May 1959

17. Sibley, W. L. and Vestine, E. H. Lines of Force of the Geomagnetic Field in Space (RAND Report T-1541), 7 November 1958.

18. Hendrick, R. W. Minimum Argotron Heights as Determined by the Geomagnetic Field (RM 59TMP-48). Santa Barbara: Technical Military Planning Operation, General Electric Co., 1959.